WATER SCIENCE SERIES

Assessment of Aquifer-Stream Connectivity Related to Groundwater Abstraction in the Lower Fraser Valley: Phase 2 Field Investigation at Otter Park, Langley

Diana M. Allen, Brynje Johnson, Andrew Garnet, Kira Howe, Michele Lepitre and Mike Simpson

November 2020

BRITISH COLUMBIA

SFU SIMON FRASER UNIVERSITY
THINKING OF THE WORLD

No. 2020-03

The **Water Science Series** are scientific technical reports relating to the understanding and management of B.C.'s water resources. The series communicates scientific knowledge gained through water science programs across B.C. government, as well as scientific partners working in collaboration with provincial staff. For additional information visit: http://www2.gov.bc.ca/gov/content/environment/air-land-water/water/water-science-data/water-science-series.

ISBN: 978-0-7726-7970-3

Citation:
Allen, D.M., Johnson, B., Garnet, A., Howe, K., Lepitre, M., Simpson, M. 2020. Assessment of Aquifer-Stream Connectivity Related to Groundwater Abstraction in the Lower Fraser Valley: Phase 2 Field Investigation at Otter Park, Langley. Water Science Series 2020-03, Province of British Columbia, Victoria.

Author's Affiliation:
Diana M. Allen, P.Geo.
Department of Earth Sciences
Simon Fraser University

Brynje Johnson, B.Sc. Honours student
Department of Earth Sciences
Simon Fraser University

Andrew Garnet, B.Sc. student
Department of Earth Sciences
Simon Fraser University

Kira Howe, B.Sc. student
Department of Earth Sciences
Simon Fraser University

Michele Lepitre, M.Sc., P.Geo.
Groundwater Section, Water Authorizations, South Coast Natural Resource Region
Ministry of Forests, Lands, Natural Resource Operations and Rural Development

Mike Simpson, M.Sc., P.Geo.
City of Vancouver
Formerly, Groundwater Section, Water Authorizations, South Coast Natural Resource Region
Ministry of Forests, Lands, Natural Resource Operations and Rural Development

Cover Photographs: Allen, D.M.

Acknowledgements

The authors gratefully acknowledge the Township of Langley for allowing the use of Otter Park for the study site and for providing LiDAR data for the numerical groundwater flow model. We also thank staff from the Ministry of Forests, Lands, Natural Resource Operations and Rural Development (Tyler Andersen, Lauren Hunter, Nida Asad, Tara Despault, Emily Elsliger, Cameron Stooshnoff, Emma Webster, Kumar KC) and Aspen Anderson from Simon Fraser University for assisting with the installation and removal of piezometers, making instream and streamflow measurements; and staff from the Ministry of Environment and Climate Change Strategy (Jon Goetz and Robin Pike) for installing the hydrometric stations. We also thank Klaus Rathfelder and Shirley Wang for reviewing this report.

EXECUTIVE SUMMARY

Abstraction of groundwater from a pumping well located beside a stream can result in sourcing of the pumped water directly from the stream and consequent depletion of stream discharge. The ability to accurately estimate stream depletion due to pumping is necessary for water rights management. This requires an understanding of the hydraulic connectivity between the aquifer and the stream. In British Columbia, evaluation of hydraulic connectivity is required for water licensing decisions under the *Water Sustainability Act*. Sensitive streams, as designated under the Water Sustainability Regulation under the *Water Sustainability Act*, are particularly at risk if hydraulically connected to an aquifer from which groundwater is abstracted.

The main goal of this multi-phase study is to build an understanding of the interaction between groundwater and sensitive streams for the purpose of identifying streams that are more vulnerable to groundwater abstraction. The study is being carried out collaboratively between Simon Fraser University and the Ministry of Forests, Lands, Natural Resource Operations & Rural Development. Phase 1 of the study (2015-2017) consisted of a targeted field study in Langley, B.C. (Union Creek at Steele Park) to determine the impacts of pumping on aquifer-stream interactions in an unconfined aquifer, including testing various analytical methods for quantifying streamflow depletion from groundwater pumping (Hall et al. 2017). Phase 1 yielded valuable data and provided critical knowledge surrounding how to conduct a field study to assess hydraulic connectivity. The study team identified several improvements to data collection that would achieve even better success in future studies, both at Steele Park and elsewhere (Hall et al. 2017).

The original intent of this study was to undertake a comparison of hydraulic connectivity in the unconfined Hopington AB Aquifer #35 at Union Creek at Steele Park in Langley, B.C., and a confined aquifer (provisionally identified Aldergrove CD #1192 at West Creek in Langley, B.C.). However, the study team determined that Phase 2 should focus on an unconfined aquifer at a different site, because unconfined aquifers are in principle more strongly hydraulically connected to surface water, and as such, are a more critical target for investigation. The team identified the Abbotsford-Sumas Aquifer #15 at Otter Park, situated south of Steele Park (the site used for Phase 1) in the Township of Langley, B.C. Bertrand Creek passes through the park and is easily accessible for deployment of instream instrumentation, and the drilling site had adequate overhead clearance. In contrast to Steele Park, which provided access to only a short reach of Union Creek with several obstructions that impacted flows (e.g. upstream by bramble and downstream by a culvert), Bertrand Creek has a longer and straighter reach through the park. Thus, Otter Park was considered ideally suited for this study.

Phase 2 was carried out from May 2018 to October 2018 and had four main objectives 1) Estimating the hydraulic conductivity (K) of the aquifer and streambed sediments using grain size analysis and slug testing; 2) Estimating the transmissivity (T), hydraulic conductivity and specific yield (Sy) of the aquifer from pumping test data; 3) Characterizing the hydraulic connectivity between the stream and the aquifer; and 4) Quantifying streamflow depletion during pumping and evaluate against a streamflow depletion model. Four wells were drilled at the site in close proximity to Bertrand Creek; one was completed as a pumping well (PW01) and the three others as monitoring wells (MW01, MW02 and MW03). PW01, MW01 and MW02 are screened from 16.8-18.3 m, while MW03 is screened from 27.4-29.0 m. The aquifer is unconfined and comprised of mostly coarse sands and gravel with very few fines. A deeper confining unit comprised of silt and clay was intersected by MW03 from 33.5 to 36.6 m. The confining unit is at least 6.01 m thick.

The site was instrumented with five hydrometric stations (HS1, HS2, HS3, HS4 and HS5). HS3 is located in-line with the pumping well. HS1, the furthest upstream, is ~150 m upstream of HS3, and ~100 m

outside of the park's boundary. HS2 is located ~40 m upstream of HS3. HS4 is ~40 m downstream of HS3, and HS5 is ~175 m downstream of HS3 along the western park boundary. The hydrometric stations were equipped with pressure transducer dataloggers to measure stage at 15-minute intervals. Streamflow measurements were made periodically from May to October 2018 and used to construct a rating curve for each hydrometric station. The accuracy of the rating curve diminished during the summer low flow period due to difficulties in measuring flow accurately, growth of instream vegetation and beaver activity.

Ten pairs of nested piezometers were installed in Bertrand Creek. Each piezometer nest had a longer and shorter partner with a difference in length of approximately 32 cm between their screened intervals (as measured at the mid-point of each screen). Four pairs were positioned across the creek, in line with the pumping well, and five pairs were positioned along the edge of the creek (one additional pair was installed for redundancy and one single piezometer was installed on the creek bank). Pressure transducer dataloggers were deployed to measure water levels at varying sampling intervals (non-pumping conditions and pumping conditions). Two networks of streambed temperature Tidbit loggers were also installed. One Tidbit network was installed in May and recorded temperatures hourly at the streambed surface and at a depth of approximately 16 cm. A second Tidbit network recorded temperature every 10 seconds during the pumping tests.

Several methods were used to determine the hydraulic conductivity (K) of the aquifer and the streambed sediments at Otter Park. Streambed sediment samples were collected from locations near each instream piezometer for grain size analysis. Five different analytical grain size distribution methods were used to estimate the minimum and maximum K for each sample. Based on the Chapuis (2004) method, considered the most accurate for the sediment at this site, the geometric mean of the minimum K values was 6.79×10^{-4} m/s and the geometric mean of the maximum K values was 4.75×10^{-3} m/s.

Slug tests were carried out in the deep and shallow instream piezometers to estimate K of the streambed sediments. The Bouwer-Rice and Hvorslev methods were used to analyze the data. The deeper piezometers had a geomean K lower than that of the shallow piezometers. For the deep piezometers, the Hvorslev method gave a geomean K of 1.46×10^{-5} m/s and the Bouwer-Rice method a geomean K of 1.39×10^{-5} m/s. In the shallower piezometers, the Hvorslev method gave a geomean K of 3.41×10^{-5} m/s and the Bouwer-Rice method a geomean K of 3.77×10^{-5} m/s. The slightly lower K of the deeper piezometers may reflect retention of fines of the deeper piezometer in the streambed compared to the shallower piezometers in the streambed.

Grain size analysis was also carried out for the aquifer sediments collected from PW01 and MW03. The geomean K, determined using the Chapuis method, ranged from 2.12×10^{-4} to 1.55×10^{-3} m/s for sediments from PW01, and from 1.44×10^{-4} to 1.11×10^{-3} m/s for sediments from MW03. Slug/bail tests conducted in monitoring wells MW01 and MW02 resulted in K values that were about half an order of magnitude lower than the minimum K calculated by the grain size analysis. The Hvorslev method gave a geomean K of 7.62×10^{-4} m/s and the Bouwer-Rice method gave a K of 5.49×10^{-4} m/s.

Two constant rate discharge pumping tests were conducted at the site; the first in July 2018 and the second in October 2018. The intent was to complete a constant rate test for 72 hours, followed by 24 hours of recovery. Pumping test 1 (PT1) was preceded by a step test to determine an appropriate pumping rate for the constant rate test (287 US gpm). PT1 began on July 4 at 10:15 and ended prematurely on July 5 at 15:15. Unfortunately, two mishaps resulted in a less than ideal dataset for the pumping test. First, the pumping contactor adjusted the flow rate early in the test. This resulted in a very poor drawdown dataset that was difficult to analyze. Second, Department of Fisheries and Oceans Canada visited the site during the pumping test and expressed concern that pumping could have a

detrimental impact on the critical habitat of the Nooksack Dace within Bertrand Creek, particularly at this time of the year (July). Therefore, the test was voluntarily terminated. A second pumping test was conducted in October, outside the low flow season. Pumping test 2 (PT2) began on October 11 at 19:15 and ended on October 14 at 19:15 (72 hours). The well was pumped at a higher rate than used in PT1 (324 US gpm). Data collected during PT2 were analyzed using the Neuman method for unconfined aquifers. The recovery data were analyzed using the Theis recovery method. A geomean K value of $1.29x10^{-4}$ m/s was estimated with the Neuman method and a geomean K value of $6.51x10^{-4}$ m/s was estimated from the Theis Recovery method. The Neuman method also provided estimates of transmissivity (geomean $3.26x10^{-3}$ m^2/s), specific yield (geomean $2.72x10^{-1}$), and specific storage (geomean $1.78x10^{-5}$ m^{-1}).

The hydraulic connectivity between the aquifer and the stream immediately prior to PT2 and during PT2 was investigated using streamflow, vertical hydraulic gradients from the instream nested piezometers, and streambed temperature. A similar analysis was carried out by Johnson (2018) for PT1. Under non-pumping conditions and outside the low flow period, HS1 (the most upstream) consistently had the highest discharge, followed by HS2, then HS3, and with similar values at HS4 and HS5. The reduction in streamflow from HS1 to HS5 suggests that Bertrand Creek is losing under natural conditions from upstream to downstream through the site. The lower magnitude decrease in streamflow from HS4 to HS5 suggests that there is little to no groundwater contribution (or indeed loss to groundwater) along this reach. Vertical hydraulic gradients at each piezometer pair location were complex both prior to pumping and during pumping. Overall, the general pattern under non-pumping conditions prior to PT2 was upward gradients upstream of the center line, mostly upward across the center line, and downward downstream of the center line. This suggests groundwater was contributing to streamflow in the upstream / center areas, and that the stream is losing downstream of the center line. The results are somewhat inconsistent with those reported by Johnson (2018) prior to PT1. However, the vertical gradients are influenced by streamflow conditions as well as the water table height in the aquifer, so it is unsurprising that the vertical gradients in the streambed were both temporally and spatially variable between May and October.

Immediately prior to PT2, streamflow was declining, which made it difficult to determine whether any streamflow depletion was occurring during pumping. The water levels in all of the individual instream piezometers immediately dropped when pumping began. All piezometers recorded drawdown until approximately 24 hours into the pumping test when maximum drawdown was attained. Thereafter, until pumping ended, the magnitude of drawdown reduced and in fact became negative (water levels in the piezometers were higher than before pumping commenced). Overall, during the pumping test, most piezometers pairs had downward flows. Streambed temperatures also differed noticeably pre-pumping, during pumping, and during recovery. The streambed temperatures had a wider range during the pumping test, compared to non-pumping conditions, and during recovery the lag between the temperatures all but disappeared.

Different approaches were used to estimate streamflow depletion including 1) using fluxes across the streambed based on the measured gradients in the nested instream piezometers, 2) using measured streamflow, 3) using a streamflow analytical model, and 4) using a numerical groundwater flow model to simulate PT2. The variability in gaining or losing conditions along the stream made it difficult to characterize streamflow depletion with absolute certainty. Over the 72 hours of pumping during PT2, streamflow depletion estimated from the vertical hydraulic gradients was 1510 m^3. An estimate of actual streamflow depletion of 500 m^3 was made using the rate of decline of streamflow over the last 14.25 hours of the test. While this value cannot simply be extrapolated to 72 hours, it was likely higher than 500 m^3. The Hunt (1999) model estimated streamflow depletion to be approximately 1460 m^3 over

the 72 hours, similar to the value estimated from the vertical hydraulic gradients (1510 m^3). A numerical groundwater flow model of the PT2 estimated streamflow depletion at 1576 m^3 over that last 37 hours of the pumping simulation. Prior to 37 hours, the stream continued to be gaining, with a switchover from gaining to losing occurring at 37 hours.

Overall, Phase 2 of the study was highly successful. Continuing research at the site in Phase 3 involves a hydroecological component to develop a more comprehensive understanding of the linkages between instream flow conditions (streamflow, groundwater exchanges, streambed temperature, streambed morphology, water chemistry) and aquatic communities (benthic invertebrates and possibly fish). A more in-depth analysis of the datasets acquired during Phase 2 under summer background (non-pumping) conditions alongside additional data collected in summer 2020 will be carried out.

Finally, to further explore and quantify exchanges between the aquifer and Bertrand Creek at a regional scale, a numerical groundwater flow model of Bertrand Creek Watershed has been developed and will be described in a forthcoming report.

CONTENTS

FIGURES

TABLES

ACRONYMS AND NOMENCLATURE

BTOC	Below the top of casing
ccf2	Cross-correlation function in R
D	Streambed piezometer
DEM	Digital elevation model
DFO	Department of Fisheries and Oceans Canada
ECCC	Environment and Climate Change Canada
gpm	Gallons per minute
HS	Hydrometric station
HSU	Hydrostratigraphic unit
K	Hydraulic Conductivity
MW	Monitoring well
NAVFAC	Naval Facilities Engineering Command
PW	Pumping well
OW	Provincial observation well
PT1	Pumping test 1 – July 2018
PT2	Pumping test 2 – October 2018
R	R statistical software
RMSE	Root mean squared error
SFU	Simon Fraser University
S	Storativity
Ss	Specific storage
Sy	Specific yield
T	Transmissivity
TB	Tidbit temperature data logger
TOL	Township of Langley
USBR	United States Bureau of Reclamation
USGS	United States Geological Survey
WTN	Well tag number

1. BACKGROUND

Groundwater is vital for sustaining community economic development and social well-being (e.g., industrial use, agricultural use and municipal and rural uses). Groundwater abstraction, however, can have detrimental impacts on streamflow in some aquifer-stream systems. Many streams are in direct hydraulic connection with groundwater and demonstrate a direct correlation between streamflow and groundwater level. However, in most studies of hydrologic systems, each system component (groundwater, surface water) is analyzed and/or modeled individually, treating the other interconnected component as a source or sink. In reality, these components are intricately linked and must be considered simultaneously. Therefore, we need a better understanding of the basic principles of groundwater and surface water interaction. Specifically, knowledge of the hydraulic connectivity between aquifers and streams is essential for effective integrated management of water resources.

The overall purpose of Phase 1 of this study, conducted from 2015 to 2017, was to build an understanding of the interaction between groundwater and surface water (with a focus on designated sensitive streams or streams with water allocation restrictions), and to identify streams that might be similarly impacted by and/or vulnerable to groundwater abstraction.

Phase 1 of the study consisted of a targeted field study in Langley, B.C. (Union Creek at Steele Park) to determine the impacts of pumping on aquifer-stream interactions in an unconfined aquifer, including testing various analytical methods for quantifying streamflow depletion from groundwater pumping. A final report entitled "Assessment of Hydraulic Connectivity Related to Groundwater Extraction on Selected Sensitive Steams: Phase 1 Field Investigation" (Hall et al. 2017) provides guidance on these various approaches and provides recommendations for further work that will lead to better tools to support science-based allocation decision making. Also, as part of Phase 1, a regional stream vulnerability assessment was carried out to determine the vulnerability of other similar types of stream-aquifer systems in the Lower Fraser Valley. A final report entitled "Assessment of Hydraulic Connectivity Related to Groundwater Extraction on Selected Sensitive Streams: Stream Vulnerability Mapping" (Middleton and Allen 2017) describes the results of a Level 1 Vulnerability Assessment for 53 aquifer-stream systems in the Lower Fraser Valley, as well as the results of a Level II Vulnerability Assessment for 10 aquifer-stream systems within the Lower Fraser Valley.

1.1 Key Findings from the Phase 1 Field Investigation

Phase 1 of this study yielded valuable data and provided critical knowledge surrounding how to conduct a field study to assess hydraulic connectivity. Following Phase 1, the study team identified several improvements to data collection that would achieve even better success in future studies, both at Steele Park and elsewhere:

1. Monitoring stream stage and groundwater levels at the site for at least one full year prior to and following the pumping test. This will allow baseline conditions to be firmly understood before stressing the aquifer.
2. Measuring streamflow periodically throughout the year to construct a stream rating curve.
3. Investigating the feasibility of installing weirs during low flow conditions.
4. Measuring streamflow both upgradient and downgradient, outside the zone of influence of pumping, and at consistent times.
5. Measuring streamflow before pumping begins and continuing to measure streamflow for a sufficiently long period after the pumping test ends to re-establish baseline conditions.
6. Carrying out a pumping test during mid- to late-summer, during a period of limited rainfall.

7. Pumping the aquifer at a slightly higher rate, if possible. This could be accomplished by setting the pump depth lower in the well at Steele Park.
8. Obtaining multiple samples of streambed sediments and carry out grain size analysis and/or carry out pneumatic slug testing to estimate streambed hydraulic conductivity. The streambed thickness should also be measured at different locations. Together, hydraulic conductivity and streambed thickness will better constrain the leakance parameter in the streamflow depletion models that include impedance.

1.2 Purpose and Objectives of Study

The overall goal of this study is to build an understanding of the interaction between groundwater and sensitive streams for the purpose of identifying streams that are more vulnerable to groundwater abstraction. While the original intent of this study was to undertake a comparison of hydraulic connectivity in an unconfined (i.e. Union Creek at Steele Park) and a confined aquifer (provisionally identified as West Creek in Langley, B.C.), the study team determined that Phase 2 should focus on an unconfined aquifer at a different site, because unconfined aquifers are in principle more strongly hydraulically connected to surface water, and as such, are a more critical target for investigation.

The objectives of Phase 2 included:

1. Estimating the hydraulic conductivity (K) of the aquifer and streambed sediments using grain size analysis and slug testing.
2. Estimating the transmissivity (T), hydraulic conductivity and specific yield (Sy) of the aquifer from pumping test data.
3. Characterizing the hydraulic connectivity between the stream and the aquifer using field measurements of water levels, streamflow and streambed temperature prior to and during pumping.
4. Based on field data, quantifying streamflow depletion during pumping, and then evaluating against an analytical streamflow depletion model and a numerical groundwater flow model.

These objectives were met through a field investigation that spanned from May 2018 to October 2018, which partially culminated in a BSc Honours thesis (Johnson 2018). Johnson was supervised by Diana Allen in the Department of Earth Sciences at Simon Fraser University (SFU). Andrew Garnet (former BSc student at SFU) developed the preliminary numerical groundwater flow model, and Kira Howe (former BSc student at SFU) assisted with the analysis of the streambed temperature data.

This report summarizes Phase 2 of the study.

2. THE STUDY SITE

2.1 Field Site Selection

Field site selection was challenging. The original plan was to select a field site underlain by a confined aquifer, so as to investigate the potential hydraulic connection in a contrasting setting to that used in Phase 1 (Hall et al. 2017). Provisionally, the team identified West Creek, a designated sensitive stream, situated to the north of Highway 1 in the Township of Langley (TOL), B.C.; however, access for drilling proved too poor at several sites visited. The team then reconsidered options and identified Otter Park, situated south of Steele Park (the site used for Phase 1) (Figure 1). Bertrand Creek passes through the park and is easily accessible for deployment of instream instrumentation, and the drilling site had adequate overhead clearance. In contrast to Steele Park, which provided access to only a short reach of

Union Creek with several obstructions that impacted flows (e.g. upstream by bramble and downstream by a culvert), Bertrand Creek has a longer and straighter reach through the park. Thus, Otter Park was considered ideally suited for this study.

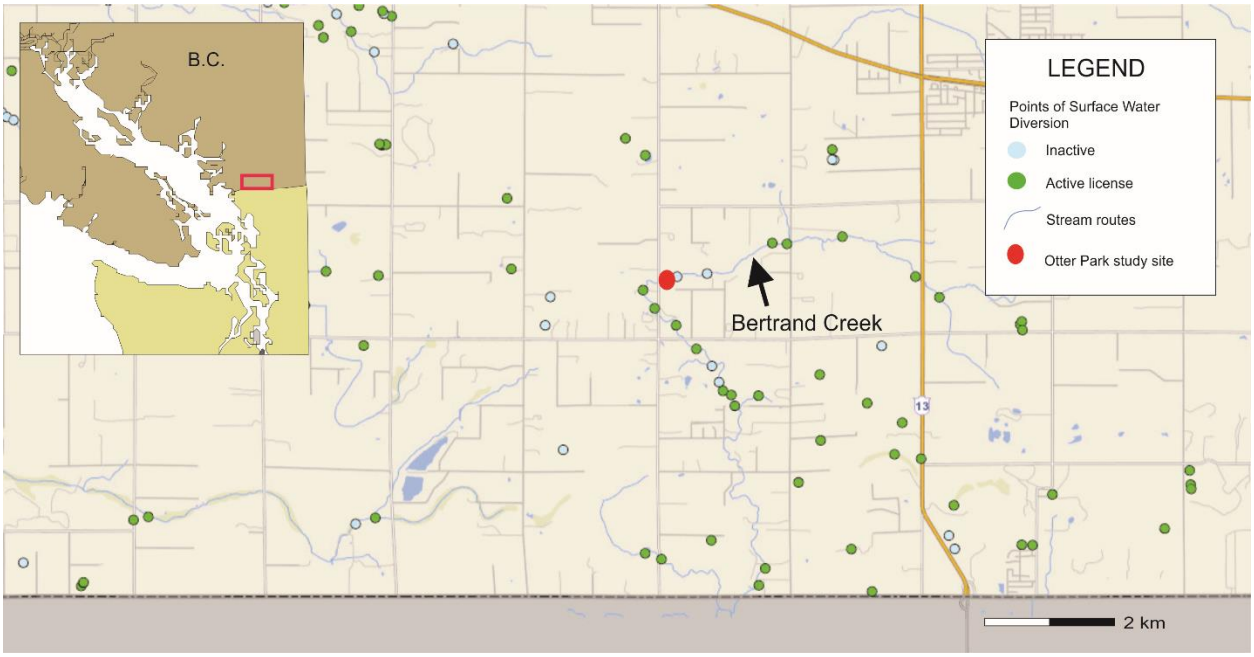

Figure 1: Location of Bertrand Creek and the Otter Park study site in the Township of Langley, BC. Also shown are points of surface water diversion. The inset map shows the approximate location of the map area in the Lower Fraser Valley of B.C. The Canada-USA border is shown at the bottom.

2.2 Regional Setting

2.2.1 Climate and Hydrology

The Fraser Valley is located in a temperate rainforest climate region, characterized by hot summers, mild winters, and rain throughout the fall, winter and spring months. Climate normals within the TOL are not available; therefore, climate normals were obtained for the period spanning 1981-2010 from the Environment and Climate Change Canada (ECCC) climate station at Abbotsford International Airport (Climate ID: 110030). This climate station is closest in proximity to Otter Park and is ~13 km east of the site (Figure 2). The climate normals (Figure 3) indicate that precipitation is highest from October to March, with November having the highest precipitation average of 248 mm and the lowest average precipitation in July at 43 mm. The annual average rainfall is 1538 mm. Temperatures are highest in the summer months when precipitation is lowest. August is the hottest month of the year with average daily maximum temperatures of 24°C, and December is the coldest, with maximum daily temperatures of 6°C.

Otter Park is located within the Bertrand Creek Watershed (Figure 2), which covers 113 km^2 over both Canada and the USA (Bertrand Creek Enhancement Society (BCES) 2008). The topography is relatively flat at ~80 masl but is locally hummocky due to previous glaciations (Starzyk 2012). The Bertrand Creek Watershed is home to several species of fish including Coho salmon, the Nooksack Dace, and the Salish Sucker, of which the latter two are endangered (BCES 2008; Pearson 2004).

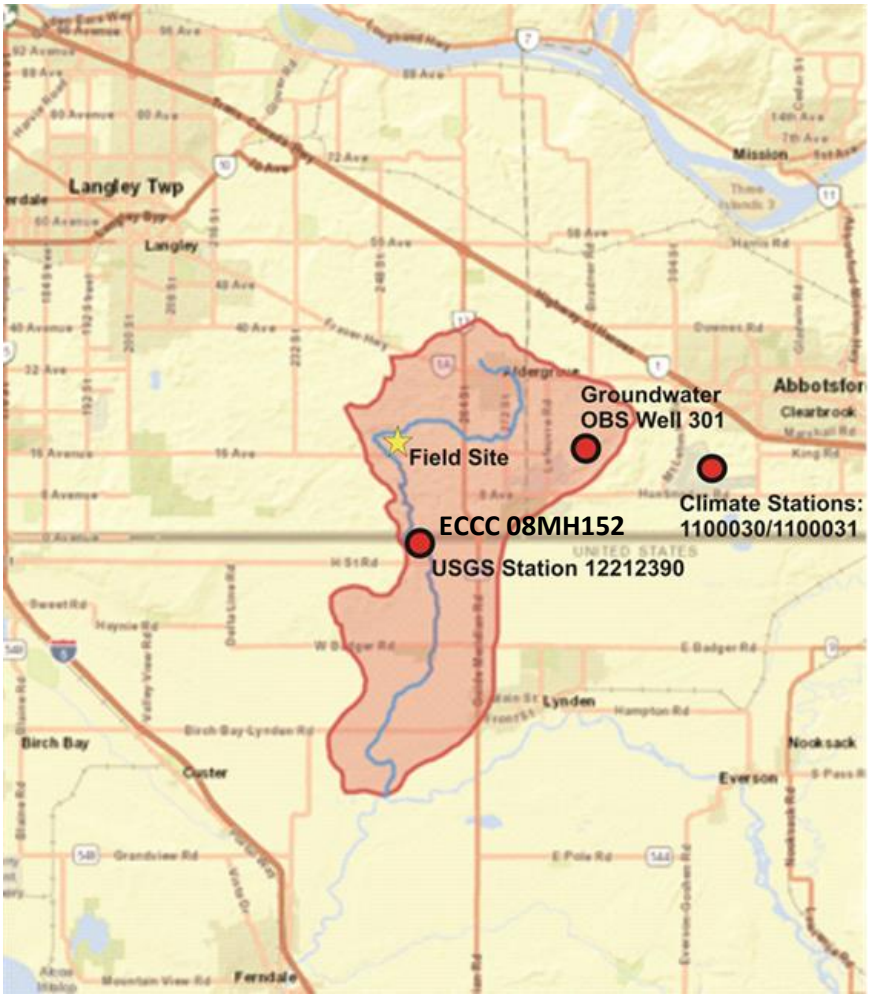

Figure 2: Location of the Otter Park field site within the Bertrand Creek watershed. The hydrometric station at the international border (USGS Station 12212390), the ECCC climate stations at the Abbotsford International Airport (1100030/1100031), and B.C. Provincial Observation Well 301 are shown.

ECCC operates a hydrometric station on Bertrand Creek (08MH152), which is located along the Canada-USA border approximately 5 km south of the field site. The United States Geological Survey (USGS) also operates a hydrometric station on Bertrand Creek at the Canada-USA border (station 12212390 – Bertrand Creek at international border). The USGS station is used to represent the discharge in Bertrand Creek over the period 2007-2017 because it had the most recent and complete record.

Figure 4 shows that discharge in the creek follows the same pattern as precipitation throughout the seasons. Discharge is highest from November to April, which coincides with the months of highest precipitation. The discharge in the Bertrand Creek Watershed is flashy as it is heavily influenced by precipitation. Average monthly discharge is greatest in January and lowest in August. Discharge rates are considerably lower in June and July, but still retain a moderately flashy discharge pattern. August through mid-October have minimal discharge that is less flashy.

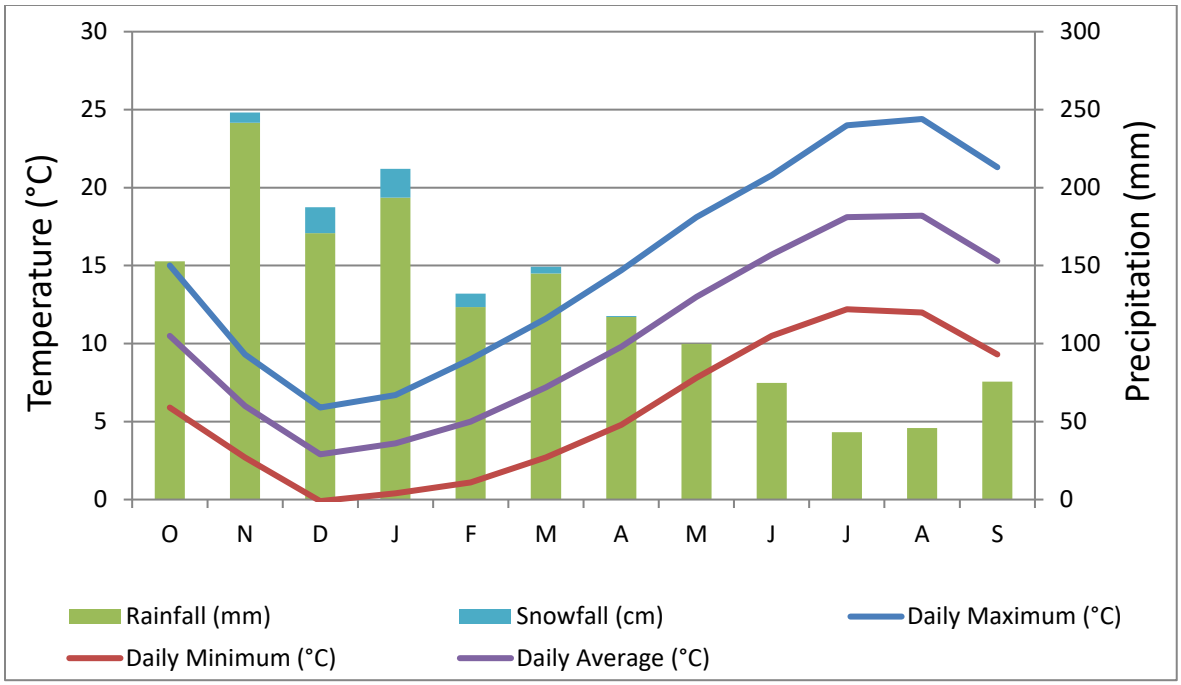

Figure 3: Climate normals from ECCC station 1100030 at Abbotsford International Airport from 1981-2010. Shown are the total monthly precipitation averages and the maximum, minimum, and average monthly temperatures in degrees Celsius.

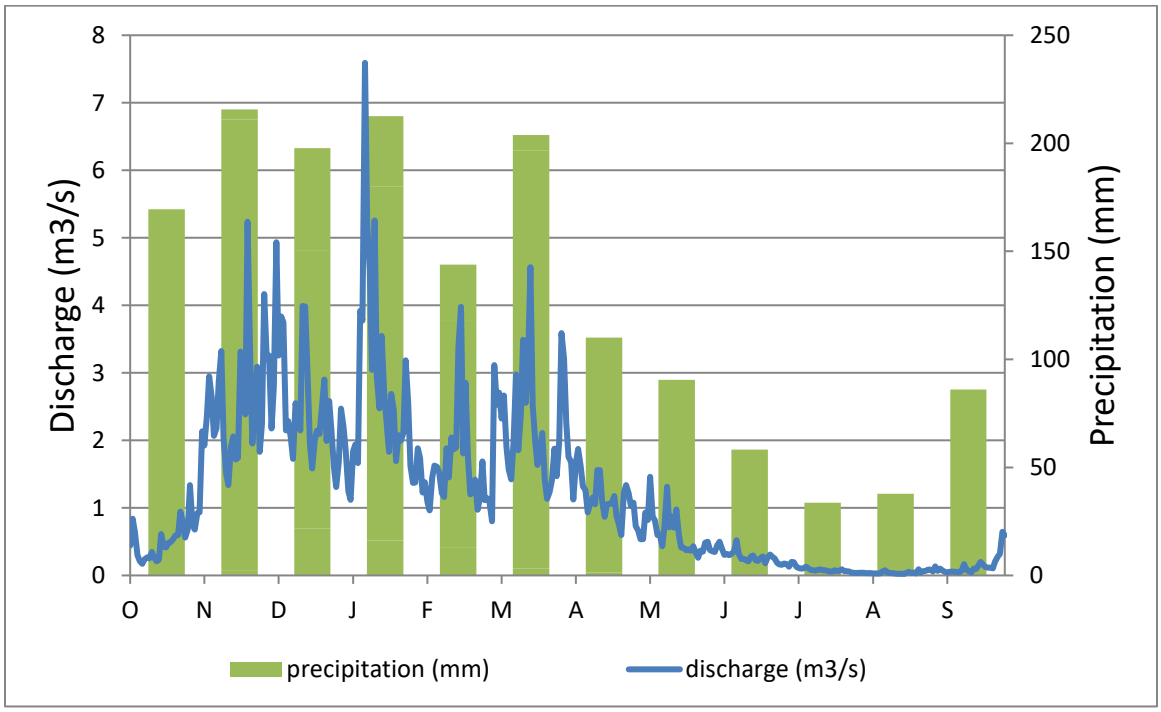

Figure 4: Hydrograph of Bertrand Creek at the Canada-USA border with daily average discharge values over the period 2007-2017 from the USGS station at the international border (station 12212390) along with total monthly precipitation averages from Environment Canada at the International Abbotsford Airport for the period of 2007-2017.

2.2.2 Regional Geology and Hydrogeology

The majority of surficial sediments in the Fraser Valley were deposited by glaciers or through glacial processes. These glacial sediments consist of till, ice-contact deposits and proglacial deltaic deposits (Armstrong 1981). Within Otter Park, Bertrand Creek flows across the Late Wisconsin aged Fort Langley Formation, which consists of interbedded, marine, glaciomarine, and glacial drift sediments (Armstrong 1981). The interbedding of the fine sand, silt and clayey silt from the marine sediments with the coarser sands and gravels from the glacial deposits led to the formation of confined and unconfined aquifers. Other surficial sediments surrounding Otter Park include the Sumas Drift, also of Late Wisconsin age, which is comprised of till, glaciaofluvial, glaciolacustrine, and ice-contact deposits (Armstrong 1981).

The stratigraphy in areas surrounding Otter Park is highly variable based on a review of well logs from BC GWELLS database. Many of the wells surrounding Otter Park contain a blue clay that commonly occurs interstratified with sands and gravel, but non-blue clays interstratified with sands and gravels are also common. Wells without clay (or minimal amounts of clay) are present, but uncommon. The variety of sediments seen in the well logs is consistent with the sediment descriptions of Armstrong (1981). Many of the wells peripheral to the site have an upper confining clay layer, which is not present within Otter Park itself, as described in Section 3.5.

Three aquifers have been mapped in the vicinity of Otter Park: the Abbotsford-Sumas Aquifer (#15), the Langley Upland Aquifer (#52) and the West of Aldergrove Aquifer (#33) (Figure 5). Both the Abbotsford-Sumas Aquifer and the West of Aldergrove Aquifer occur within the field site, and the Langley Upland Aquifer is directly adjacent to the park. The Abbotsford-Sumas Aquifer is the only unconfined aquifer of the three and is the focus of this field study. It is a sand and gravel aquifer that extends across Abbotsford and into Langley Township as well as south into the United States and is classified as having high productivity and high vulnerability.

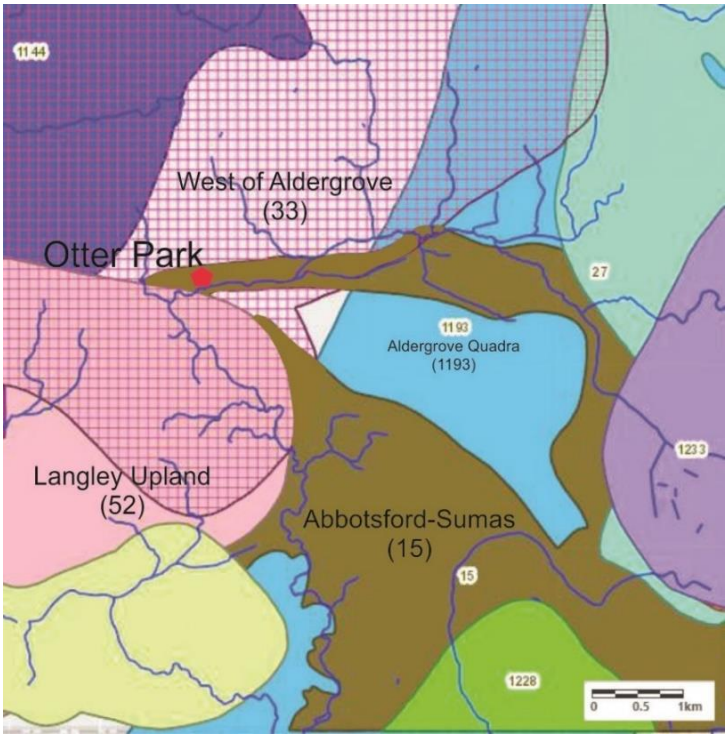

Figure 5: The three aquifers in the vicinity of the field site: Abbotsford-Sumas (unconfined), West of Aldergrove (confined) and Langley Upland (confined). The field site is indicated with a star. (source: iMapBC).

Historical groundwater levels for the region were obtained from the BC Provincial Observation Well OW301 (Figure 6). The well is located ~7 km east of Otter Park (see Figure 2) and is screened in Abbotsford-Sumas Aquifer. Groundwater elevation (in metres above sea level; masl) is shown from October 2007 to September 2017. The 10-year period shows seasonal variability. The lowest groundwater levels typically occur August through October and the highest levels typically occur in December through May. Throughout the year, the groundwater levels vary by approximately 2.3 m between the highest and lowest levels. There is no visible long term increasing or decreasing trend.

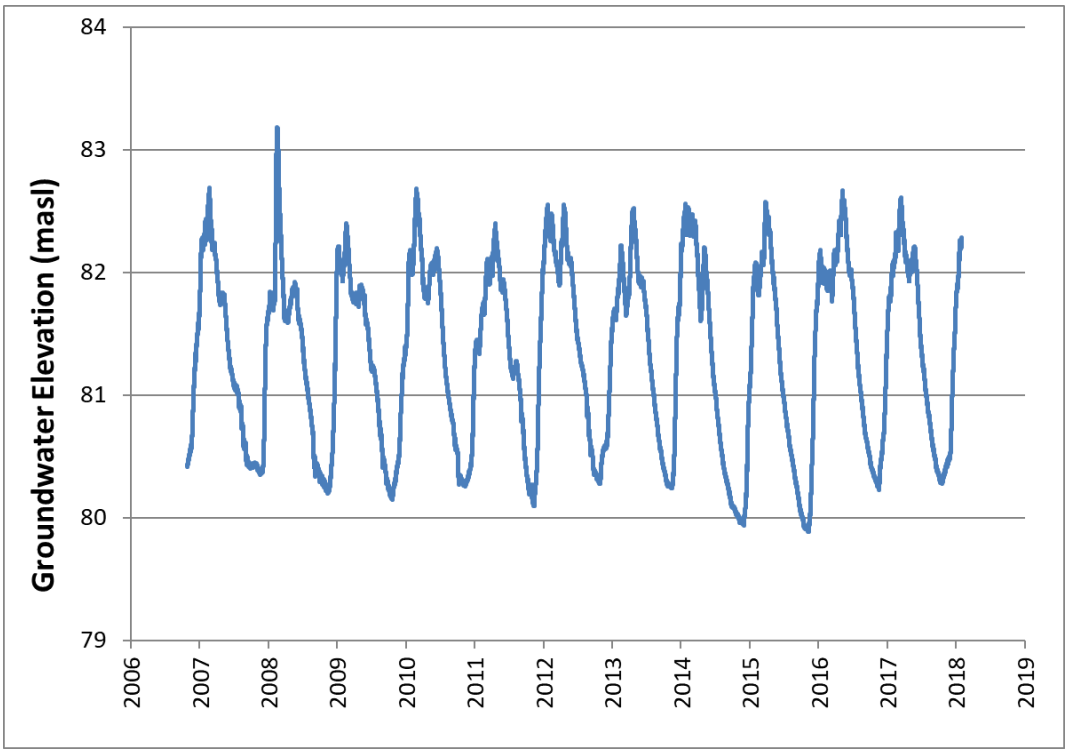

Figure 6: Groundwater elevation in BC Observation Well OW301 from October 1, 2007 until December 31, 2018.

3. FIELD INVESTIGATION

3.1 Site Description

Otter Park is a relatively small (<0.5 km^2) forested park that is primarily used as a day use area for walking and horseback riding. The area surrounding Otter Park is mostly rural with some small-scale agricultural use (e.g., hobby farms). Otter Park is relatively flat at ~80 masl with approximately 3 m of relief, with most of the change in elevation occurring as a drop from the main park area down to the creek itself. Bertrand Creek flows from east to west through the park, diverts south after exiting the park and flows towards the border into the US (Figure 7).

The stream width varies throughout the site spatially and temporally. The stream is widest as it first enters the park from the east and becomes constricted by vegetation and gravel deposits as it flows through the park, snaking through the rest of the park before exiting the park through a culvert at 248th street. In May 2018, the creek was ~10 m in width at its widest upstream section. The residents visiting the park have noted that the stream has more frequently run dry in the last several years. In 2018, the stream was dry by August 7, leaving only a few small isolated pools.

There are two manholes at Otter Park along 248th Street (Figure 7). The first is at the northwest corner of the park and the second is further south before the stream. Both manholes discharge through a storm sewer outlet back into Bertrand Creek before the creek flows through the culvert and exits the park.

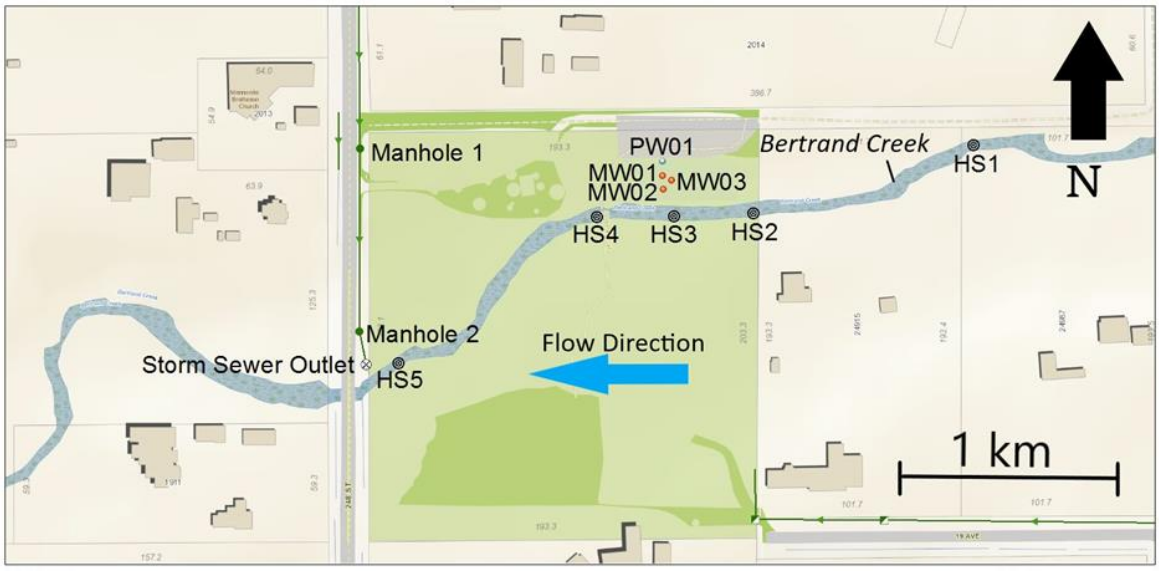

Figure 7: Otter Park field site showing the locations of the pumping well (PW01) and the monitoring wells (MW01, MW02, and MW03) along with the site hydrometric stations (HS1, HS2, HS3, HS4, and HS5).

3.2 Wells

One pumping well (PW01, Well Tag Number: 114933, in GWELLS) and three monitoring wells (MW01, MW02, MW03) were installed at Otter Park (Figure 7). The wells are located along the dirt road within the park on the terrace north of the creek in the northeast corner of the site. All three monitoring wells were drilled using sonic drilling by Blue Max Drilling, and the pumping well was drilled using a dual air rotary drill by Field Drilling. PW01 was drilled on March 8, 2018 to a depth of 75 ft (22.86 m) and is screened from 55-65 ft (16.8-19.8 m). MW01 and MW02 were drilled on March 20, 2018 and are both screened from 55-60 ft (16.8-18.3 m). MW03 was drilled on March 21, 2018 and is screened from 90-95 ft (27.4-29.0 m) (Appendix A. Borehole Logs). Each well (pumping and monitoring) has a top of casing elevation of 30 inches (76.2 cm) above the ground surface. PW01, MW01, and MW02 are positioned in a line perpendicular to Bertrand Creek, and MW03 is positioned east of the other wells and between MW01 and MW02 forming a triangle (Figure 7). PW01 is farthest from Bertrand Creek and MW02 is the closest. MW01 is 7 m from PW01, MW02 is 14 m from PW01, and MW03 is 10.6 m from PW01. Figure 14 (shown later) gives a cross-sectional view of the wells in relation to the stream. Figure A3 in Appendix A shows a satellite image of the site, along with nearby water wells relative to PW01.

Each well was equipped with a Solinst Levelogger (pressure transducer) set to record every 15 minutes under background (non-pumping) conditions. Logging intervals were adjusted during each of the two pumping tests conducted at the site (see Section 4.3). A dedicated barologger was installed in the pumping well to record atmospheric pressure variations. An additional barologger was installed in a tree near the wells.

3.3 Streamflow

Five hydrometric stations (HS1, HS2, HS3, HS4, and HS5) were installed at the field site on May 11 and 12, 2018 (Figure 7). HS3 is positioned in line with PW01, MW01, and MW02. HS1 and HS2 are located upstream of HS3; HS2 is 40 m upstream of HS3 and is located on Otter Park's eastern boundary. HS1, the furthest upstream, is ~150 m upstream of HS3, and approximately 100 m outside of the park's boundary. HS4 and HS5 are both downstream of HS3. HS4 is approximately 40 m downstream of HS3, and HS5 is approximately 175 m downstream of HS3 along the western park boundary. HS1 and HS5 were positioned with the intention of being outside the zone of influence of PW01 during a pumping test. The hydrometric stations are situated on the southern edge of the creek bed, and were equipped with HOBO pressure transducer loggers, programmed to record water level every 15 minutes. Several HOBO barologgers were available for barometric compensation. Ultimately, the data from a single barologger (Baro3) were used, but a portion of the data had to be compensated using a redundant barologger (Baro1) due to missing Baro3 data.

Streamflow measurements were made along cross-sections approximately 0.5 m upstream of each hydrometric station (Figure 8). Two flow meters were used, the FlowTracker and the FlowTracker2 by SonTek. Flow measurements were made every 0.2 to 0.5 m across the stream width. Streamflow was measured on approximately 11 occasions at each hydrometric station between May and September. The first set of measurements (~4 at each station) spanned late May to June. The second set was in early July immediately prior to pumping, during pumping and during recovery for pumping test 1 (PT1). The third set was prior to, during and following PT2, on September 20, October 12 and October 15, respectively. Pumping test 2 (PT2) started on October 11 and ended on October 14.

Figure 8: Streamflow measurements being taken at HS3 in Bertrand Creek on May 11, 2018.

The streamflow measurements were used to construct specific rating curves for each cross- section so that streamflow could be estimated from the continuous stage measurements. Construction of the rating curves proved very challenging. Specifically, during the late summer there was some beaver activity in Bertrand Creek, and the amount of canary grass increased throughout the summer. Several stream rating curves were modeled using an R script (Jon Goetz, personal communication) as well as using Excel (curve fitting functions). The "best" rating curves (using R) were ultimately used for calculating streamflow at each hydrometric station, but the discharge results are very poor during the late summer and there is very low confidence in the streamflow during this low flow period (Figure 9). The visible flow in Bertrand Creek at the site was very low in late July to early September, so it is not surprising that the calculated discharge is extremely low. Local residents have observed that Bertrand Creek had been running dry during the summer. It is noted that measurements from times deemed 'high flow' were also excluded from the ratings curves and for this reason the rating curves are also not appropriate for calculating discharge at higher flow rates.

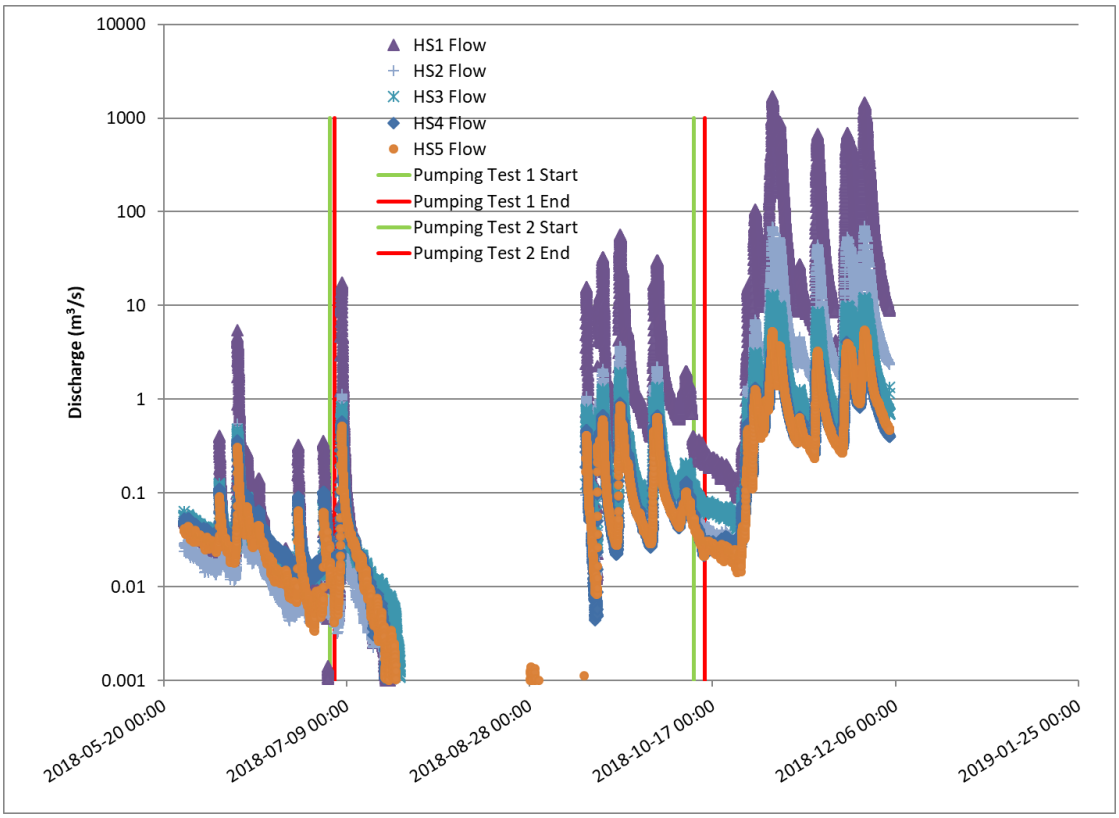

Figure 9: Stream discharge at the five hydrometric stations in Bertrand Creek from May to December 2018. Streamflow was calculated using the "best" rating curve for each hydrometric station. Beaver activity and canary grass growth in the stream over the summer significantly affected the rating curves for the hydrometric stations (HS). The start and end times for PT1 and PT2 are shown as red and green vertical lines.

3.4 Instream Piezometers and Temperature Loggers

A network of instream piezometers was installed in Bertrand Creek on May 11 and 12, 2018. The piezometers were assembled from 32 cm long sections of 1.905 cm diameter stainless steel pipe connected using a pipe coupler (Figure 10a). At one end of each piezo, a drive point with a screen assembly was attached. The screen section consisted of 10 holes evenly spaced along 6 inches of pipe with wire screening backing the holes (Figure 10b).

Figure 10: a) Assembled links of the piezometers before installation; b) the screened interval of the piezometers.

The piezometers were installed as nested pairs in the creek. Each piezometer nest had a longer and shorter partner with a difference in length of one pipe section. The longer piezometers had 6 sections and were 2.046 m long, the shorter piezometers were 5 sections and 1.725 m long. They were installed to have their tops at an approximately equal level, resulting in a difference of one pipe section (32 cm) between their screened intervals (as measured at the mid-point of each screen).

Ten pairs of piezometers were installed in Bertrand Creek and one single piezometer was installed on the creek bank (Figure 11). Five pairs were installed across the creek in line with PW01, MW01, and MW02. Piezometer pairs D7/D8, D9/D10, D37/D38, were installed evenly across the width of the stream. D7/D8 and D37/D38 were installed 2.68 m from the south and north bank, respectively, and D9/D10 was installed halfway between (i.e. 5.35 m from each bank).

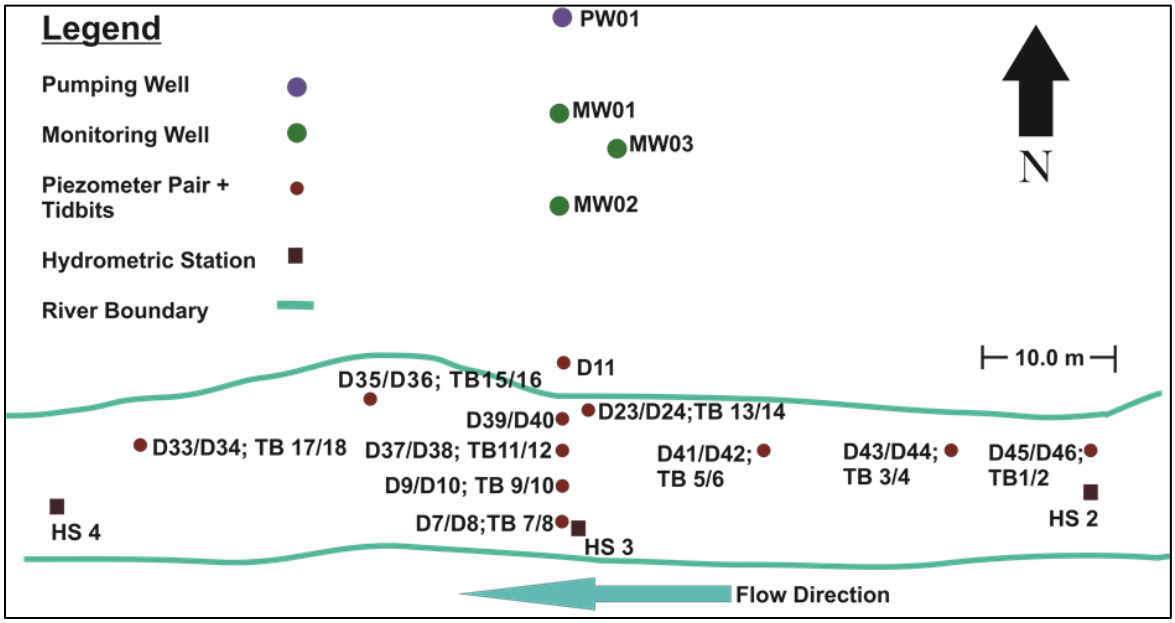

Figure 11: Instream piezometers (DX/DX) and temperature TidBit loggers (TB) installed on May 11-12, 2018.

Two pairs of piezometers were installed at the same location, 30 cm from the edge of the northern bank (D39/D40 and D23/D24). The additional pair, D23/D24, was installed to test a different water level logger (as described below). This pair was of a narrower diameter. The same piezometer tip end was used. The single piezometer (D11) was installed on the stream bank, in line with PW01, MW01, and MW02 to monitor groundwater level.

Five piezometer pairs were installed along the length of the stream; three pairs upstream (D45/D46, D43/D44 and D41/D42) and two pairs downstream (D33/D34 and D35/D36) relative to D39/D40. The three upstream are spaced 14.7 m apart, and D35/D36 and D33/D34 are 15 m and 35 m downstream, respectively. Figure 12 shows a photograph of a section of the installed instream piezometer network that spans across Bertrand Creek.

Figure 12: The piezometers and PVC tubes housing the background TidBits that were installed on May 10, 2018 in Bertrand Creek.

Solinist Leveloggers were installed in the larger diameter piezometers. Rather than suspending them, the loggers were lowered to rest at the bottom of the piezometer. This allowed them to be reinstalled at the same depth after data were downloaded (i.e., after slug tests, or between pumping/recovery periods). The loggers were programmed to record the pressure of the overlying water column every 15 minutes. During the pumping test, a different logging interval was used as described in Section 4.3. Three barologgers were also installed at the site to record atmospheric pressure variations at the same interval (one was paired with the hydrometric stations). This water level was used to determine the hydraulic head in each piezometer using the surveyed elevation of the top of the piezometer. VanEssen Micro-divers were also installed into the three small diameter piezometers (D11, D23/D24) in the streambank and set to record at the same interval.

Streambed temperature logging was done using two separate networks: a background network and a pumping test network. The **background streambed temperature network** was installed on May 11 and 12 and loggers were retrieved on October 15, 2018. The logging interval was one hour. The Solinst TidBit v2 Temp Loggers were installed in pairs next to each piezometer pair, with the exception of D39/D40

and D23/D24 which shared a pair of TidBits because of their proximity and the likelihood of the creek running dry at that location. The TidBits were installed at two different depths, one at the streambed-water interface and the other 16 cm below the interface. To provide shielding from solar radiation, these temperature loggers were affixed (using zip ties) to the inside of a 4-inch diameter section of white PVC sewer pipe. The streambed was excavated by hand, the sewer pipe eased in, and then strapped to a piece of rebar to hold it in place.

The **pumping test network of streambed temperature loggers** was installed solely for the purpose of monitoring streambed temperature during the pumping tests. This second network was necessary because the logging interval in the background network was too long and if the loggers were removed to re-program them, it was unlikely that they could be returned to their exact depth. Therefore, two additional Tidbit loggers were affixed to the rebar slightly beneath the streambed-water interface (Figure 13). These loggers were set to record every 30 seconds. They were installed just prior to the first pumping test on July 4 and were retrieved on July 19, roughly two weeks after the first pumping test. These loggers were re-deployed at the same locations for the second pumping test. The loggers were finally removed on October 15, 2018.

Figure 13: TidBit temperature logger installed attached to the rebar on the outside of the PVC tubing for the pumping test. Background TidBits are installed inside the tube.

3.5 Overview of Site Hydrogeology

The Otter Park field site sits atop an unconfined aquifer, which is comprised mostly of coarse sands and gravel with very few fines (Appendix I, Borehole Logs). Three of the wells (PW01, MW01, and MW01) are completed within this aquifer (Figure 14). A deeper confining unit was intersected by monitoring well (MW03) from 33.5 to 36.6 m (110-120 ft) and consists of silt and clay. The confining unit is at least 6.01 m (20 ft) thick. Drilling ceased at 42.7 m (140 ft) and the confining unit was still present.

Bertrand Creek at Otter Park is ~5 m below the ground surface where the pumping and monitoring wells are located, and likely cuts through the unconfined aquifer. In addition, the static water levels in the wells were approximately 4 m below the top of casing (BTOC) on October 11, 2018, suggesting that the

water table sloped slightly away from Bertrand Creek (Figure 14). This suggests that the stream was losing at that time. However, Johnson (2018) measured slightly higher water levels in the wells in July 2018, suggesting a sloping water table towards Bertrand Creek and gaining conditions.

The coarse grain size of the aquifer sediments also indicates that the hydraulic conductivity is high. Therefore, it is likely that the aquifer-stream connectivity is high, meaning the stream will be sensitive to changes in groundwater levels and may experience streamflow depletion during pumping.

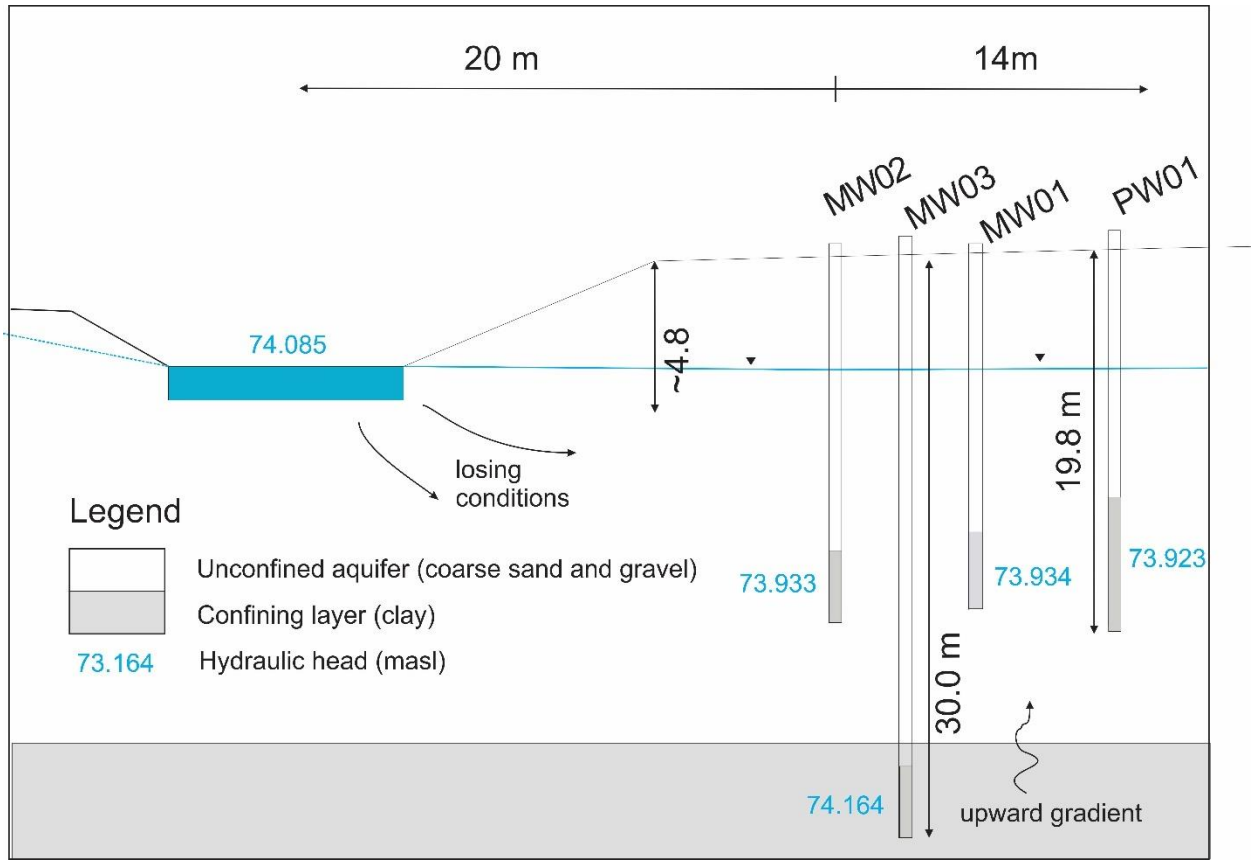

Figure 14: Cross-sectional view of the study site from the well network to Bertrand Creek (shown in blue on the left). Groundwater level is from measurements made on October 11, 2018 before the start of pumping test 2. Note that MW03 is offset from the cross-section but is included for conceptual purposes.

4. AQUIFER AND STREAMBED HYDRAULIC PROPERTIES

To characterize aquifer-stream connectivity, representative values of the hydraulic conductivity (K) of both the aquifer and the streambed sediments are needed. For this study, three approaches were used.

- Grain size analysis of aquifer materials and streambed sediment
- Slug testing of instream piezometers and wells
- Two pumping tests

This section summarizes the methodology and main results. Additional details can be found in Bryn Johnson's BSc Honours Thesis (Johnson, 2018), which is available upon request from Diana Allen.

4.1 Grain Size Analysis

4.1.1 Method

Fifteen samples were taken from the streambed between HS2 and HS4 (see Figure 11). Nine of the samples were taken adjacent to each piezometer pair (within 0.5 m) (these samples are identified by a D in the sample ID). The other six samples were taken between piezometer pairs lengthwise down the creek (these samples are identified by an A in the sample ID, where the numbers in the sample ID correspond to the piezometer pair upstream of it).

Shovels were used to dig ~30 cm deep holes in the streambed sediment and the samples were collected from the bottom of the holes. Using this sample collection method, some fines may have been lost. Additionally, cobbles and boulders were present in the streambed but were too large to collect using the sample collection method. Exclusion of the cobbles and boulders is not expected to influence the results because the finer grain sizes limit the permeability.

Core samples from drilling were collected from PW01 and MW03 were also analysed. Twelve samples were collected from PW01 every 5 ft (~1.5 m) between 15 ft and 70 ft (~4.6 m and 21.3 m). The core from MW03 was sampled when there was variation in the material. Ten samples were collected, but the two deepest samples that represent the confining unit were not analyzed for grain size as they were not representative of the aquifer (Appendix I. Borehole Logs).

The samples were mechanically sieved according to the lab procedures outlined in the 2002 ASTM standard D422 (American Society of Testing and Materials, 2014). Before sieving, the samples were oven dried at 105°C for at least 24 hours and until the weights had not changed by more than 1% for two hours. Any aggregates were broken apart and the samples were then run through a mechanical sieve shaker with 11 sieves for 15 minutes. The results were used to construct grain size distribution curves for analysis (see Appendix III A. Grain Size Distributions in Johnson, 2018).

The grain size distributions were analysed using six different analytical methods to estimate hydraulic conductivity. The Hazen method (Fetter 2001), NAVFAC (1974), Chapuis (2004), Beyer (1964), Sauerbrei (1932, as cited in Vukovic and Soro 1992) and the USBR (1978 as cited in Vukovic and Soro, 1992) (Table 1) were used to analyze the data (as recommended by Dr. Romain Chesnaux at l'Université du Québec à Chicoutimi). Each method has specific conditions that need to be met for the equation to be valid. These conditions are based on the sediment type, several effective grain size diameters, void ratio and porosity, and the coefficient of uniformity.

The NAVFAC, Chapuis, and Sauerbrei equations all include void ratio or porosity that could not be measured directly. To estimate values of hydraulic conductivity for these methods, upper and lower limits for void ratio or porosity (Chapuis, NAVFAC and Sauerbrei methods) and for the C parameter (Hazen method) were obtained through the literature for the different sediment types. Given the uncertainty in these parameters, the NAVFAC, Chapuis, Sauerbrei, and Hazen methods provide a range of estimated hydraulic conductivity. The Beyer and USBR equations only include known values, and therefore, a single estimate of hydraulic conductivity was calculated. The Hazen, Beyer, Chapuis and NAVFAC all use the effective grain size d_{10}, whereas Sauerbrei uses d_{17} and USBR uses d_{20} (see Appendix II in Johnson, 2018 for additional details on these parameters).

Table 1: Methods with the equations and conditions that were used to calculate the hydraulic conductivity from the grain size distribution of the streambed and aquifer samples.

Method	Empirical equation	Conditions
Hazen	$K\left(\frac{cm}{s}\right) = C(d_{10})^2$ with d_{10} in cm	1) loose and uniform sand 2) Cu≤5 3) 0.1mm≤d_{10}≤3mm
NAVFAC DM7	$K\left(\frac{cm}{s}\right) = 10^{1.291e-0.6435} * (d_{10})^{0.5504-0.2937e}$ with d_{10} in mm	1) Sand and mixtures of sand & gravel 2) 2≤Cu≤12 3) d_{10}/d_5 ≤1.4 4) 0.1mm ≤ d_{10} ≤ 2mm 5) 0.3 ≤ e ≤ 0.7
Chapuis	$K\left(\frac{cm}{s}\right) = 2.4622 * \frac{(d_{10})^2 * e^3}{(e+1)^{0.7825}}$ With d_{10} in mm	1) All natural soils without plasticity 2) 0.003mm ≤ d_{10} ≤ 3mm 3) 0.3 ≤ e ≤ 1
Beyer	$K\left(\frac{cm}{s}\right) = 0.45(d_{10})^2 * \log\left(\frac{500}{Cu}\right)$ with d_{10} in mm	1) Uniform to moderately uniform sand 2) 0.06 mm ≤ d_{10} ≤ 0.6 mm 3) 1 ≤ Cu ≤ 20
Sauerbrei	$K\left(\frac{cm}{s}\right) = \frac{2.436n^3(d_{17})^2}{(1-n)^2}$ With d_{17} in mm	1) Sand and silty sand 2) d_{17} ≤ 0.5mm
USBR	$K\left(\frac{cm}{s}\right) = 0.36(d_{20})^{2.3}$ With d_{20} in mm	1) medium size sand 2) Cu≤5
where: K = hydraulic conductivity C = Unitless empirical coefficient for different types of sand dn = The effective grain size parameter at the percent indicated by the subscript n Cu = the coefficient of uniformity (d60/d10) e = void ratio n = porosity; n=e/(1+e)		

4.1.2 Results for Streambed Sediments

The streambed sediment consists of rounded to subrounded pebble-sized clasts with sand and is poorly sorted. The sieve analysis showed little to no fines in the samples, although as noted above, some fines may have been lost during sample collection.

The estimates of K for each empirical method are listed in Table 2. The Hazen, Chapuis, NAVFAC, and Sauerbrei all had unknown parameters in their equations (e and C), therefore, for these methods the minimum and maximum values of hydraulic conductivity (K) are reported. Each analytical method has conditions that must be met (Table 1) if it is to be used for calculating the hydraulic conductivity. Therefore, following the grain size analysis, the applicability of each method was assessed by Johnson (2018). Because the porosity/void ratio is unknown and estimated from the literature, it was not used to determine whether a particular method was applicable to the sample.

Johnson (2018) determined that the NAVFAC method has no applicability to the streambed samples. All the streambed samples met the sand or sand + gravel condition, and all fell within the accepted range for d_{10}. Only 6 of the 15 samples fell below the max Cu acceptable, and only two met the d_{10}/d_5 condition, but no samples met both these conditions. Four samples (D9/D10, A33/A34, D41/D42, and A41/A42) are within 10% of the accepted maximum Cu value; however, none of these are samples that also meet the d_{10}/d_5 condition. The d_{10}/d_5 values are clustered close to the threshold but still above it.

Based on the evaluation of the applicability of each method, Johnson (2018) determined that the Chapuis method is the most applicable of all the methods. All the samples are natural soils without plasticity and they all fall within the accepted effective grain size at d_{10}, and all but four samples are outside 10% of the accepted void ratio range. The Chapuis method also has the largest ranges for void ratio and effective grain size, which makes it more likely that samples will meet the conditions.

Table 2: Estimates of hydraulic conductivity (K) in m/s for the streambed sediments using the six empirical methods: Hazen, Chapuis, NAVFAC, Beyer, Sauerbrei, USBR. The Chapuis method yielded the best estimates.

Streambed Sample ID	Hazen m/s		Chapuis m/s		NAVFAC m/s		Beyer m/s	Sauerbrei m/s		USBR m/s
	K min	K max	K min	K max	K min	K max	K	K min	K max	K
D7/D8	5.78E-03	8.67E-03	**6.74E-04**	**3.98E-03**	4.56E-03	1.27E-02	5.37E-03	5.74E-04	5.56E-03	1.98E-02
D9/D10	5.78E-03	8.67E-03	**8.56E-04**	**6.27E-03**	4.99E-03	2.00E-02	5.16E-03	7.78E-04	9.92E-03	1.58E-02
A33/A34	5.78E-03	8.67E-03	**8.56E-04**	**6.27E-03**	4.99E-03	2.00E-02	5.16E-03	7.78E-04	9.92E-03	1.39E-02
D33/D34	5.78E-03	8.67E-03	**6.74E-04**	**3.98E-03**	4.56E-03	1.27E-02	5.29E-03	8.70E-04	8.42E-03	1.98E-02
D35/D36	3.38E-03	5.07E-03	**5.62E-04**	**4.12E-03**	4.40E-03	1.83E-02	2.72E-03	3.33E-04	4.24E-03	4.48E-03
D37/D38	3.92E-03	5.88E-03	**6.31E-04**	**4.63E-03**	4.56E-03	1.88E-02	3.40E-03	4.61E-04	5.87E-03	5.48E-03
A39/A40	2.42E-03	3.63E-03	**4.33E-04**	**3.17E-03**	4.07E-03	1.73E-02	2.06E-03	3.73E-04	4.76E-03	3.60E-03
D39/D40	5.78E-03	8.67E-03	**8.56E-04**	**6.27E-03**	4.99E-03	2.00E-02	4.82E-03	9.03E-04	1.15E-02	1.77E-02
D41/D42	4.50E-03	6.75E-03	**7.03E-04**	**5.16E-03**	4.71E-03	1.92E-02	4.04E-03	5.57E-04	7.11E-03	1.06E-02
A41/A42	4.50E-03	6.75E-03	**7.03E-04**	**5.16E-03**	4.71E-03	1.92E-02	4.04E-03	7.78E-04	9.92E-03	1.39E-02
A43/A44	7.22E-03	1.08E-02	**1.02E-03**	**7.46E-03**	5.25E-03	2.08E-02	6.81E-03	1.04E-03	1.32E-02	1.98E-02
D43/D44	6.48E-03	9.72E-03	**7.38E-04**	**4.36E-03**	4.68E-03	1.30E-02	6.19E-03	5.74E-04	5.56E-03	1.22E-02
A45/A46	2.42E-03	3.63E-03	**4.33E-04**	**3.17E-03**	4.07E-03	1.73E-02	2.09E-03	4.61E-04	5.87E-03	5.48E-03
D45/D46	3.92E-03	5.88E-03	**6.31E-04**	**4.63E-03**	4.56E-03	1.88E-02	3.62E-03	5.57E-04	7.11E-03	7.81E-03

4.1.3 Results for Aquifer Materials

The six empirical methods used to analyze the grain size data for the streambed sediments were also used to analyze the grain size data for the sediment cores extracted from PW01 and MW03. The aquifer sediments are more varied in their grain size compared to the streambed sediments, ranging from clay and silt to coarse sand and gravel. The sediments in each sample are mostly poorly sorted, but there are a few well sorted samples. The majority of samples are sands mixed with gravel.

The estimates of K for PW01 for each empirical method are listed in Table 3. The results show a range in K based on the range in C (Hazen method) and the range of void ratios estimated by the literature (Chapuis, NAVFAC and Sauerbrei methods). The Hazen method had a geomean of minimum K values of 1.06×10^{-3} m/s and geomean of maximum K values of 1.67×10^{-3} m/s. The other methods had larger ranges in K, from 1.54×10^{-4} m/s to 1.40×10^{-2} m/s.

The K results from the grain size analysis for MW03 are presented in Table 4. The Hazen method had a geomean of minimum K of 6.11×10^{-4} m/s and a geomean of maximum K of 9.98×10^{-04} m/s. The Chapuis, NAVFAC, and Sauerbrei methods all produced approximately an order of magnitude difference between the minimum and maximum estimates, from 1.20×10^{-4} to 1.38×10^{-2} m/s.

Similar to the streambed sediments, the applicability of each method was assessed by Johnson (2018). Ultimately, Johnson (2018) determined that the Chapuis method is the most applicable for the aquifer samples. All samples are natural soils without plasticity and fall within the accepted d_{10} range. As well, the estimates of void ratio were also all close to accepted values.

Table 3: Hydraulic conductivity for PW01 from the Hazen, Chapuis, NAVFAC, Beyer, Sauerbrei and USBR methods using the minimum and maximum void ratios or C values. The Chapuis method is considered to give the best estimates (Johnson, 2018).

	Hazen		Chapuis		NAVFAC		Beyer	Sauerbrei		USBR
Sample ID	m/s		m/s		m/s		m/s	m/s		m/s
PW01	K min	K max	K min	K max	K min	K max	K	K min	K max	K
15 ft	2.40E-04	4.80E-04	8.89E-05	6.52E-04	2.55E-03	1.24E-02	3.06E-04	5.02E-05	6.40E-04	4.38E-04
20 ft	8.00E-03	1.20E-02	8.70E-04	7.87E-03	4.92E-03	2.05E-02	7.85E-03	1.36E-03	2.27E-02	2.21E-02
25 ft	1.80E-02	2.70E-02	1.64E-03	5.58E-03	5.97E-03	1.06E-02	1.94E-02	1.80E-03	8.59E-03	4.17E-02
30 ft	1.28E-03	1.92E-03	2.07E-04	7.05E-04	3.19E-03	6.10E-03	9.07E-04	4.11E-04	1.97E-03	1.77E-02
35 ft	2.42E-03	3.63E-03	3.41E-04	3.09E-03	3.71E-03	1.68E-02	2.02E-03	5.74E-04	9.59E-03	1.77E-02
40 ft	9.80E-04	1.47E-03	1.68E-04	1.52E-03	2.99E-03	1.45E-02	7.39E-04	5.17E-05	8.63E-04	4.63E-04
45 ft	9.80E-04	1.47E-03	1.68E-04	1.52E-03	2.99E-03	1.45E-02	8.08E-04	9.55E-05	1.59E-03	1.53E-03
50 ft	7.20E-04	1.08E-03	1.32E-04	1.20E-03	2.78E-03	1.37E-02	5.66E-04	1.26E-04	2.11E-03	1.86E-03
55 ft	9.80E-04	1.47E-03	2.13E-04	1.56E-03	3.30E-03	1.49E-02	9.05E-04	9.75E-05	1.24E-03	8.00E-04
60 ft	9.80E-04	1.47E-03	1.68E-04	1.52E-03	2.99E-03	1.45E-02	8.28E-04	9.55E-05	1.59E-03	1.29E-03
65 ft	7.20E-04	1.08E-03	1.68E-04	1.23E-03	3.07E-03	1.42E-02	6.88E-04	7.01E-05	8.93E-04	5.17E-04
70 ft	4.00E-05	8.00E-05	3.97E-05	3.75E-04	2.13E-03	2.29E-02	1.00E-04	1.48E-05	2.61E-04	1.22E-02
Geomean	1.06E-03	1.67E-03	2.12E-04	1.55E-03	3.26E-03	1.40E-02	1.03E-03	1.54E-04	1.96E-03	3.18E-03

Table 4: Hydraulic conductivity for MW03 from the Hazen, Chapuis, NAVFAC, Beyer, Sauerbrei and USBR methods using the minimum and maximum void ratios or C values. The Chapuis method is considered to give the best estimates (Johnson, 2018).

	Hazen		Chapuis		NAVFAC		Beyer	Sauerbrei		USBR
Sample ID	m/s		m/s		m/s		m/s	m/s		m/s
PW03	K min	K max	K min	K max	K min	K max	K	K min	K max	K
5 ft	1.28E-03	1.92E-03	2.07E-04	1.22E-03	3.19E-03	9.60E-03	8.10E-04	4.11E-04	3.98E-03	1.39E-02
24 ft	1.62E-03	2.43E-03	2.49E-04	1.47E-03	3.37E-03	1.00E-02	1.27E-03	1.39E-04	1.35E-03	1.92E-03
45 ft	5.00E-04	7.50E-04	9.94E-05	9.24E-04	2.55E-03	1.34E-02	3.28E-04	4.65E-05	8.04E-04	4.63E-04
57 ft	1.28E-03	1.92E-03	2.07E-04	1.93E-03	3.19E-03	1.56E-02	8.80E-04	4.11E-04	7.11E-03	1.77E-02
61 ft	9.80E-04	1.47E-03	2.13E-04	1.56E-03	3.30E-03	1.49E-02	5.45E-04	1.89E-04	2.41E-03	1.86E-03
93 ft	4.00E-05	1.00E-04	3.97E-05	3.75E-04	2.13E-03	2.29E-02	1.04E-04	1.48E-05	2.61E-04	5.32E-05
Geomean	6.11E-04	9.98E-04	1.44E-04	1.11E-03	2.92E-03	1.38E-02	5.06E-04	1.20E-04	1.64E-03	1.67E-03

4.2 Slug Tests

4.2.1 Method

Slug tests were performed in all the instream piezometers and the three monitoring wells (not the pumping well) to obtain estimates of hydraulic conductivity of the streambed and aquifer sediments, respectively. Bail tests were also performed in the monitoring wells. Most of the tests were conducted on May 12, 2018, but repeat tests were done on July 19, 2018 on select piezometers and MW03 because the original data were poor.

The small diameter of the instream piezometers dictated a water injection method. Water (≤600 mL) was poured directly into the piezometer and the water level allowed to equilibrate back to its initial level. A minimum of three slug tests was carried out in each piezometer. Solinist Leveloggers were set to record every second during testing. Following testing, the loggers were reprogramed back to every 15 minutes to continue background monitoring.

A solid slug was used to conduct the tests in the monitoring wells rather than the water injection method as the well diameters could accommodate a slug. A minimum of three sets of slug and bail tests were carried out in the monitoring wells. HOBO data loggers were installed in the monitoring wells to record every second during the slug and bail tests.

All data were analyzed in AquiferTestPro 9.0 using the Hvorslev (1951) method and the Bouwer-Rice (1976) method. The Hvorslev method is generally used to analyze data from confined aquifers, but it is commonly applied to unconfined aquifers. The Bouwer-Rice method is commonly used for unconfined aquifers but can be used for confined aquifers. The assumptions of each method were met or assumed to be met at the field site (see Johnson, 2018). The datasets collected in each instream piezometer and monitoring well are provided in Johnson (2018; Appendix IV). On each graph, one test illustrates the line for which the slope was calculated. For the Bouwer-Rice method, only one dataset, considered the "best" one, was used for analysis. The "best" dataset had the greatest displacement in water level and/or had the least discrepancy between the initial water level and the recovered water level.

4.2.2 Results for Streambed Sediments

The streambed slug tests were separated into shallow and deep piezometers (Table 5). Using the Hvorslev method, the deep piezometers had a geomean K of 1.46×10^{-5} m/s with a standard deviation of 1.57×10^{-5} m/s, and the shallow piezometers had a geomean K of 3.41×10^{-5} m/s with a standard deviation of 3.30×10^{-5} m/s. Using the Bouwer-Rice method, the deep piezometers had a geomean K of 1.39×10^{-5} with a standard deviation of 1.17×10^{-5} m/s, and the shallow piezometers had a geomean K of 3.77×10^{-5} m/s with a standard deviation of 3.27×10^{-5} m/s.

Table 5: Hvorslev and Bouwer-Rice estimates of hydraulic conductivity (m/s) from slug tests by water injection into the streambed piezometers.

Hvorslev (m/s)				Bouwer-Rice (m/s)			
	Deep		Shallow		Deep		Shallow
D7	2.00E-05	**D8**	3.20E-05	**D7**	1.17E-05	**D8**	8.40E-05
D9	2.15E-05	**D10**	2.15E-05	**D9**	1.69E-05	**D10**	1.51E-05
D33	1.35E-06	**D34**	5.25E-07	**D33**	9.53E-07	**D34**	2.00E-05
D37	6.50E-06	**D38**	5.30E-06	**D37**	5.50E-06	**D38**	3.83E-06
D39	3.50E-06	**D40**	5.25E-05	**D39**	2.91E-05	**D40**	3.90E-05
		D42	1.00E-04			**D42**	8.75E-05
D43	4.00E-06	**D44**	1.05E-05	**D43**	3.83E-06	**D44**	8.63E-06
D45	4.50E-05	**D46**	5.06E-05	**D45**	2.91E-05	**D46**	4.37E-05
Geomean	1.46E-05		3.41E-05		1.39E-05		3.77E-05
Standard Deviation	1.57E-05		3.30E-05		1.17E-05		3.27E-05

Notably, the geomean K values for the deep piezometers are lower than for the shallow piezometers. Therefore, a student t-test was performed on both the Hvorslev and Bouwer-Rice results to determine if the mean K values of the deep and shallow piezometers are the same (at the 0.1 significance level). The t-test produced different conclusions for the two methods. For the Hvorslev method, the test indicated that there is no statistical difference in the K values between the two depths. For the Bouwer-Rice method, the test indicated that there was a difference in the K values between the two depths (although the t-value was only slightly larger than the critical t-value).

4.2.3 Results for Aquifer Material

All three monitoring wells were tested on May 12, but only satisfactory data were obtained for MW01 and MW02. MW03 was re-tested on July 19; however, a good dataset was still not obtained. During the slug test, the water level in MW03 immediately dropped to approximately half of the initial head displacement but had only partially recovered after one hour. When the slug was pulled out (bail test) the same anomaly occurred, and the water levels returned to approximately half of the 'static' water level and ceased recovering. The immediate change in water level after the slug and bail tests indicates the well is screened in a material that has high K, but the failure to return to the static water level suggests a possible skin effect[1], possibly because the piezometers were not developed. The data from MW01 showed a similar effect, but to a much smaller degree. This effect was not observed in MW02.

Table 6 shows the K values determined using each of the Hvorslev and Bouwer-Rice methods for monitoring wells MW01 and MW02. No estimate is available for MW03.

Table 6: Hvorslev and Bouwer-Rice results for hydraulic conductivity in the monitoring wells.

	Hvorslev (m/s)	Bouwer-Rice (m/s)
MW01	6.25E-04	6.00E-04
MW02	9.00E-04	4.97E-04

4.3 Pumping Tests

4.3.1 Method

The aquifer hydraulic properties of the aquifer (transmissivity T, storativity S, and specific yield Sy) were estimated from the analysis of pumping and recovery test data. Ultimately, two pumping / recovery tests were completed, and the data analyzed for each test.

A step test was first conducted on July 3, 2018 to determine an appropriate pumping rate for the constant rate discharge test. Four steps were planned. The first step test was carried out at a rate of 157 US gpm. Unfortunately, due to unforeseen complications with the pump, none of the steps was completed. Time constraints on the project dictated that the constant rate test must commence on July 4, 2018. Therefore, a pumping rate of 287 US gpm was selected for the first constant rate test based on an estimated drawdown of approximately 1 m in MW01. This drawdown was estimated with the Theis equation, using the geomean K for the aquifer of 7.6×10^{-4} m/s determined from the slug/bail tests in MW01 and MW02 (Table 6) and a specific storage (Ss) value of 1×10^{-4} m^{-1} based on literature values.

The step test data were downloaded prior to the pumping test and the loggers were reprogrammed using custom time intervals to maximize data resolution and most efficiently use the data logger

[1] A positive skin effect indicates extra flow resistance near the wellbore, leading to slower recovery during a slug test. See Butler (1998).

memory. Three different time intervals were used. The constant rate test was initially planned for 72 hours, starting at 10:15 a.m. on July 4. Loggers were set to record data every second for the beginning of the pumping test when the changes in drawdown would be greatest. The data loggers recorded data every second from 10:15 a.m. to 12:00 p.m. for a total of 1 hour and 45 minutes. The recording interval was then changed to record every minute from 12:00 p.m. to 5:00 p.m. for a total of 5 hours, and then every 15 minutes for the rest of the test when it was estimated that the aquifer would be approaching steady state. The constant rate test was not completed for the full 72 hours. During the constant rate test, the Department of Fisheries and Oceans Canada (DFO) expressed concerns about the effects of the test on the critical habitat of the Nooksack Dace and Salish Sucker within Bertrand Creek. Therefore, the test was terminated at 3:15 p.m. on July 5 to prevent potential impacts on the habitat. Thus, the first constant rate test was 29 hours in length and was followed immediately by a recovery test. Before the pump was shut off, the data were downloaded and the loggers reprogrammed for the recovery period. A varying time interval was also used for the recovery period. The recovery period logged data every second for 3 hours, every minute for the following 5 hours, and then 15 minutes until the end of the test. However, due to a programming error, the data loggers did not start logging at the same time. The loggers in MW03 and MW02 started logging at the first interval together, then MW01 had a 15-minute delay before it started logging, and PW01 started logging last and had a 25-minute delay. All of the data loggers were logging at 1-second intervals at the same time for 2 hours 25 minutes between 2:55 p.m. until 5:30 p.m.

The second constant rate test was initiated at 7:10 p.m. on October 11, 2018. The well was pumped at a constant rate of 324 US gpm. The pump was shut off at 7:15 p.m. on October 14, 2018. Therefore, the constant rate test duration was ~72 hours. Similar to the first constant rate test, a variable logging interval was used. The data loggers recorded data every second from 7:10 p.m. to 1:00 a.m. on October 12 for a total of 5 hours and 50 minutes. The recording interval was then changed to record every minute from 1:00 a.m. to 1:00 p.m. on October 12 for a total of 12 hours, and then every 5 minutes to the end of pumping on October 14 and through recovery until the loggers were retrieved and downloaded at 10:40 a.m. on October 15.

4.3.2 Results for Pumping Tests

The drawdown response in all wells during PT1 is shown in Figure 15. At the beginning of the constant rate test, the pumping rate was unfortunately adjusted by the pumping contractor, which resulted in the water table equilibrating with the new flow rate. This can be seen in the water levels of PW01, MW01, and MW02 at ~15 minutes (953 s) into the test. The change in water level is not seen in MW03, perhaps because its lower K buffered the change in flow rate. Drawdown in MW01 had the greatest response, which is expected as it is the closest in proximity to the pumping well. However, MW02 had more drawdown than MW03, despite MW03 being 3.5 m closer to the pumping well. This is consistent with MW03 being screened in a zone of lower K. While Johnson (2018) attempted to analyze the data to obtain estimates of the hydraulic properties of the aquifer, the dataset is so poor that it is no longer examined here.

Figure 16 shows the drawdown response in all wells during PT2. The dataset is much cleaner because the pumping contractor was directed not to adjust the pumping rate early in the test. Therefore, this dataset is used to estimate the hydraulic properties of the aquifer at Otter Park.

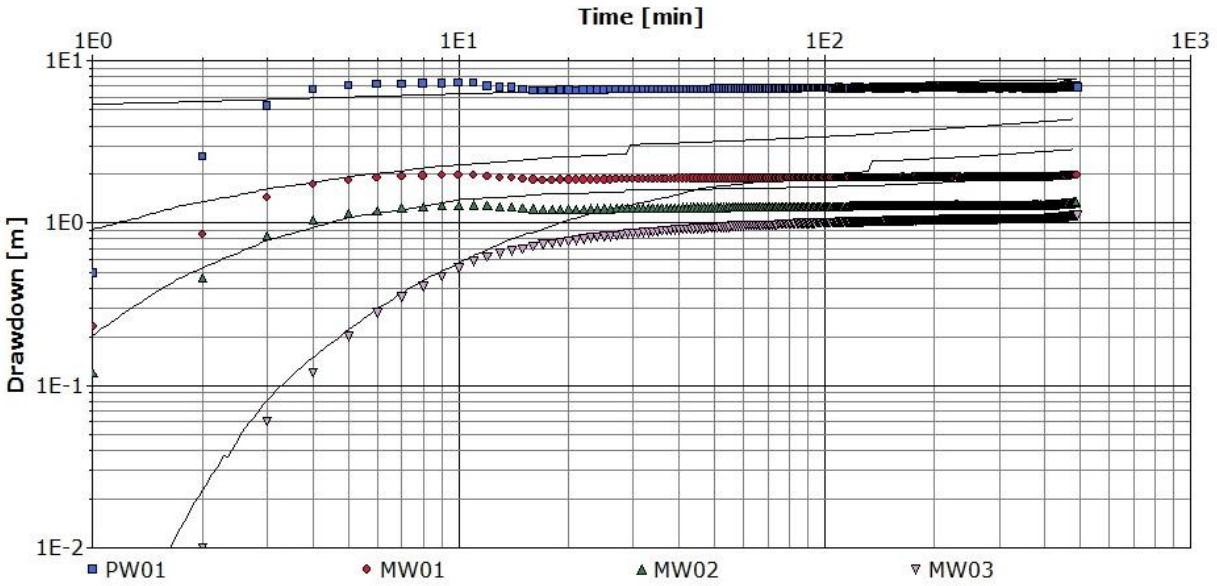

Figure 15: Drawdown data for PT1 at Otter Park. Shown are the data for pumping well (PW01), and three monitoring wells (MW01, MW02 and MW03). Also shown are the early portions of the Neuman curves. Note: the time axis is in seconds.

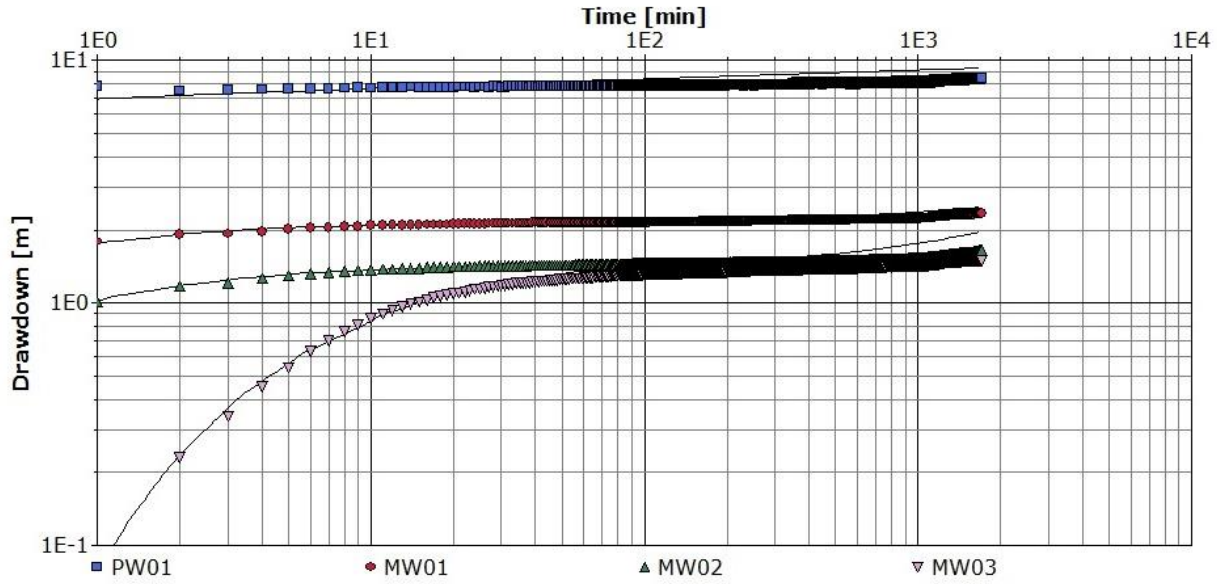

Figure 16: Drawdown data for PT2 at Otter Park. Shown are the data for pumping well (PW01), and three monitoring wells (MW01, MW02 and MW03). Also shown are the best fit Neuman curves. Note: the time axis is in minutes.

The Neuman method (1975) for unconfined anisotropic aquifers was identified as the most appropriate analytical method for estimating the hydraulic properties of the aquifer. The Neuman type curve is made up of three segments a) a steep segment (Theis-like), b) a flat segment at intermediate time, and c) a steeper segment at later time (also Theis-like), although segment c) was only just noticeable in the pumping test data (Figure 16). Not all of the conditions for the Neuman method were fully met. The Neuman method assumes: 1) the aquifer has infinite areal extent; 2) the aquifer is homogenous, isotropic and of uniform thickness; 3) the pumping well is fully or partially penetrating; 4) the aquifer is unconfined with delayed gravity response; 5) flow is unsteady; and 6) the diameter of the pumping well is very small so that storage in the well can be neglected. As described in Section 3, the unconfined aquifer in Otter Park is limited in its extent, particularly because Bertrand Creek is an important boundary condition and hydraulic connection is anticipated. It is unlikely that the aquifer is homogenous based on the variability in grain sizes vertically in PW01 and MW03. The aquifer is likely anisotropic, with vertical K less than horizontal K. And finally, because the aquifer thickness was determined only from a single well (MW03), it is uncertain if the aquifer is of uniform thickness. These assumptions are rarely met in real aquifers and are commonly accepted limitations in the pumping test analyses.

The software AquiferTestPro (Waterloo Hydrogeologic Inc. 2019) was used to analyze the constant rate discharge test data for all monitoring wells MW01, MW02, and MW03. The test data at the pumping well (PW01) were analyzed, but as is typical of pumping wells, the storage parameters are excluded. The aquifer T, Sy and Sy/S were obtained directly from manual curve fitting (Table 7). Then, K, S and Ss were calculated by dividing by the average saturated thickness (b) of the aquifer (Table 7). The average saturated thickness (25.3 m) is the difference between the average water table depth in each well prior to pumping (3.2 m) and the top of the confining layer based on the borehole log for MW03 (28.5 m). The saturated thickness in an unconfined aquifer changes during a pumping test; however, the effect on the calculated K and Ss values is minor because the saturated thickness only decreased by ~2 m in MW01 (8% of saturated thickness) and by ~1 m in MW02 and MW03 (2.5% of saturated thickness).

Table 7: Hydraulic properties of the aquifer estimated using the Neuman method for data collected during PT2 at Otter Park.

	T (m^2/s)	Sy	Sy/S	K (m/s)	S	Ss (m^{-1})
PW01	5.16E-03	n/a	n/a	2.04E-04	n/a	n/a
MW01	4.34E-03	3.50E-02	6.46E+02	1.72E-04	5.42E-05	2.14E-06
MW02	5.00E-03	4.10E-02	3.39E+02	1.98E-04	1.21E-04	4.78E-06
MW03	2.18E-03	4.63E-01	7.00E+01	8.63E-05	6.61E-03	2.61E-04
Geomean	**3.26E-03**	**2.72E-01**		**1.29E-04**		**1.78E-05**
StDev	**1.10E-03**	**4.79E-01**		**4.37E-05**		**1.47E-04**

Curve fitting was somewhat challenging because it had to be done manually. The automated curve fitting could not converge on a best fit. Fits were sensitive to a combination of parameters, such that slight adjustments of one would result in another parameter with a value that was unreasonable. Fits were generally insensitive to Sy/S and to K_V/K_H, except in MW03. The T (and K) values are relatively consistent between the wells (Table 7). The values at MW03 are slightly lower, which is expected based on the small grain size sediments that intersect the lower portion of the well (see Appendix I, Borehole Logs). The Sy values are more variable, but still within an order of magnitude of each other. The uncertainty is high for Ss.

To investigate varied response times in the wells, the data were plotted as drawdown vs time/radius^2 - a Cooper-Jacob III (Cooper and Jacob, 1946) composite plot (Figure 17). PW01 plots further to the right than the other wells because its radial distance is simply the well radius. The Cooper-Jacob III plot is useful because it allows for determining if the aquifer is homogenous. The three monitoring wells generally plot together indicating that the aquifer is relatively homogenous. However, MW01 has more drawdown than MW02 and MW03, which is consistent with the lower Sy value obtained for this well (Table 7). The higher drawdown at PW01 is possibly related to well inefficiency, which is the result of the water flowing into the well meeting resistance as it passes through the well screen. This causes more drawdown in the pumping well than would be expected based on the aquifer properties and pumping rate. The steep slope at early time for the pumping well (not apparent in Figure 17, but is inferred because drawdown starts at zero metres) illustrates this point. Inefficiency could also come from pumping equipment or the discharge line into the culvert. The hose that discharged the groundwater into the culvert was very long and had numerous turns that could add resistance to water flow, resulting in energy loss. The presence of inefficiencies would result in large (but unknown) errors in the estimates of the hydraulic properties for the pumping well.

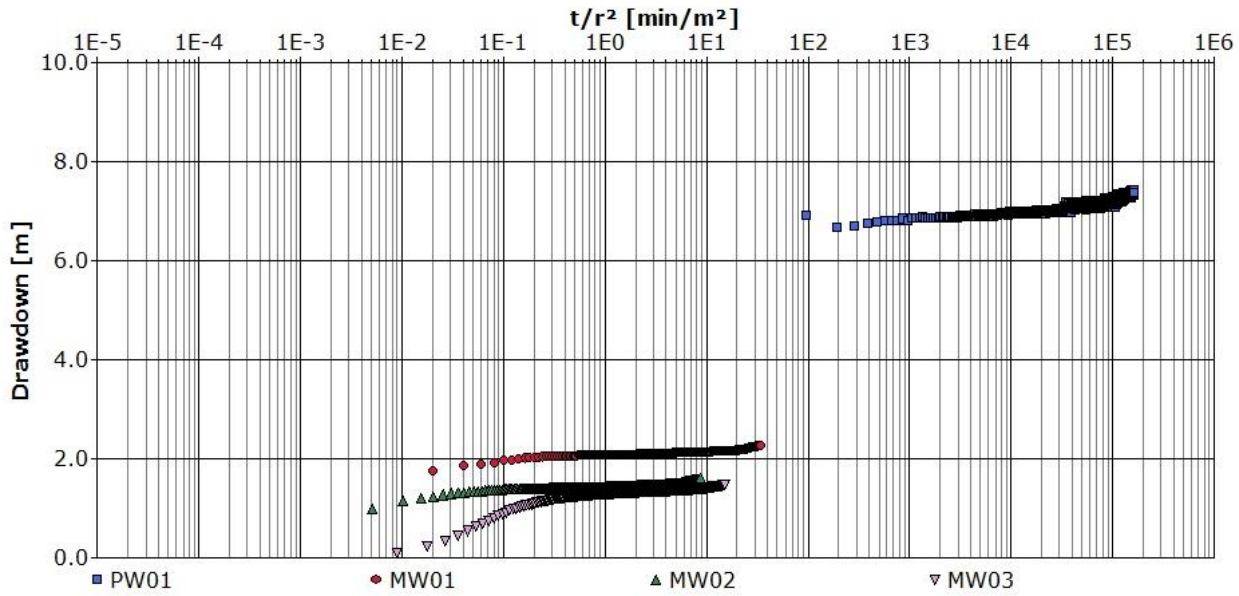

Figure 17: Cooper-Jacob III composite plot of drawdown versus t/r^2 for PT2 at Otter Park. Shown are the data for pumping well (PW01), and three monitoring wells (MW01, MW02 and MW03).

4.3.3 Results for Recovery Tests

The pump was shut off in PT2 at 7:15 p.m. on October 14, 2018. The water level immediately began to recover in the pumping well, followed closely by MW01 and MW02. The water level response in MW03 was slightly delayed (Figure 18).

The Theis Recovery method was used to analyze the recovery data for PT2. Due to the very rapid recovery in the pumping well and the two shallower monitoring wells (MW01 and MW02), the curve could only be fit to the later recovery data (t/t' less than 1000; Figure 18). Consequently, with the shallower slope of the lines, the T (and K) values are higher by almost an order of magnitude (Table 8) compared to the values estimated from the pumping test data (Table 8). The T (and K) values for MW03 are very similar between the pumping and recovery tests.

Johnson (2018) analyzed the recovery data for PT1 and estimated a geomean T of 3.2×10^{-3} m^2/s for MW01, MW02 and MW03; the results for PW01 were excluded due to difficulties in analyzing the data.

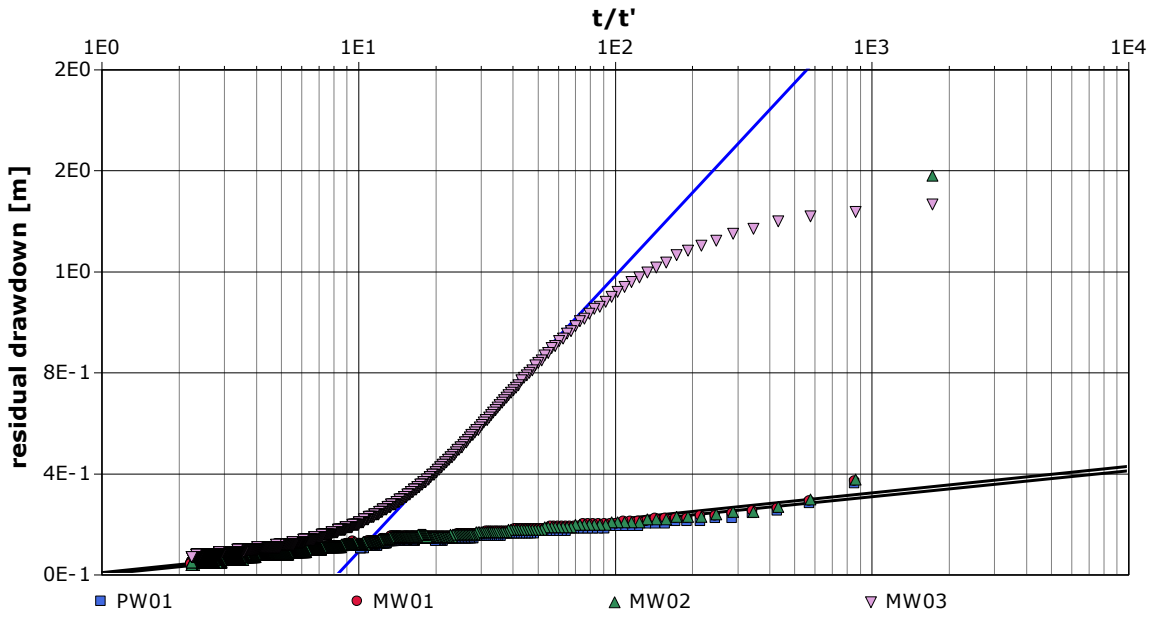

Figure 18: Recovery data for PT2 pumping test 2 at Otter Park. Shown are the data for pumping well (PW01), and three monitoring wells (MW01, MW02 and MW03). Also shown are the best fit Theis Recovery curves. Note: PW01 and MW01 underlie the data for MW02.

Table 8: Transmissivity and hydraulic conductivity values of the aquifer estimated using the Theis Recovery method for data collected during recovery following PT2 at Otter Park.

	T (m^2/s)	K (m/s)
PW01	4.95E-02	1.74E-03
MW01	5.11E-02	1.79E-03
MW02	3.65E-02	1.28E-03
MW03	3.42E-03	1.20E-04
Geomean	**1.85E-02**	**6.51E-04**
StDev	**2.44E-02**	**8.57E-04**

4.4 Summary of Hydraulic Properties

4.4.1 Streambed Sediments

As mentioned above, the Chapuis method was the most applicable grain size analysis method for the streambed samples. The other methods failed to meet the sediment requirements. The Chapuis method gave a lower estimate of K than the other methods, ranging from 6.79×10^{-4} m/s to 4.75×10^{-3} m/s depending on the void ratio values used (Table 9).

The grain size analysis results are not entirely consistent with the slug tests results. The slug tests performed in the instream piezometers and analysed using the Hvorslev and Bouwer-Rice methods produced K values two orders of magnitude lower than those from the grain size analysis (Table 9). For the deep piezometers, the Hvorslev method produced a geomean K of 1.46×10^{-5} m/s and for the shallow

piezometers, the geomean K was $3.41x10^{-5}$ m/s. The Bouwer-Rice method produced similar results; the deep piezometers had a geomean K of $1.39x10^{-5}$ m/s, and the shallow piezometers had a geomean K of $3.77x10^{-5}$ m/s.

It is not uncommon for grain size analysis methods to overestimate hydraulic conductivity because grain size methods can neglect the finer material and instead focus on material that can be sieved. Thus, the K values from the slug tests are considered more representative of the in-situ field conditions. The geomean K for both deep and shallow piezometers, based on both methods of analysis, is $2.5x10^{-5}$ m/s.

Table 9: Summary of hydraulic conductivity values for the streambed sediments.

	Grain size		Slug test			
Method	**Chapuis min**	**Chapuis max**	**Hvorslev deep**	**Hvorslev shallow**	**Bouwer-Rice deep**	**Bouwer-Rice shallow**
Geomean K (m/s)	6.79E-04	4.75E-03	1.46E-05	3.41E-05	1.39E-05	3.77E-05

4.4.2 Aquifer

Again, the Chapuis method was also the most applicable method for the aquifer samples. The geomean values using the minimum and maximum void ratios produced a minimum geomean for the samples from PW01 of $2.12x10^{-4}$ m/s and a maximum of $1.55x10^{-3}$ m/s (Table 10). The monitoring well MW03 had a similar range, with a minimum geomean of $1.44x10^{-4}$ m/s and a maximum of $1.11x10^{-3}$ m/s.

The minimum and maximum K values produced by the Chapuis method bracket the K values from the other methods. The Hvorslev method produced a geomean K of $7.62x10^{-4}$ m/s and the Bouwer-Rice method a geomean K of $5.49x10^{-4}$ m/s for sediments from MW01/02.

The aquifer K estimated from PT2 using the Neuman method produced a geomean K of $1.29x10^{-4}$ m/s for PW01 and all three monitoring wells. Using the Theis Recovery method for PT2, the geomean K for the wells was $6.51x10^{-4}$ m/s, which is approximately a half order of magnitude higher than the Neuman result.

Overall, the results for K from all methods suggest that the aquifer has a higher K than the streambed sediments, which indicates the likelihood of the instream piezometers being screened in a clogging layer (layer of lower hydraulic conductivity).

Table 10: Summary of hydraulic conductivity values for the aquifer samples.

	Grain size				Slug test		Pumping test	
Method	**Chapuis PW01 min**	**Chapuis PW01 max**	**Chapuis MW03 min**	**Chapuis MW03 max**	**Hvorslev MW01/02**	**Bouwer-Rice MW01/02**	**Neuman**	**Theis Recovery**
Geomean K (m/s)	2.12E-04	1.55E-03	1.44E-04	1.11E-03	7.62E-04	5.49E-04	1.29E-04	6.51E-04

5. PUMPING EFFECTS ON INSTREAM CONDITIONS

As mentioned in Section 4.3, two constant rate discharge pumping tests were conducted at the Otter Park field site; the first in early July and the second in mid-October 2018. Johnson (2018) describes the instream conditions prior to and during the July pumping test. This report summarizes the instream conditions prior to and during the second pumping test carried out in October.

5.1 Stream Discharge

As described in Section 3.3, the hydrometric stations were equipped with data loggers that measured stream stage every 15 minutes. Loggers were installed in May and the data downloaded periodically throughout the summer. Ultimately, the loggers were retrieved in December. Stream discharge was estimated using a location-specific rating curve as described in Section 3.3

Figure 19 shows streamflow at each hydrometric station from October 1 to December 4, 2018. The start and end of PT2 are indicated by the green and red vertical lines, respectively. During the summer recession in the months prior to PT2, streamflow at HS3 was higher than at HS2 indicating that the stream was gaining over that section (see Figure 7 for locations), while during periods of higher flow, discharge was lower at HS2 compared to HS3. Throughout the monitoring period, the discharge at HS4 and HS5 were of similar magnitude (curves almost overlap), despite being closer together than HS3 and HS4. The reduction in streamflow from HS1 to HS5 suggests that Bertrand Creek was losing under natural conditions from upstream to downstream through the site. The lower magnitude decrease in streamflow from HS4 to HS5 suggests that there was little to no groundwater contribution (or indeed loss to groundwater) along this reach.

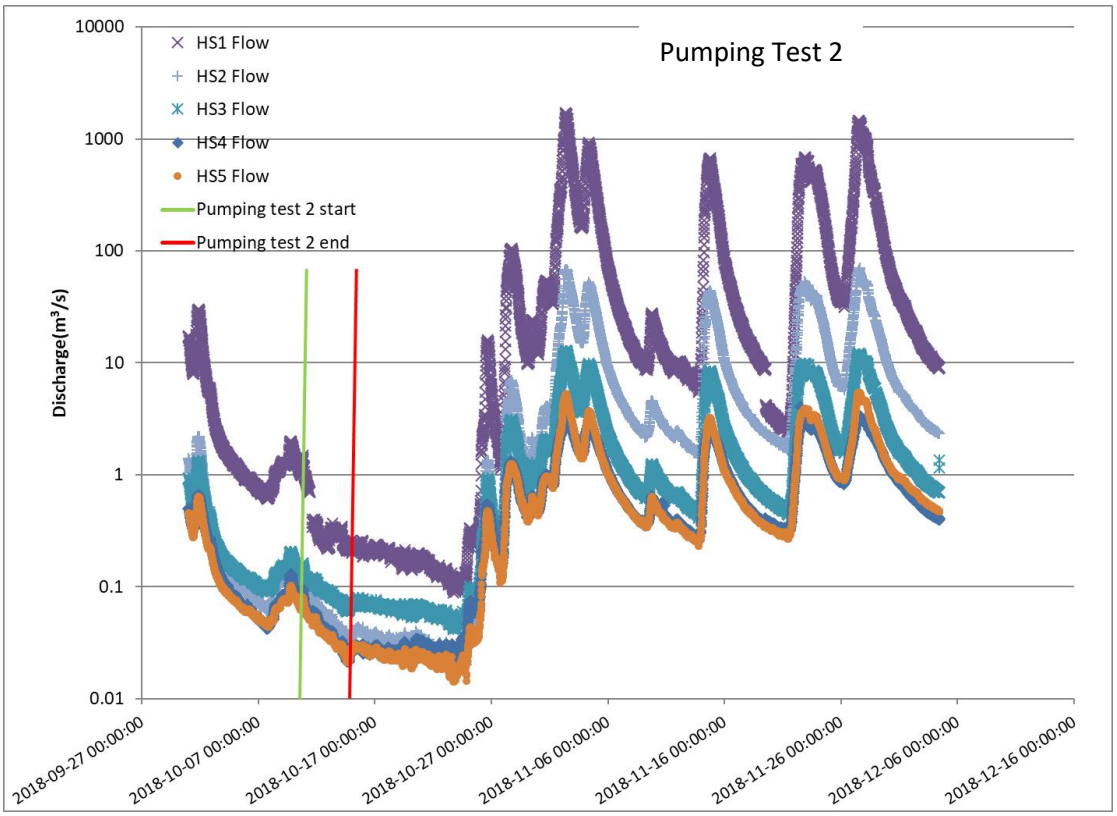

Figure 19: Stream discharge at the five hydrometric stations in Bertrand Creek from October 1 to December 4, 2018. The start and end times for PT2 are shown as red and green vertical lines.

Figure 20 shows the stream discharge for a narrower time interval, from just prior to PT2 on October 11 to October 19, 2018. Importantly, streamflow was declining prior to the pumping test. Precipitation data from Abbotsford Airport indicate light rain, showers of light rain, drizzle and mist from October 7-9. There was no further rain until October 23. Therefore, it is likely that streamflow was declining due to rainfall in the previous days.

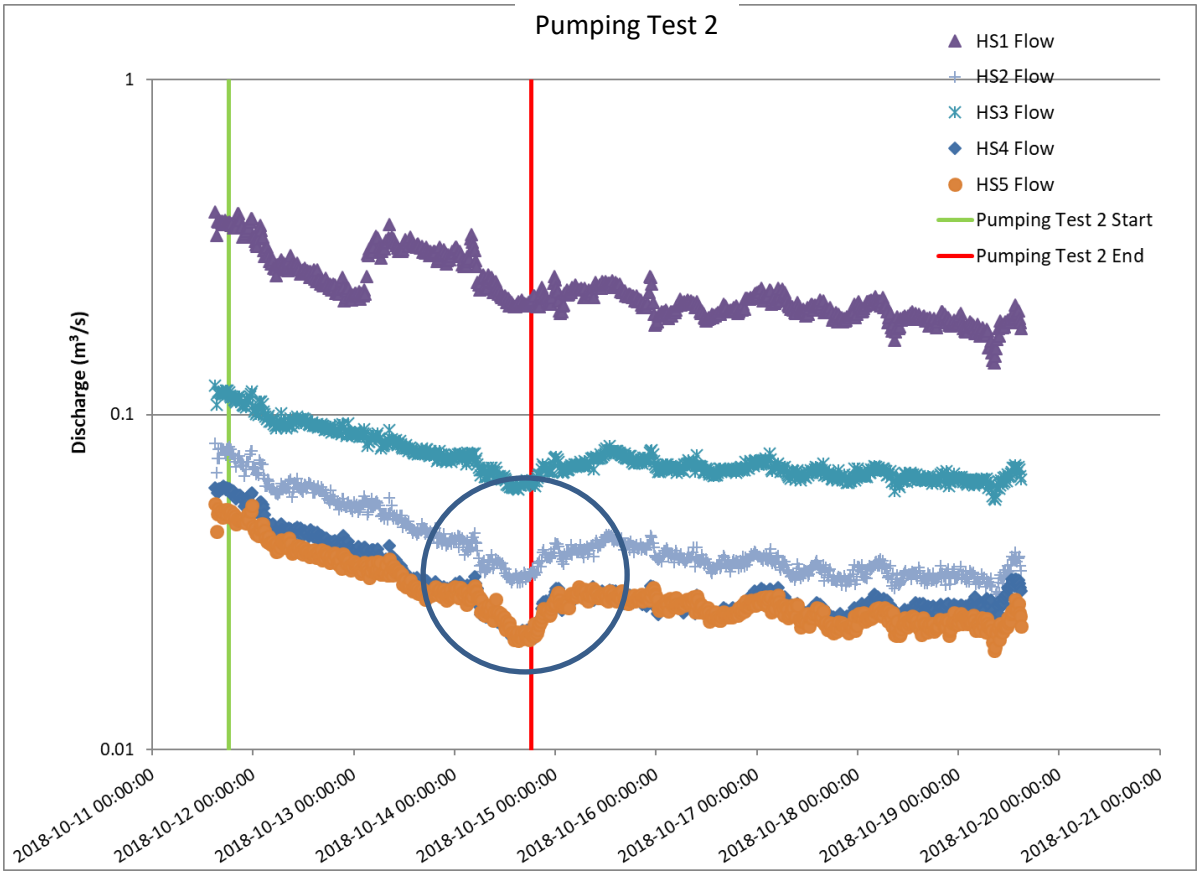

Figure 20: Stream discharge at the five hydrometric stations in Bertrand Creek from October 11-19, 2018. The start and end times for PT2 are shown as red and green vertical lines.

During the pumping test, streamflow continued to decrease at all hydrometric stations. At HS1, there appears to be greater variability – perhaps related to pumping from another well. While the negative trend observed during the pumping test could suggest streamflow depletion was occurring, the results are not conclusive because as shown in Figure 19, streamflow was declining prior to pumping. However, there are several lines of evidence that indicate streamflow depletion occurred during pumping.

- During PT2, streamflow decreased gradually at all hydrometric stations, but most notably right near the end of the test (Figure 20). The same phenomenon was observed during PT1 (Figure 21). A delay in streamflow depletion is expected as water pumped from the aquifer initially comes from storage, possibly intercepting groundwater if the gradient is toward the stream. Then, as the extent of the cone of depression increases, the stream is intersected, and water can begin to flow into the aquifer.
- Once the pump was shut down (red vertical line in Figure 20) the streamflow rebounded slightly.

- Prior to and following PT2, the streamflow at HS4 was consistently higher than at HS5, while during the pumping test the streamflow was almost the same magnitude as at HS5. Interestingly, the opposite was observed during PT1 - the difference in streamflow between HS4 and HS5 was greater than it had been at any time during non-pumping conditions. However, after the pump was shut off, the difference remained similar until the next precipitation event.
- During PT2, the streamflow magnitudes at HS1, HS3 and HS4 were more similar than at any other time during non-pumping conditions (see Figure 19). The same phenomenon was observed during PT1.

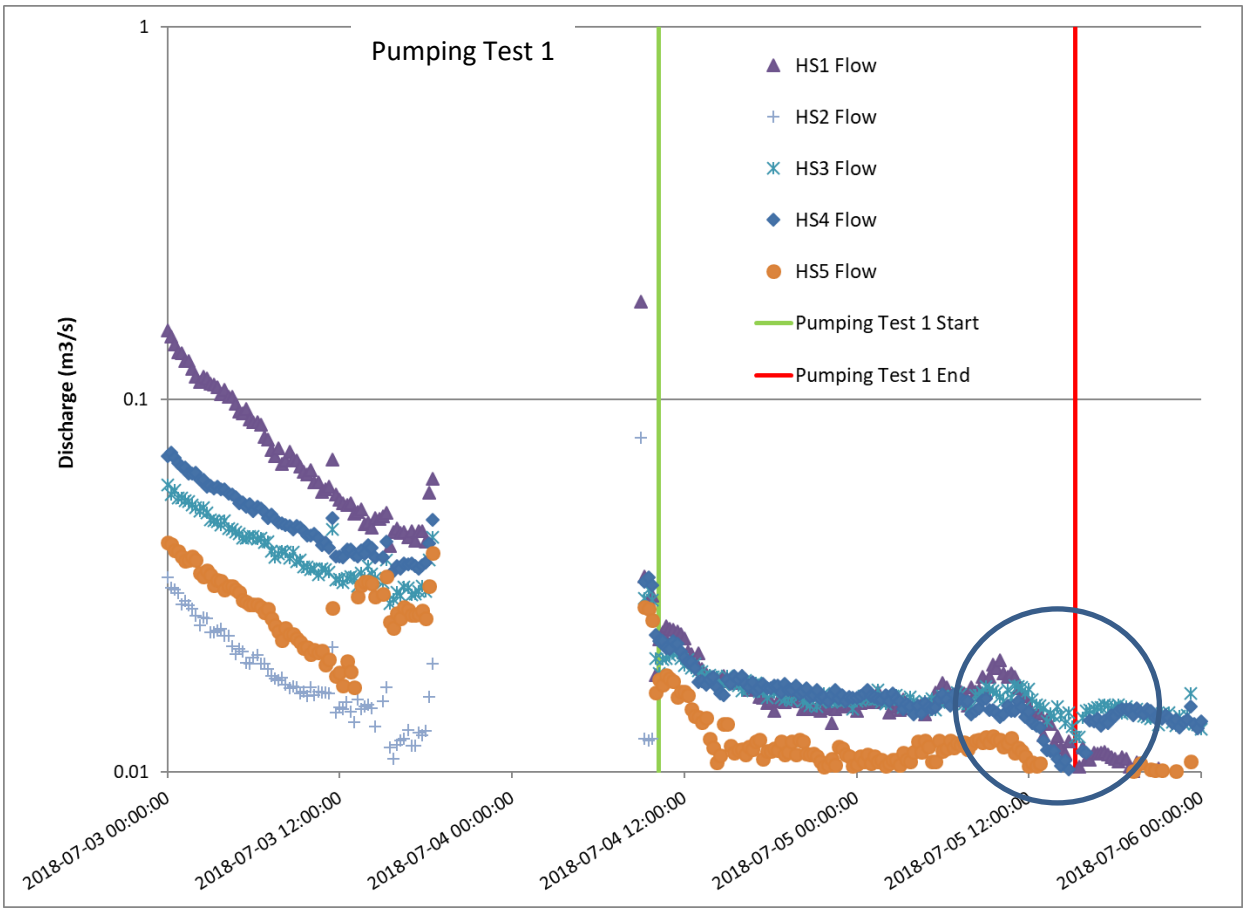

Figure 21: Stream discharge at the five hydrometric stations in Bertrand Creek from July 3-6, 2018. The start and end times for PT1 are shown as red and green vertical lines.

5.2 Instream Piezometers

This report focuses on instream conditions immediately prior to PT2, during PT2, and during recovery. Emphasis is placed on how the instream conditions changed over the monitoring period (October 11, 2018 at 15:00 to October 15, 2018 at 9:00).

5.2.1 Data Collection and Processing

The nested instream piezometers (as described in Section 3.4) were used to measure groundwater levels before and during pumping. Natural fluctuations (magnitude and possibly direction) in groundwater levels are expected throughout the year due to relative changes between the water table

and the stream stage. During pumping, if a stream is hydraulically connected to the aquifer, the groundwater levels in the piezometers are expected to decrease. The drawdown in the instream piezometers may be accompanied by either a change in the magnitude of the hydraulic gradient whereby it would become more negative (where negative indicates a downward gradient) or a lessening or reversal of the hydraulic gradient if the pre-pumping gradient was positive. However, interesting variations in the gradient can occur if one piezometer in the nested pair responds differently, for example, due to differences in the hydraulic conductivity of the streambed sediments surrounding the piezometers. Some of these unusual variations in gradient were observed at the site.

Prior to PT2, the loggers were reprogrammed to record measurements every 10 seconds. Loggers began logging at 15:00 on October 11th and continued to log at a 10-second interval until they were retrieved on October 16th. The pumping test started at 19:15 on October 11th and ended at 19:15 on October 14th. Thus, groundwater levels were recorded immediately prior to the start of the pumping test and continued logging for approximately two days following the end of pumping.

As mentioned in Section 3.4, the design for the instream piezometer network was to install at each location one deep and one shallow piezometer, with a difference in length of one pipe section between the pair (approx. 32 cm). The loggers were installed in the piezometers so that they rested on the bottom. In practice, however, the installation of the piezometers met with several challenges, which led to difficulties in calculating the hydraulic gradient (dh / dl):

1. The elevations of the top of casing was not the same at each nested pair, so the separation dl had to be adjusted accordingly to account for minor differences in the vertical offset.
2. Some of the piezometers were installed at a bit of an angle, so again an adjustment to dl had to be made.
3. At one location (D37/D38), both piezometers were accidentally installed to the same depth.
4. At one location (D41/D42), the piezometers had a greater difference in depth compared to the other pairs.

Appendix B describes the approach for determining the vertical hydraulic gradient in instream piezometers (vertical installation and tilted).

5.2.2 Results: Drawdown

Drawdown in all instream piezometers was calculated from the start of pumping. Figure 22 shows the drawdown in piezometers located along the stream reach, and Figure 23 show the drawdown in piezometers located along the midline of the creek, in line with the pumping well. The green vertical line on the graphs marks the beginning of PT2 at 19:15 on October 11th, and the red vertical line marks the end of the pumping test at 19:15 on October 14th. Drawdown was zero at the start of pumping and increased (note y-axis reversal) until approximately 18:45 on October 12th. Then, drawdown began to lessen and eventually became negative in several piezometers (head values greater than head values at the start of pumping). At approximately 12:00 on October 14th, a few hours before pump shutdown, the drawdown increased slightly in all piezometers. Therefore, the drawdown response in the instream piezometers was somewhat complex.

Notably, all piezometers responded immediately with a decline in head at the beginning of pumping. The magnitude of the drawdown differed between different pairs. For example, pair D35/D36 had less of a difference than pair D33/D34 (Figure 22).

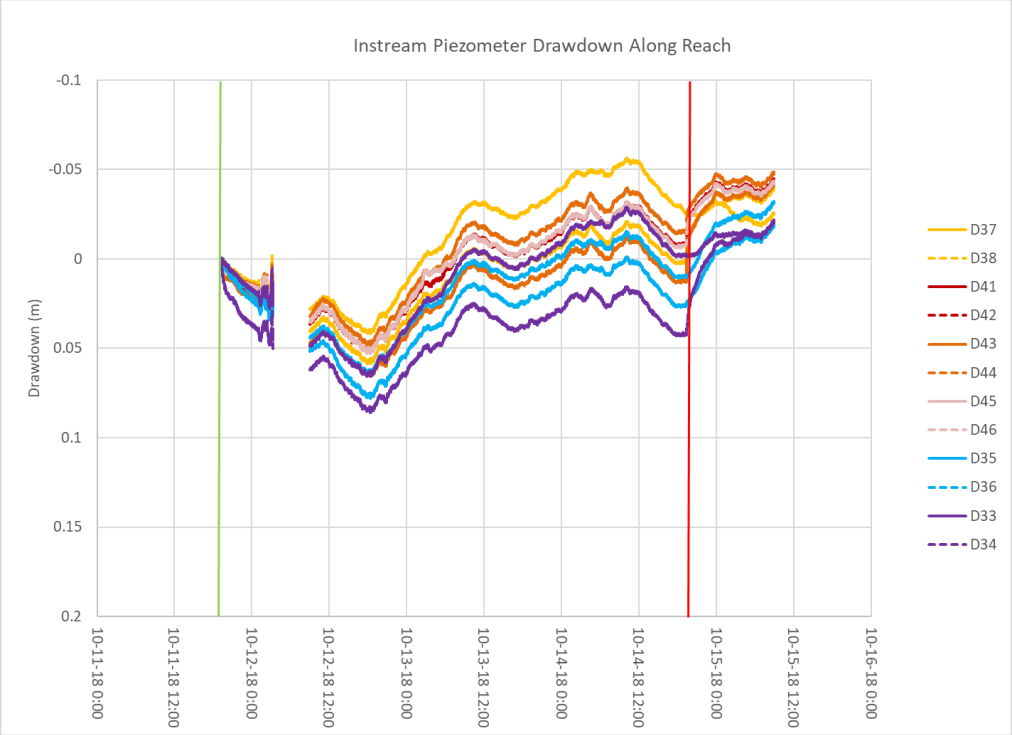

Figure 22: Drawdown measured in instream piezometers located along the length of the reach during PT2. Pumping began on October 11 at 19:15 and ended on October 14 at 19:15.

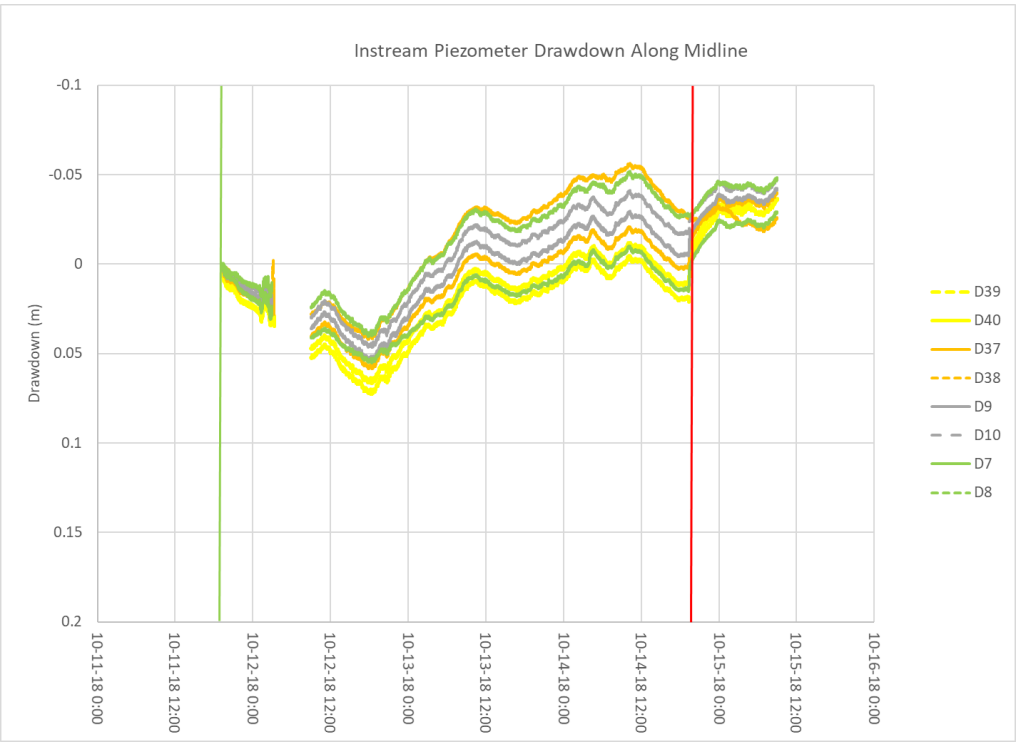

Figure 23: Drawdown measured in instream piezometers located along the midline of the creek during PT2. Pumping began on October 11 at 19:15 and ended on October 14 at 19:15.

5.2.3 Results: Vertical Hydraulic Gradient

Figure 24 displays the vertical gradient between each nested pair. The green vertical line represents the start of the pumping test, and the red vertical line represents the end of the pumping test. A positive gradient indicates upward groundwater flow and a negative value indicates downward groundwater flow. Hereafter, the terms upward and downward gradient will be used. To understand changes in the gradient, it is instructive to recall the drawdown characteristics. In all cases, the drawdown increased initially (from the start of pumping) until roughly 24 hours into the test (see Figure 22 and Figure 23). The drawdown rate differed between the deep and shallow piezometers, so the curves diverge as pumping progressed. The maximum drawdown ranged from approximately 0.04 to 0.08 m at the 24-hour mark. Once the maximum drawdown was attained, the drawdown began to lessen, but because of each piezometer in the pair responded at a different rate, the difference in water levels continued to increase, and according, the magnitude of the gradient increased. The drawdowns measured in each of D9/D10, D39/D40, D45/D46 and D35/D36 are very similar, so the gradients changed very little in these pairs. Appendix C shows the individual graphs for each piezometer pair, including the drawdown in each piezometer and the gradient.

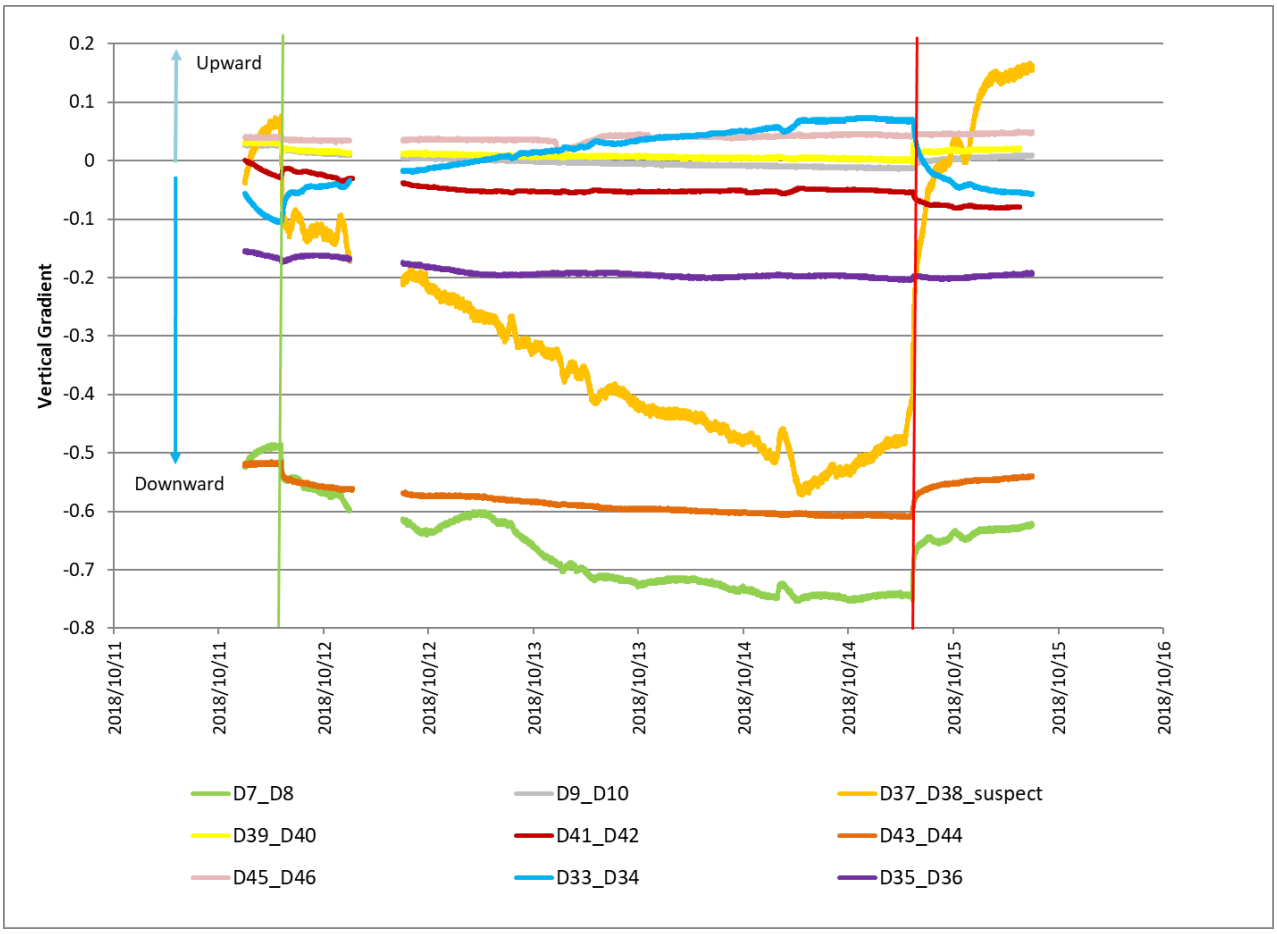

Figure 24: Vertical hydraulic gradients between the nested instream piezometers from October 11 to October 15, 2018. Pumping began on October 11 at 19:15 and ended on October 14 at 19:15. The green vertical line represents the start of the pumping test and the red vertical line the end of pumping. See Figure 23 for piezometer locations.

The gradients across the streambed ranged from +0.15[2] to -0.75 over the full period. Most of the piezometer pairs show an abrupt change in gradient when pumping began and again when it ended. In most cases, the gradient gradually became more negative (i.e. increasing upward flow) when pumping began, and then abruptly became less negative when pumping ended. This occurred because for all piezometer pairs except D33/D34 (the furthest downstream) the drawdown was greater in the shallower piezometer than in the deeper piezometer (see drawdown graphs in Appendix C). As noted in Section 4.4.1, on average the shallower piezometers had a K value approximately 2.5 times that of the deeper piezometers. Thus, it is possible that the shallower piezometers are more strongly hydraulically connected to the aquifer.

Results are summarized below in three categories: upstream of the pumping well, in line with the pumping well, and downstream of the pumping well, in reference to Figure 24.

Upstream of the Pumping Well: Furthest upstream of the pumping well, piezometer nest D45/D46 had a downward, albeit very low, gradient throughout the entire period. The water levels (and drawdown) were almost identical in both piezometers. At D43/D44, the gradient was strongly upward throughout and reduced only slightly, but there were more abrupt changes at the beginning and end of pumping compared to D45/D46. At D41/D42, the gradient was weakly upward throughout, but interestingly the upward gradient increased at the end of pumping (i.e. the negative gradient increased, suggesting a greater difference in the water levels between these two piezometers when pumping ended). It is noted, however, that D41/D42 had a larger vertical separation than the other piezometer pairs (approximately double), which may have confounded the results.

In line with the Pumping Well: Furthest from the pumping well, but in line with it, is D7/D8. This pair had the greatest upward gradient at the site, and the second largest reduction in gradient. D9/D10 and D39/D40 initially had downward gradients prior to pumping, switched to upward throughout most of the pumping period, and then returned to downward at the end of pumping. The gradients, however, were weakly negative at these two locations. Finally, at D37/D38 the gradient was upward throughout, but the reduction in the gradient was the largest at the site. This large reduction in gradient is likely due to the fact that these piezometers were accidentally installed to the same depth, so any changes in groundwater level recorded in these wells is magnified when the gradient is calculated because of the small vertical separation between the screens. It is likely that the gradient is indeed upward at this pair, but the magnitude of the change in the gradient is incorrect.

Downstream of the Pumping Well: D35/D36 had a moderate upward gradient over the monitoring period. The upward gradient increased at the beginning of pumping, but then stabilized. The response at D33/D34 is interesting because it is the only pair at which more drawdown occurred in the deeper piezometer. Unfortunately, the slug test results are inconclusive; Hvorslev method gave a higher K value for the deeper piezometer (by an order of magnitude), but Bouwer-Rice gave a lower K value for the deeper piezometer.

The spatial variation of the gradients immediately prior to PT2 (i.e., background conditions) is shown in Figure 25. Upstream of the center line D45/D46 and D41/D42 had upward gradients, while D43/D44 had a downward gradient. Along the center line, D39/D40 and D9/D10 had upward gradients, D7/D8 a downward gradient, and D37/D38 a neutral (or indeterminant) gradient. The gradient at D37/D38 was neutral because the vertical separation of these piezometers was minimal due to an installation error. Downstream of the center line, at D34/D35 and D33/D34, the gradients were downward.

[2] This maximum positive gradient was measured in D37/D38, suspected to have been installed accidentally at the same depth. Therefore, the gradient is magnified and likely incorrect. A more realistic maximum positive gradient was measured at D33/D34 at a value of 0.075.

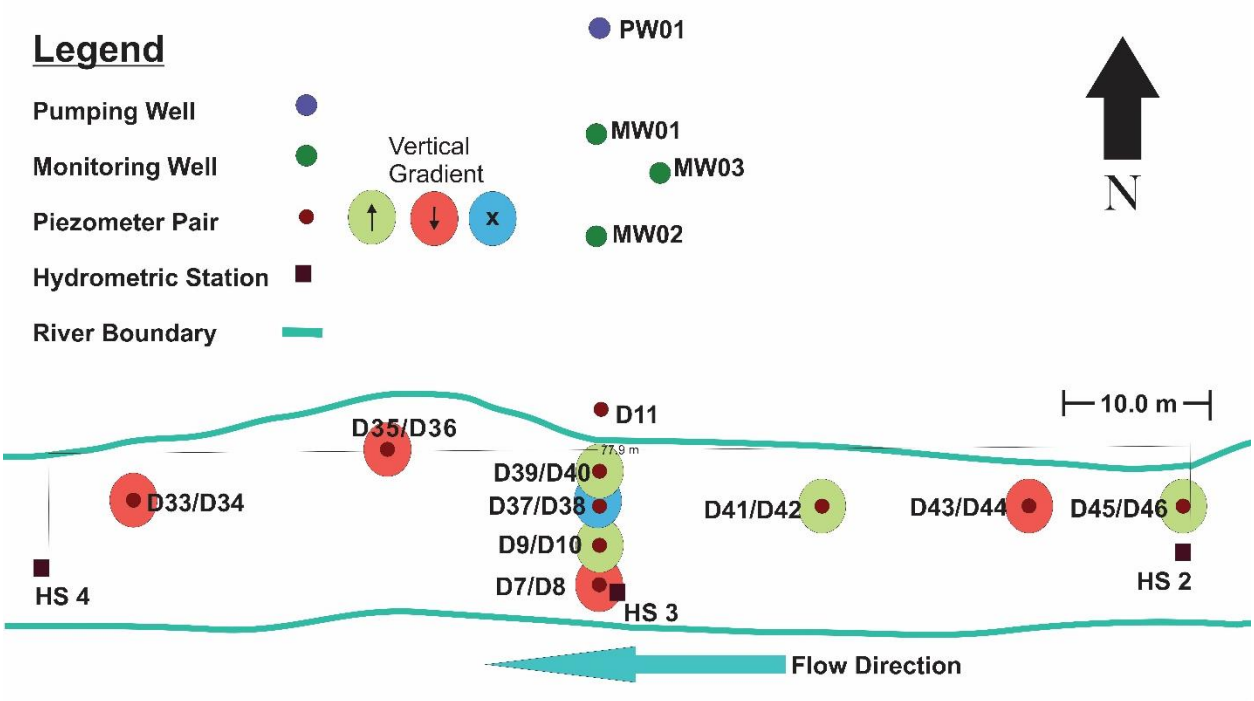

Figure 25: Spatial distribution of the vertical hydraulic gradients immediately prior to PT2. Green circles indicate a positive (upward) gradient; red circles indicate a negative (downward) gradient; blue circles indicate an (approximately) neutral gradient. Piezometer pair D37/D38 had a neutral gradient because of the similar depths of the piezometers.

The spatial variations in the vertical gradient are interesting, and somewhat inconsistent with gradients measured prior to PT1, between May 25 and July 3, as described by Johnson (2018). As noted in Section 3.5, Johnson (2018) measured slightly higher water levels in the wells in July 2018, suggesting a sloping water table towards Bertrand Creek and likely gaining stream conditions across much of the streambed. The measured vertical fluxes across the streambed in the summer are generally consistent with gaining conditions. Prior to PT1, from May to July, the average gradient was upwards at all piezometers between HS2 and HS3 (upstream locations), and upward at D35/D46 and neutral at D33/D34 (between HS3 and HS4). Across the center line, all piezometers had a downward gradient, except D7/D8 which had a neutral gradient. The dominantly downward gradient along the center line is interesting and may be related to the fact that the streambed is slightly raised near the center line (a low hump extending from the north to south banks). If the streambed is raised, some streamflow may be directed downward underneath the raised section, and then re-emerge downstream as upward flow.

The spatial variation of the gradients during PT2 is shown in Figure 26. Upstream of the center line D45/D46 retained its upward gradient, while D43/D44 and D41/D42 switched to downward gradients. Along the center line, gradients were downward except at D39/D40. Downstream of the center line, the gradient at D34/D35 was downward, and at D33/D34 the gradient was upward. Overall, throughout the stream, there was a noticeable change to dominantly downward gradients. Johnson (2018) observed that during pumping, the gradient was consistently upward upstream of the center line, downward across the center line, and upward downstream of the center line (Johnson, 2018).

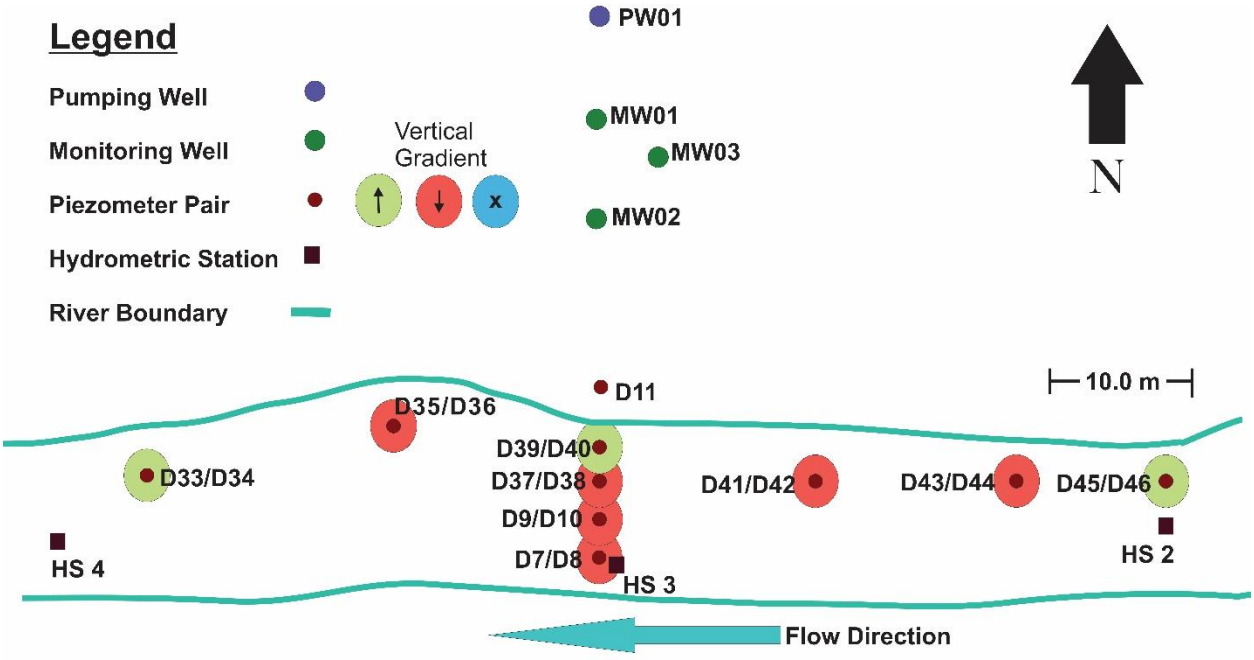

Figure 26: Spatial distribution of the vertical hydraulic gradients in the instream piezometers during PT2 in October 2018. Green circles indicate a positive (upward) gradient; red circles indicate a negative (downward); blue circles indicate an (approximately) neutral gradient (none observed during the test).

5.2.4 Uncertainty

The gradient changes during PT2 are similar to PT1, but there are inconsistencies. There could be a number of reasons for this. First, the pumping rates were different; 287 US gpm for PT1 and 324 US gpm for PT2. Second, the tests were conducted at different times of the year - July and October, and groundwater levels in the aquifer and streamflow (and stage and wetted area) were considerably different during these times. These factors combined would likely influence how the gradients would transition from non-pumping to pumping conditions. For example, whether a gradient was upward or downward prior to pumping and how strong that gradient was would dictate how the gradient might subsequently change. Also, the response time of each piezometer is influenced by the K of the streambed material surrounding that piezometer. A piezometer that is completed in a lower K material compared to its partner, significantly impacts the gradient response. It is beyond the scope of this report to fully explore these relationships.

Uncertainty in the vertical gradient estimates is associated with measurement error, corrections and multiple calculations. The error associated with each measurement of the hydraulic gradient is shown in Table 11. It was very challenging to measure water levels accurately. Loggers were deployed, then removed, re-deployed, etc. over a period from May to October (multiple time series for each piezometer). While the loggers were intended to sit on the bottom of the piezometer (to avoid issues related to depth corrections), there were inconsistencies with the manually measured water depths that were used to determine the relative water levels measured by the dataloggers. One of the main reasons for this was the slow response time of the piezometers. Each time a water level tape was dipped into the narrow piezometer tube to obtain a manual measurement of water depth, the water level rose in the piezometer, by perhaps a centimeter. Likewise, when the loggers were deployed there was a jump in water level that took up to a half hour in most piezometers to recover. Manual water depth measurements were made frequently prior to PT1, but when it became obvious that the water levels

were not recovering following measurement, this practice ended, and the logger water levels were all corrected (height above logger) using the same "assumed" depth of logger. Thus, there may be some unaccounted minor shifts in water levels between each time series. Overall, error propagation accounts for ~4.5 mm for dh and ~6.2 mm for dl.

Table 11: Measurement error associated with the vertical hydraulic gradient determination. Variables are defined in Appendix B.

Parameter	variable	Error	
Water level tape	a_s, a_d	3 mm	Readability of water level tape + possible change in hydraulic head in response to inserting the water level tape in the piezometer
Survey data	n/a	1 mm	difference between starting point and the same point at end of test
Survey data	c	1.4 mm	The error propagation of the elevation difference
data loggers	b_s, b_d	3 mm	Instrument error
Length of piezometer	L(a or b) and H uncorrected	10 mm	Due to measuring tape usage and slightly varying lengths from links
Length of piezometer	L(a or b) corrected	variable	Error is variable depending on the magnitude of the measurement
Top of piezometer to streambed	a	10 mm	Readability and difficulty of use of the measuring tape
Hypotenuse of top of piezometer to streambed	h	10 mm	Readability and difficulty of use of the measuring tape

5.3 Streambed Temperature

The TidBit Data loggers were installed as described in Section 3.4. As mentioned, two streambed temperature monitoring networks were installed. The background network was installed in May and left in place until late October, and temperatures were logged at 1-hour intervals. These loggers were attached to the inside of sewer pipe (for shielding) at two different depths (one at the streambed-water interface and the other 16 cm below the interface). The background network captured both background conditions and conditions during the two pumping tests. The second network was installed for each of the two pumping tests to accommodate a shorter sampling interval (30 seconds) as well as easy installation (attached to rebar placed beside the piezometers). The temperature data from both networks were compared and there were no significant differences in either the patterns or magnitudes of the temperatures from both networks. Therefore, in this report, the background Tidbit time series data are shown (the locations of the Tidbit loggers are shown in Figure 27). This report focuses on general observations of the streambed temperatures over the full time period and specifically how they changed during PT2.

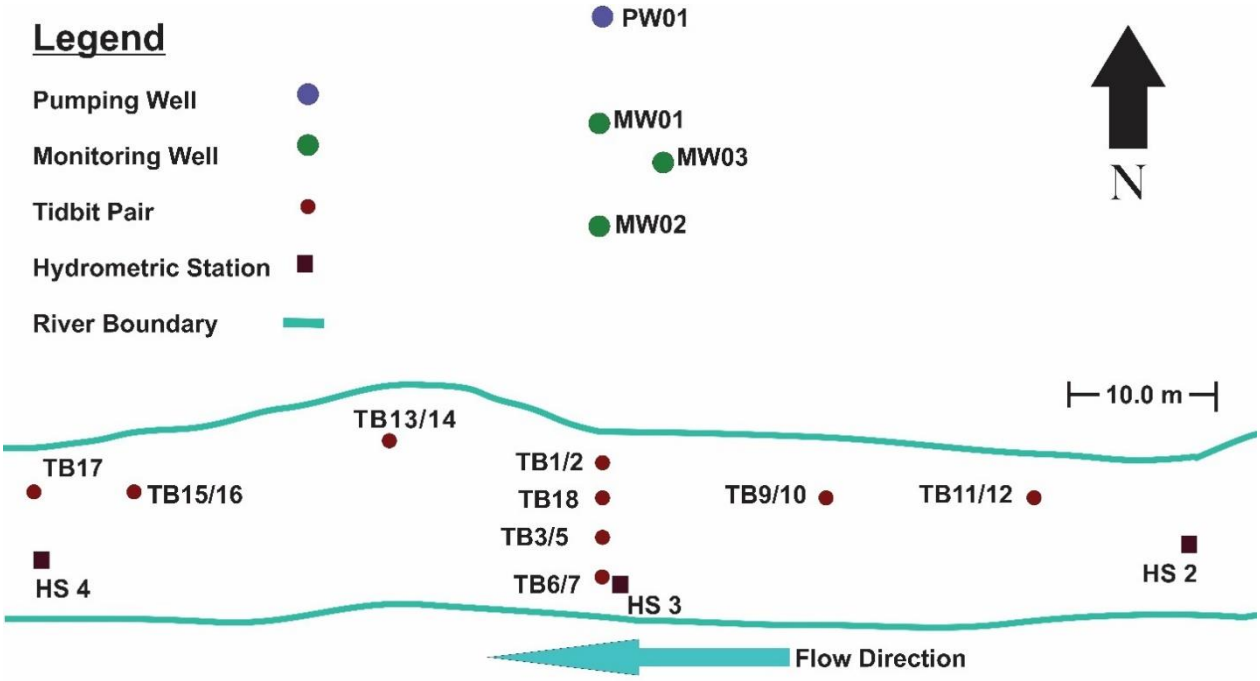

Figure 27: Location map for background streambed temperature loggers. Loggers recorded streambed temperatures at two depths (near the streambed surface and 16 cm depth below the streambed).

Figure 28 shows the full streambed temperature time series. Hourly air temperature recorded at Abbotsford International Airport is shown in grey. From May through mid-July, and from early-September to mid-October, daily air temperature variations exceed streambed temperature variations. From mid-July through to early-September, some of the daily streambed temperature variations exceed air temperature variations, notably in TB9/10, but also in TB1/2 and TB13/14. All of these loggers were situated near the north stream bank, and during this low flow period, the area was exposed. It is likely that the proximity of the piezometer tubes and rebar (used for the pumping Tidbit network) caused localized heating.

Generally, from May to mid-summer, streambed temperatures gradually increased at all locations and then began to decrease, due to changes in incident solar radiation over this time period. However, the general trend is punctuated by somewhat abrupt changes in streambed temperature, likely related to increases and decreases of streamflow and/or groundwater contributions. Ongoing examination of the hydrological dataset (streamflow and vertical gradients in the piezometers) is revealing complex interactions under background conditions related to changes in streamflow (peak flows) and possibly groundwater contributions. Such changes will undoubtedly affect the streambed temperatures. Detailed analysis of the streambed temperature data collected during the full background period (May 25 to Oct 19) is beyond the scope of this report.

Figure 29 shows the streambed temperature data measured over a 5-day prior to PT2. Streambed temperatures at all sites display a range of temperature, and generally follow the air temperature pattern. The overall trend in temperature increased, but from October 7th to 8th the range in daily air temperature was lower. Streambed temperatures similarly had a lower range on those days. Figure 19 showed that stream discharge had been steadily decreasing prior to October 7th, but on October 7th, it increased. Abbotsford recorded rain most of the day on October 7th, and it tapered off to showers on October 8th. Therefore, the lower range in temperature (air and streambed) was likely influenced by overcast conditions in combination with higher, and cooler stream discharge.

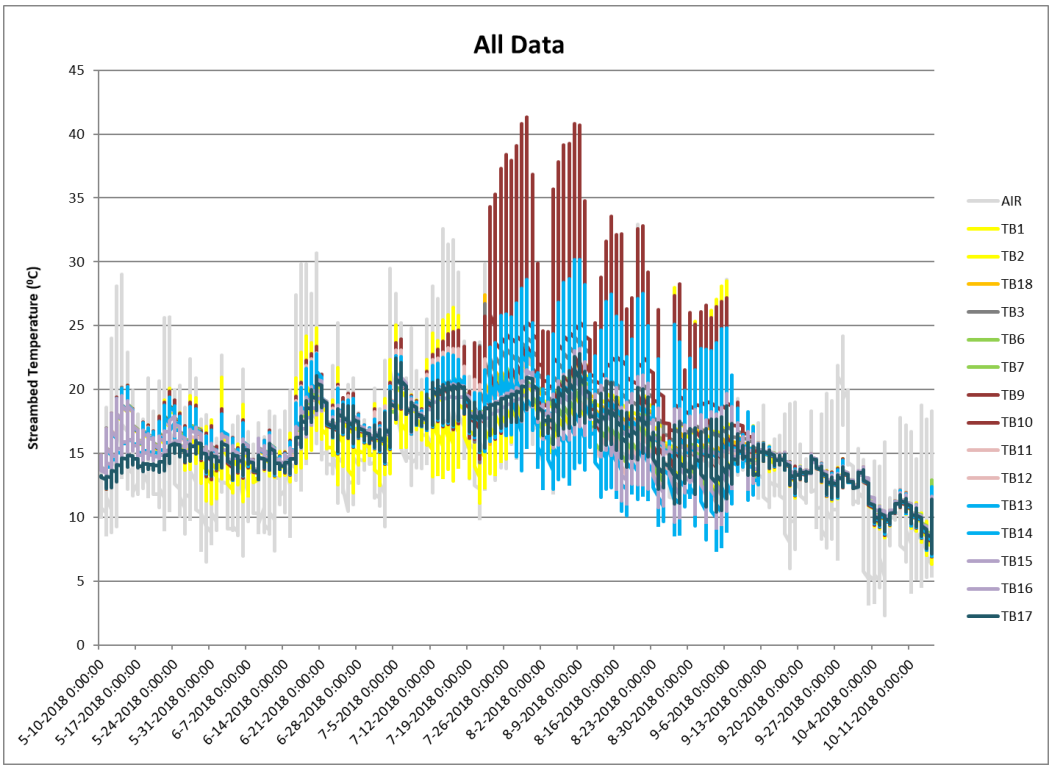

Figure 28: Full time series for background streambed temperature from May 10, 201 to October 15, 2018. Loggers in the legend are arranged progressively downgradient.

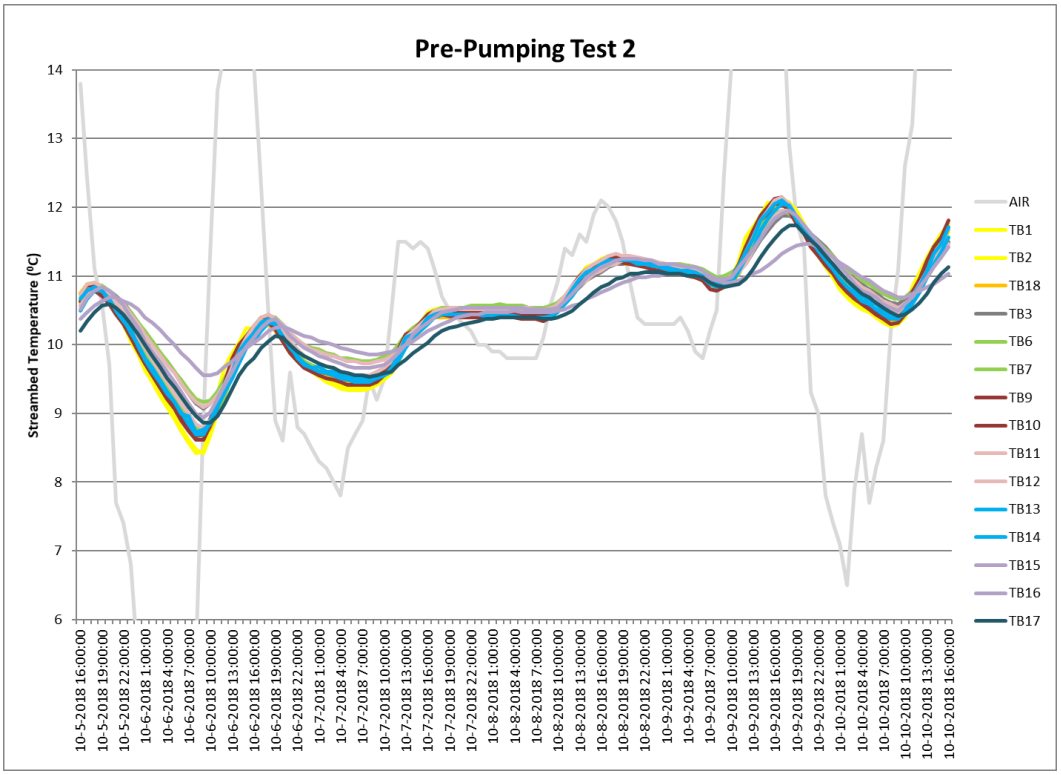

Figure 29: Streambed temperature data from October 5th to October 10th prior to PT2. Loggers in the legend are arranged progressively downgradient.

Figure 30 shows streambed temperature data from October 10th to October 19th, spanning PT2. During pumping, the streambed temperatures gradually diverged (i.e. the range increased between Tidbit pairs at some locations). This increase in temperature range is most apparent in TB1/2 (yellow in Figure 30), but also in TB13/14, likely because these TidBits were installed along the bank of the stream where water depths became shallower following the previous rain, and possibly due to streamflow depletion caused by pumping. In contrast, TB6/7 developed a lower range in temperature throughout the pumping test. Visually, comparing Figure 29 (pre-pumping) and Figure 30 (pumping) the colour spectrum is very different, despite the same scale and the same order of the Tidbits in the legend.

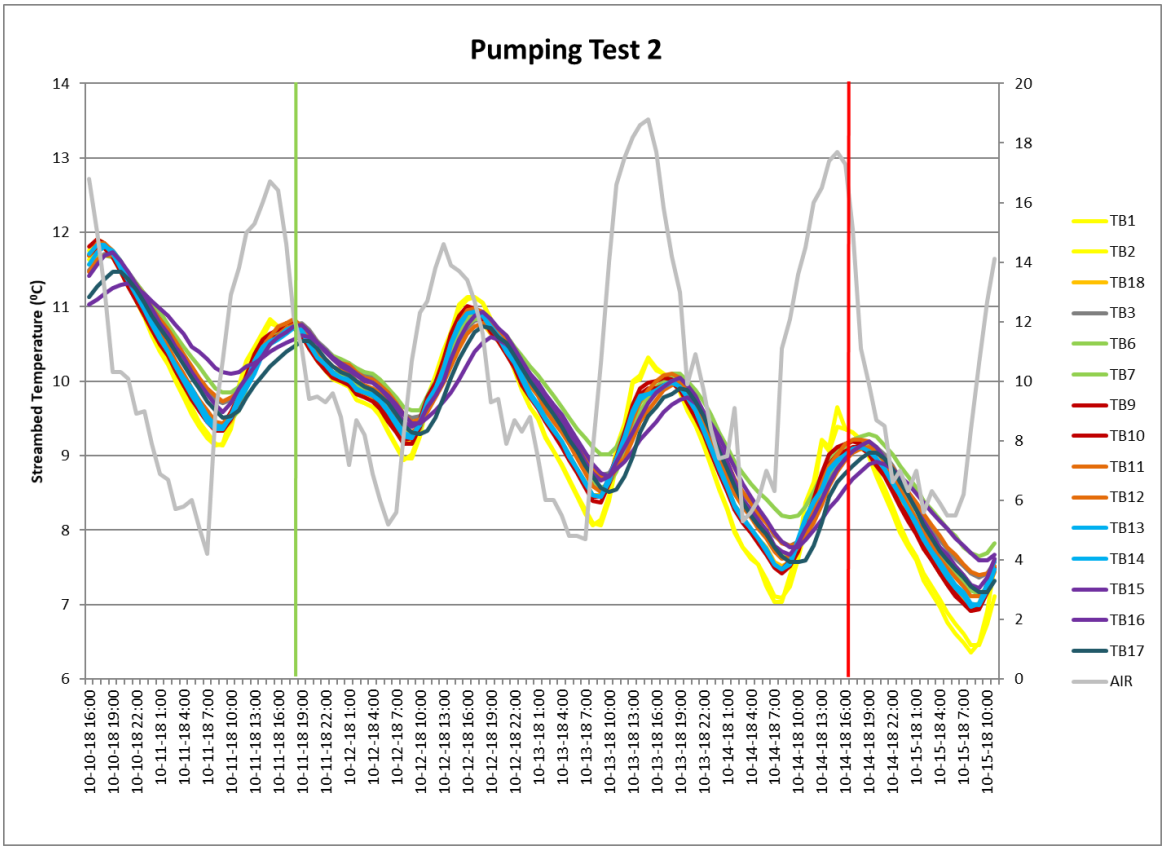

Figure 30: Streambed temperature data from October 10th to October 19th spanning PT2. The green vertical line shows the start of the pumping test and the red vertical line shows the end of the pumping test. Loggers in the legend are arranged progressively downgradient. Loggers were retrieved at the end of the record.

Following a similar approach to Whistler (2018) for Steele Park, a cross-correlation analysis was completed to examine the strength of the correlation between streambed temperature at different locations. For each monitoring location, the streambed temperatures were first examined to determine the leading Tidbit. Recall that the Tidbits were placed at two different depths in the streambed. The leading Tidbits included: 2, 18, 3, 7, 10, 12, 14, 16 and 17 (see the location map in Figure 27). Tidbits 18, 3, 16 and 17 were only single Tidbits (not one of a pair). The time series was sub-divided into four time periods spanning PT2: pre-pumping (72 hours prior to pumping), pumping for 72 hours, at the end of pumping during the last 20 hours, and during recovery for 19 hours. A cross-correlation analysis was then completed in R using ccf2 (cross-correlation function) for each of the four periods. Each Tidbit was compared with all other Tidbits. The maximum correlation and its corresponding lag were identified in the output.

Figure 31 shows the results for temperature loggers grouped by location: West of the center line, center line South to North, and Center to East (as shown in Figure 27). Correlation coefficients are positive, and most are significant above the 95% confidence level. The lag times range from -2 hours to 2 hours. The lag times are indicated as color intensity in the figure, and the direction of lag by color. The ccf2 calculates the lag for the logger across the top row, relative to the logger in the left column. Therefore, if a logger in the top row is blue, this means it has a positive lag (or lags behind the logger in the left column). In contrast, red indicates a negative lag, meaning the logger in the top row is a leading logger.

Pre-pumping, the Center to East (upstream) Tidbits (TB10 and TB12) lag the West to Center (furthest downstream) Tidbits (TB17, TB16 and TB14) by at least a ½ hour and by up to 2 hours. In fact, a general pattern is that from the center line to upstream, the Tidbits generally lag or have zero lag with Tidbits located further downstream (Figure 32). The cause is likely related to stream depth, as the stream becomes much deeper upstream and so warming of the streambed due to radiant heating would take longer. This pre-pumping pattern is generally consistent with the pattern during pumping, suggesting the streambed temperatures were only slightly impacted during pumping (considering the entire pumping period). Although, there are more cases of near zero lag during pumping conditions. At the end of pumping (the last 20 hours), there are even more cases of zero lag, and during recovery, most Tidbits have zero lag.

Interestingly, the results of this study are similar to those reported by Whistler (2018) under pre-pumping and pumping conditions at Steele Park during Phase 1 of this study. Whistler identified a high (statistically significant) correlation between streambed temperatures at different locations in the stream. Under pre-pumping conditions, a range of lag times (0 to 45 minutes) was detected between Tidbit loggers upstream and downstream. During pumping, however, there was an extreme decrease in lag times (0 to 2 seconds) and temperature changes became synchronous throughout the streambed. Whistler did not examine the recovery Tidbit data.

The thermal response at both field sites was not quite the same. During PT2 at Otter Park it was only during recovery that a notable decrease in lag occurred, while at Steele Park the decrease in lag occurred during pumping. Both pumping tests were conducted at essentially the same time of year, although the duration of pumping was different (72 hours for Otter Park and only 2 hours at Steele Park) and the stream discharge was considerably lower at Steele Park because it is a much smaller stream. Also, during the pumping test at Steele Park, streamflow remained stable over the 2-hour period. At Otter Park, streambed temperatures were increasing prior to pumping (Figure 29) and decreasing during pumping (Figure 30). Streamflow had increased a few days before PT2 due to a rain event on October 9th but was declining during the pumping test (Figure 19). Near the end of PT2, stream discharge noticeably dropped and recovered over a short period, and then generally stabilized (Figure 20). It was during this relatively short streamflow recovery period that the recovery period streambed temperatures were measured. So, possibly the general trend of decreasing streamflow during the pumping test masked an abrupt synchronization of streambed temperatures. The streambed temperatures near the end of pumping appear to be transitioning from asynchronous (lagged) to synchronous (no lag).

Finally, it is noted that the same ccf2 approach was used to analyze the data from the pumping network of Tidbits which were logging at 10-second intervals, as well as on filtered datasets (every 15 minutes and every hour). Unfortunately, the loggers were deployed only 30 hours prior to the start of the pumping test, which limited the data available for analysis pre-pumping. Moreover, one Tidbit (TB39 located near instream piezometer D39 – see Figure 11) dominated the correlation analysis. Nevertheless, the results for all datasets (10-second, 15-minute, and 1-hour) showed similar spatial and temporal patterns as the Tidbits from the Background network (discussed above), notably showing a reduction in the lag among all Tidbits during recovery.

Pre-pumping

CCF	West to Center			Center Line South to North				Centrer to East		Lag
	TB17	TB16	TB14	TB7	TB3	TB18	TB2	TB10	TB12	-2
TB17		**0.993**	**0.985**	**0.988**	**0.992**	**0.984**	**0.980**	**0.986**	**0.989**	-1.5
TB16	**0.993**		**0.995**	**0.990**	**0.998**	**0.992**	**0.984**	**0.993**	**0.992**	-1
TB14	**0.985**	**0.995**		**0.997**	**0.995**	**0.999**	**0.987**	**0.998**	**0.998**	-0.5
TB7	**0.988**	**0.99**	**0.997**		**0.992**	**0.998**	**0.989**	**0.992**	**0.999**	0
TB3	**0.992**	**0.998**	**0.995**	**0.992**		**0.994**	**0.981**	**0.993**	**0.994**	0.5
TB18	**0.984**	**0.992**	**0.999**	**0.998**	**0.994**		**0.989**	**0.997**	**0.999**	1
TB2	**0.980**	**0.984**	**0.987**	**0.989**	**0.981**	**0.989**		**0.993**	**0.990**	1.5
TB10	**0.986**	**0.993**	**0.998**	**0.992**	**0.993**	**0.997**	**0.993**		**0.994**	2
TB12	**0.989**	**0.992**	**0.998**	**0.999**	**0.994**	**0.999**	**0.990**	**0.994**		

Pumping

CCF	West to Center			Center Line South to North				Center to East	
	TB17	TB16	TB14	TB7	TB3	TB18	TB2	TB10	TB12
TB17		**0.994**	**0.977**	**0.985**	**0.995**	**0.980**	**0.947**	**0.971**	**0.983**
TB16	**0.994**		**0.981**	**0.994**	**0.998**	**0.983**	**0.946**	**0.978**	**0.990**
TB14	**0.977**	**0.981**		**0.992**	**0.979**	**0.998**	**0.971**	**0.998**	**0.995**
TB7	**0.985**	**0.994**	**0.992**		**0.993**	**0.996**	**0.962**	**0.986**	**0.999**
TB3	**0.995**	**0.998**	**0.979**	**0.993**		**0.981**	**0.940**	**0.975**	**0.988**
TB18	**0.980**	**0.983**	**0.998**	**0.996**	**0.981**		**0.969**	**0.997**	**0.998**
TB2	**0.947**	**0.946**	**0.971**	**0.962**	**0.940**	**0.969**		**0.982**	**0.970**
TB10	**0.971**	**0.978**	**0.998**	**0.986**	**0.975**	**0.997**	**0.982**		**0.991**
TB12	**0.983**	**0.990**	**0.995**	**0.999**	**0.988**	**0.998**	**0.970**	**0.991**	

End of pumping

CCF	West to Center			Center Line S to N				Center to East	
	TB17	TB16	TB14	TB7	TB3	TB18	TB2	TB10	TB12
TB17		**0.976**	0.871	**0.945**	**0.982**	0.891	0.843	0.872	**0.923**
TB16	**0.976**		**0.936**	**0.983**	**0.996**	**0.949**	**0.87**	**0.911**	**0.973**
TB14	0.871	**0.936**		**0.969**	**0.93**	**0.991**	**0.949**	**0.993**	**0.981**
TB7	**0.945**	**0.983**	**0.969**		**0.988**	**0.986**	**0.925**	**0.957**	**0.997**
TB3	**0.982**	**0.996**	**0.93**	**0.988**		**0.952**	0.884	**0.919**	**0.977**
TB18	0.891	**0.949**	**0.991**	**0.986**	**0.952**		**0.954**	**0.991**	**0.994**
TB2	0.843	0.87	**0.949**	**0.925**	0.884	**0.954**		**0.964**	**0.943**
TB10	0.872	**0.911**	**0.993**	**0.957**	**0.919**	**0.991**	**0.964**		**0.974**
TB12	**0.923**	**0.973**	**0.981**	**0.997**	**0.977**	**0.994**	**0.943**	**0.974**	

Recovery

CCF	West to Center			Center Line South to North				Center to East	
	TB17	TB16	TB14	TB7	TB3	TB18	TB2	TB10	TB12
TB17		**0.997**	**0.995**	**0.916**	**0.936**	**0.946**	**0.954**	0.733	0.612
TB16	**0.997**		**0.982**	**0.903**	**0.925**	**0.939**	**0.955**	0.725	0.592
TB14	**0.995**	**0.982**		**0.87**	**0.865**	**0.899**	**0.926**	0.651	0.507
TB7	**0.916**	**0.903**	**0.870**		**0.982**	**0.990**	**0.975**	0.690	0.590
TB3	**0.936**	**0.925**	**0.865**	**0.982**		**0.994**	**0.977**	0.730	0.638
TB18	**0.946**	**0.939**	**0.899**	**0.990**	**0.994**		**0.993**	0.713	0.600
TB2	**0.954**	**0.955**	**0.926**	**0.975**	**0.977**	**0.993**		0.727	0.595
TB10	0.733	0.725	0.651	0.690	0.730	0.713	0.727		0.972
TB12	0.612	0.592	0.507	0.590	0.638	0.600	0.595	**0.972**	

Figure 31: Stream temperature correlation coefficients for four time periods, spanning the 72-hour time period prior to the pumping test (October 8th-11th), during pumping (October 11th-14th), at the end of pumping (last 20 hours on October 14th), and during recovery (October 14th- 15th). The lag times are indicated as color intensity, and the direction of lag by color. Viewing the loggers across the top row, ***blue indicates the logger in the top row lags behind the loggers in the left column (a positive lag), whereas, red indicates that logger leads the logger in the left column (a negative lag relative).*** *High CCE, greater than 0.95, are shown in bold type – most are significant. The sampling interval was hourly. Uncertainty in lag time is ± 0.5 hour. Temperature loggers are grouped by location as shown in Figure 32).*

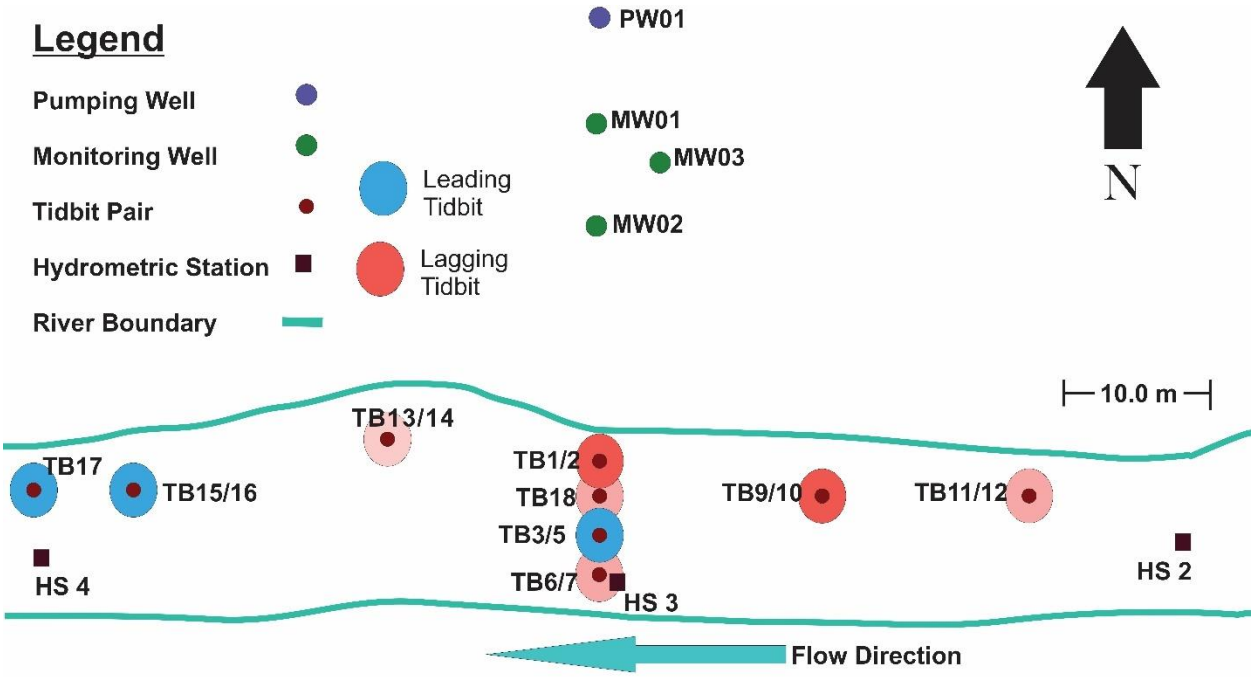

Figure 32: Location map of background Tidbits showing the lag during pre-pumping and pumping conditions when patterns are similar. ***Blue (positive lag) indicates a Tidbit generally lags behind the other ones, while red (negative lag) means it leads.*** *A lighter shade of red is used to illustrate the lags may be only slightly negative.*

Of note, from a technical perspective, the 15-minute filtered dataset was ideal for the ccf2 analysis. The 10-second logging interval was too short because the maximum correlation (peak) occurred over a wide range of lags (i.e. there was a broad flat peak). Therefore, the lag corresponding to the middle of the peak was used. The 1-hour filtered dataset was also adequate when data were analyzed over several days, but when the time period is short there are too few data.

6. STREAMFLOW DEPLETION MODELING

Streamflow depletion modeling was carried out using two approaches. First using the Hunt (1999) analytical model, and second using a numerical groundwater flow model to simulate PT2.

6.1 The Hunt (1999) Analytical Model

The Hunt model (1999) was used to model the streamflow depletion in Bertrand Creek and to make comparisons between the field study results (Figure 33). This model was preferred over others because it contains a parameter for a 'clogging layer'. The clogging layer, also known as streambed impedance, is a semi impervious layer in the streambed with a lower hydraulic conductivity than the aquifer, which impedes connectivity between the aquifer and the stream.

The Hunt model (1999) uses Equation 1 to determine stream depletion (ΔQs) normalised to the pumping rate (Qw) as a function of time. The description of the variables and the determined values are presented in Table 12.

$$\frac{\Delta Qs}{Qw} = erfc\left(\sqrt{\frac{Sd^2}{4Tt}}\right) - \exp\left(\frac{\lambda^2 t}{4ST} + \frac{\lambda d}{2T}\right) erfc\left(\frac{\sqrt{\lambda^2 t}}{4ST} + \frac{\sqrt{Sd^2}}{4Tt}\right) \quad (1)$$

where:

$$\lambda = \frac{w}{b'} K' \quad (2)$$

The Hunt Model (1999) assumes (Hunt, 1999):

- The ratio of vertical to horizontal velocity components is small
- The aquifer is of infinite extent and is homogenous and isotropic in all horizontal directions
- Drawdowns are small enough compared with saturated aquifer thickness to allow the governing equations to be linearized
- The streambed cross-section has horizontal and vertical dimensions that are small compared to the saturated aquifer thickness, and the stream extends from y = - ∞ to y = +∞ along x = 0
- The well flow rate, Qw, is constant for 0 < t < ∞
- Changes in water surface elevation in the stream created by pumping are small compared with changes created in the water table on the aquifer side of the semi pervious layer
- Seepage flow rates from the river into the aquifer are linearly proportional to the change in the piezometric head across the semi pervious layer

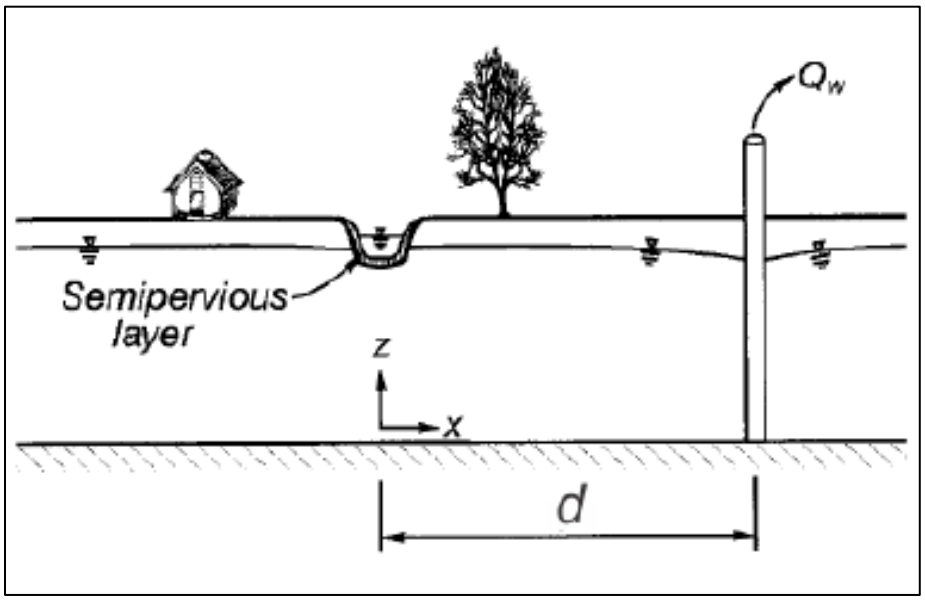

Figure 33: Conceptual model presented by Hunt (1999) of aquifer-stream connectivity that is used to frame the solution for streamflow depletion.

6.2 Application of the Hunt Model (1999) to the Field Site

Streamflow depletion using the Hunt (1999) method was modelled using a Visual Basic script in Excel developed by Dr. Bruce Hunt. The spreadsheet used for these calculations was designed by Glenn Hall for usage at Steele Park (Hall, 2017). Variables used in the model were determined from the locations of the field instrumentation and the analysis of the aquifer and streambed hydraulic properties discussed in Section 4. Table 12 briefly describes the source for each variable. Of particular note, the vertical K of

the streambed sediments was based on the K values estimated from the slug testing results for the deeper piezometers. Recall that the deeper piezometers had a lower K than the shallow piezometers, which may reflect a clogging layer. The higher K for the shallower piezometers suggests the absence of a clogging layer nearer to the streambed, possibly because finer materials have been more readily removed as a result of flowing water. The streambed thickness was determined to be the average separation (*dl)* between the piezometer pairs. This separation is highly uncertain.

Table 12: Variables for the Hunt (1999) model with their symbols as used in Equations 1 and 2, along with a brief description of how the value was determined.

Variable	Symbol	Units	Value	Description
Distance from well to stream edge	d	m	34	Field measurements
Transmissivity	T	m^2/hr	11.736	*AquiferTest* Neuman method – all wells
Specific yield	S or S_y	dimensionless	0.272	*AquiferTest* Neuman method – geomean from monitoring wells
Pumping rate	Q	m^3/hr	73.59	Field measurement
Streambed thickness	b'	m	0.3	Estimate: average separation of instream piezometers
Streambed conductivity	K'	m/hr	0.0513	Deep piezometer averages from slug test
Stream width	w	m	10	Field measurements
Streambed Conductive Coefficient	λ	m/hr	1.71	Calculated from Equation 2

6.3 Streamflow Depletion Analytical Modeling Results

The Hunt model estimates a ΔQs/Qw ratio of 0.55 according to the graph at 72 hours. Therefore, using a pumping rate of 324 US gpm (73.59 m^3/hr or 0.020 m^3/s), and by estimating the area under the curve, the streamflow depletion rate would be approximately **1460 m^3 over the 72-hour period**. Uncertainty in some input parameters, such as specific yield (Sy) and streambed thickness (b'), were briefly explored. If Sy is lowered to 0.15, streamflow depletion at 72 hours would be approximately 1740 m^3, while increasing b' to 0.5 m or 1 m, lowers streamflow depletion at 72 hours to approximately 1300 and 1000 m^3, respectively. Therefore, parameter uncertainty does impact the results, but not substantially.

All of the instream piezometers saw immediate drawdown at the start of pumping regardless of their location in the stream. Interestingly, drawdown increased in all piezometers and then peaked at approximately 24 hours into the test (Appendix C). After the ~24-hour mark, drawdown decreased and eventually became negative relative to the initial drawdown. This means that the water levels in the piezometers had recovered higher than they were at the beginning of pumping. The maximum drawdown ranged from approximately 0.04 – 0.06 m (Appendix C). Generally, the pattern of response was identical among the two piezometers in the pair, although the magnitude varied slightly, suggesting one piezometer experienced more drawdown that the other one. In all pairs except D33/D34, the deeper piezometer had the greater drawdown.

Despite the common drawdown patterns observed, there was no obvious trend in the hydraulic gradients; some piezometer pairs had upward gradients and some negative, and the direction and magnitude of the gradient varied. Therefore, it was not possible to determine an average hydraulic

gradient for the site to estimate the flux through the streambed due to pumping. Assuming the gradient during the initial 24-hour period is representative of the impact of pumping (and not a change in streamflow due to other factors), the average gradient among those piezometer pairs that had a negative gradient was **-0.28** for the first 24 hours. Piezometer pairs excluded from this average included D37/38 (for reasons mentioned previously) and D9/D10, D39/D40 and D45/D46. The average gradient among those piezometers with a negative gradient from 24 hours to 72 hours was **-0.31**, which is similar to the average negative gradient over the first 24 hours. It is noted that the gradient became negative in D9/D10, less positive in D39/D40, and remained unchanged in D45/D46 from 24 hours to 72 hours.

Using a negative gradient estimate of 0.3 to represent the entire site, and the K value of the streambed sediments ($2.5x10^{-5}$ m/s), the average downward flux at those locations would have been approximately $7.45x10^{-6}$ m/s. If the area of the entire streambed between HS2 and HS4 is approximated at 780 m^2, then the volumetric loss of water would be approximately $5.8x10^{-3}$ m^3/sec or **1510 m^3 over the 72 hour** pumping period, assuming streamflow depletion was taking place at the same rate over the entire 72 hour period (this is likely an overestimate because the rate of streamflow depletion varies over time).

The estimate of streamflow depletion based on the hydraulic gradient across the streambed (1510 m^3) is similar to the estimate from the Hunt model (1460 m^3) at the end of pumping. A rough estimate of the average change in stream discharge between HS2 and HS4 on the last day of pumping between at 5:00 and 19:15 on October 14th is 0.01 m^3/s (see circled area on Figure 20 when streamflow noticeable dropped). This equates to a loss of approximately **500 m^3 over 14.25 hours**. Because the rate of streamflow depletion varies (as shown in Figure 34), this estimate taken near the end of pumping presumably underestimates the streamflow depletion. Over the full 72-hour period it would likely approach the value estimated from the vertical gradients.

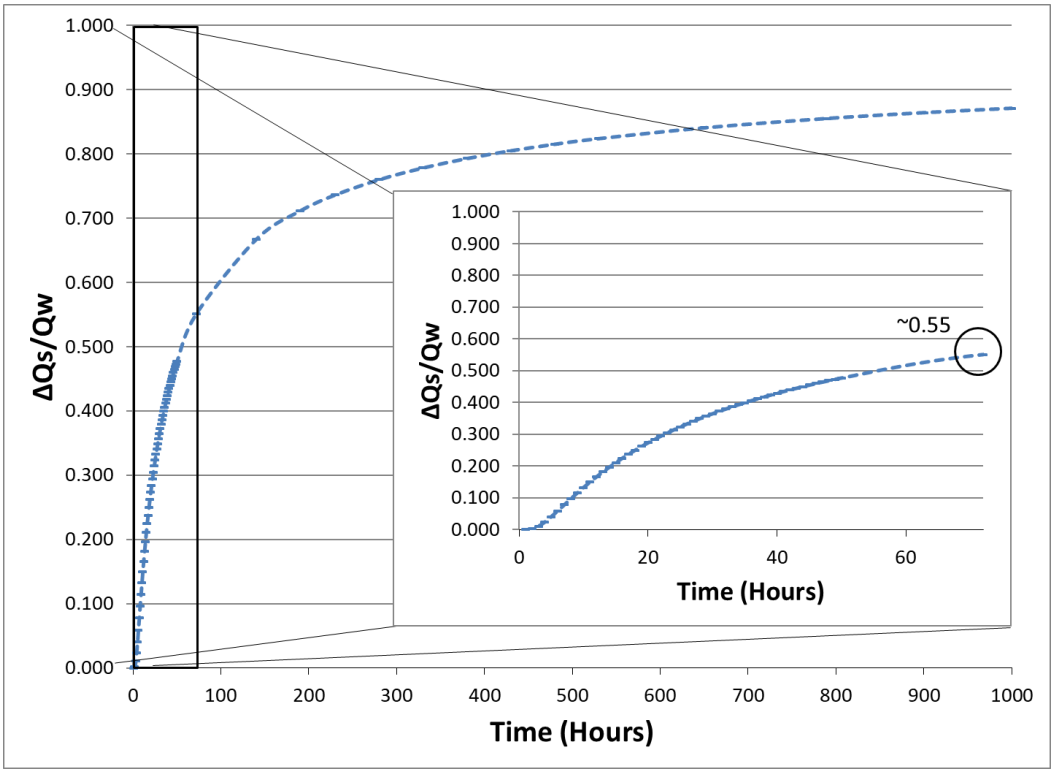

Figure 34: Hunt (1999) model of streamflow depletion (normalised with respect to the pumping rate) in Bertrand Creek using the input parameters in Table 12 and run for 1000 hours. Inset is for the time duration of PT2 (72 hours).

6.4 Numerical Groundwater Flow Modeling

A numerical groundwater flow model was developed for the site using Visual MODFLOW Classic version 2011.1 (Waterloo Hydrogeologic Inc. 2011). This particular software was selected because it includes the stream boundary condition; the newer Visual MODFLOW Flex does not include this boundary condition.

The main purpose of the modeling was to estimate streamflow depletion by simulating PT2 and calibrating the model against the observed heads in the three wells and the deep instream piezometers (recall there are deep and shallow instream piezometers; the deeper ones were selected for model calibration to align with the vertical discretization of the model).

6.4.1 Conceptual Hydrogeological Model

Two main sources of information were used to develop a conceptual hydrogeological model of the site: 1) well lithology logs for several nearby groundwater wells (available on iMapBC), and 2) well logs for PW01 and MW03 at Otter Park (Appendix A). Two geologic cross-sections were constructed for the area surrounding Otter Park (Appendix D). Only wells within 700 metres of the park were considered for site scale model. Based on the two geologic cross-sections, the aquifer directly underneath and proximal to Otter Park is considered mostly unconfined and planar (or lens-like) in shape. At distances further away from Otter Park, the thickness and extent of these HSUs becomes uncertain.

Six hydrostratigraphic units (HSUs) were identified based on these cross-sections (Table 13 and Figure 35). Table 13 gives a brief description of each HSU along with the minimum and maximum hydraulic conductivity values (Kmin and Kmax, respectively) estimated from grain size data. The interbedded sand and gravel layer (HSU #3) and the fine-to medium-sand (HSU #4) together form an unconfined aquifer. Based on the borehole logs (Appendix A) and grain size results (Table 3 and Table 4) for PW01 and MW03, HSU #3 appears to be heterogeneous and could be divided into an upper and a lower section. Due to the large difference in K between HSU #4 and the silt and clay layers (HSUs #5 and #6), the silt and clay layers can generally be considered aquitards.

Storage properties estimates were only available for the unconfined aquifer (HSU #3 and #4) based on the pumping test results. Specific storage was estimated at 1.8×10^{-5} m^{-1} and specific yield at 0.27 (see geomean values in Table 7).

Table 13: Hydrostratitgraphic units (HSUs) and minimum and maximum hydraulic conductivity values (Kmin and Kmax) estimated from grain size analysis and the literature.

HSU #	Description	Kmin (m/s)	Kmax (m/s)
1	Sandy topsoil	2.1E-04	1.4E-02
2	Stream sediments	4.3E-04	2.1E-02
3	Interbedded sand and gravel layer	4.7E-05	4.2E-02
4	Fine- to medium-sand	4.0E-05	2.3E-02
5	Silt	1.0E-09[3]	5.0E-05[2]
6	Clay	1.0E-12[2]	5.0E-09[2]

[3] Estimated from Table 2.2 in Freeze and Cherry (1979)

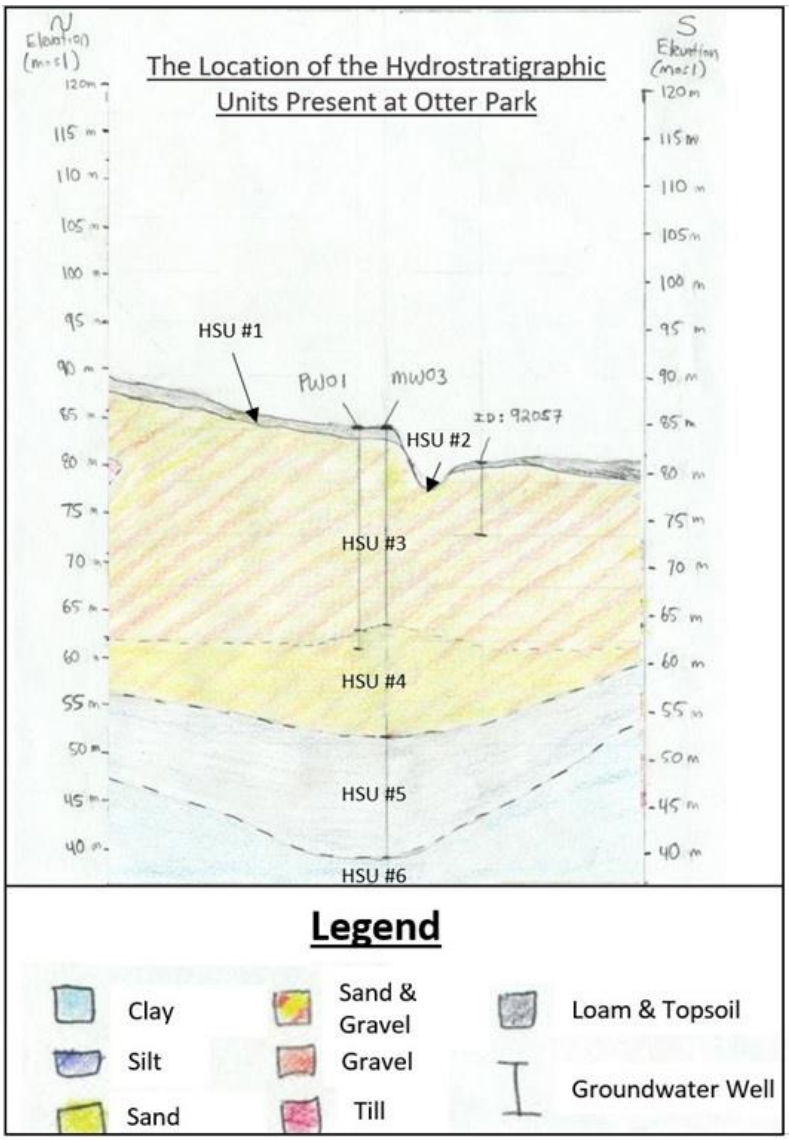

Figure 35: Hydrostratigraphic units interpreted from lithology logs from wells near Otter Park, for PW01 and MW03 at Otter Park (see Appendix A).

6.4.2 Numerical Model Construction

Model Domain and Discretization

The model domain is rectangular, 350 m wide and 450 m in length (Figure 36). This width of domain was chosen for two reasons. First, streamflow was not measured beyond HS1 and HS5, and because a stream boundary condition was to be used (see below), it was necessary to limit the domain extent to these furthest upstream and downstream hydrometric stations. Also, for the purposes of simulating a 72-hour pumping test, it was thought that the lateral domain boundaries would be sufficiently far away from PW01 to avoid influences from the model boundary. The length of the domain was based on trying to generate a roughly north-south groundwater flow system, parallel to the east and west domain boundaries. Groundwater flow is thought to be highly controlled by topography and groundwater should flow from the hillside in the north (which is higher in elevation) towards Bertrand Creek and the southern border of the model, which are both lower in elevation.

The domain was discretized into 140 columns and 176 rows. The grid was refined locally around the wells where head changes would be greatest. Close to the groundwater wells, the model cells are approximately 1.25 m x 1.3 m, while further away and close to the edges of the model their size increases to roughly 3.3 m x 8.4 m.

The surface digital elevation model (DEM) was created by merging two datasets: 1) a raster DEM created using LiDAR (Light Detection and Ranging) data provided by the Township of Langley (spatial resolution of 1m and a vertical accuracy of ±8cm) and 2) a provincial DEM from iMapBC. Because the LiDAR DEM did not cover the full model domain, both datasets were used, with the more accurate LiDAR DEM being overlaid (and taking precedence over) the lower resolution DEM. The two DEMs had a close agreement in elevation values; however, along the interface (edges) shared between both DEMs, differences in elevation were up to 1.5 m, although this magnitude of difference was rare. Commonly, the elevation discrepancies were around 20 cm. When imported into the groundwater model, this had the effect of creating small elevation gains in the areas along the interface. This difference was thought to be small enough to ignore for a groundwater model.

Elevation across the model domain ranges from 30-104 masl. The highest elevations are in the northwest corner, representing a portion of the hillside (Figure 37 and Figure 38). The bottom depth of the model was selected to be approximately at the depth of the underlying clay layer as seen in cross-section #1 (Appendix D). Furthermore, from cross-sections #1 and 2, the clay layer was assumed to extend laterally throughout the Otter Park region. The model was discretized vertically into 29 individual layers; each layer is approximately 1.4 m thick (Figure 37 and Figure 38). The bottom elevations for each layer were assigned relative to surface topography. In places where the topography was flat, or only slightly changing, such as near the groundwater wells and near Bertrand Creek, the layers are roughly planar, while in areas where topography changes rapidly, the model layers are curved.

Figure 36: Numerical model domain in plan view showing the location of the stream boundary condition (blue), and the wells, instream piezometers and hydrometric stations used for calibration. The horizontal grid is not shown for clarity purposes.

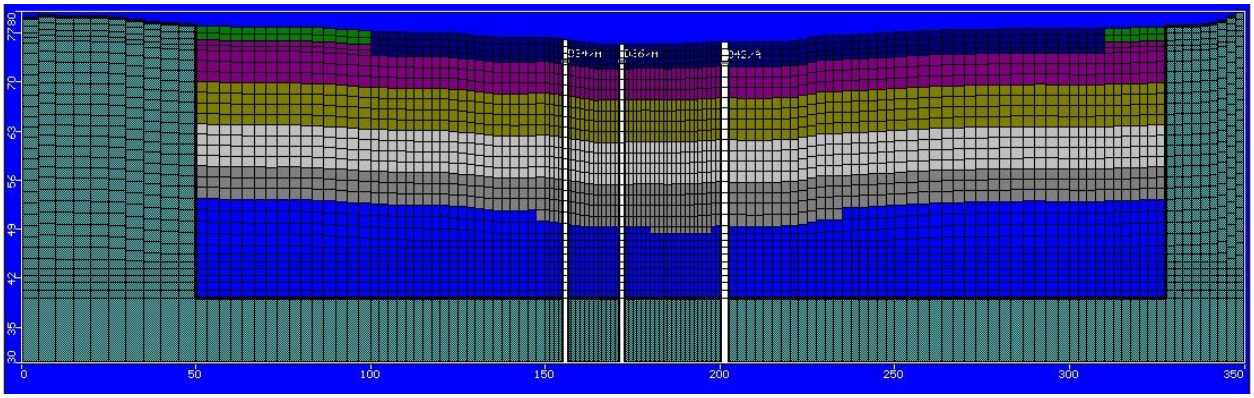

Figure 37: East-West cross-section through the numerical model domain showing HSUs that were assigned unique K values. Also shown are instream piezometers that intersect this cross-section.

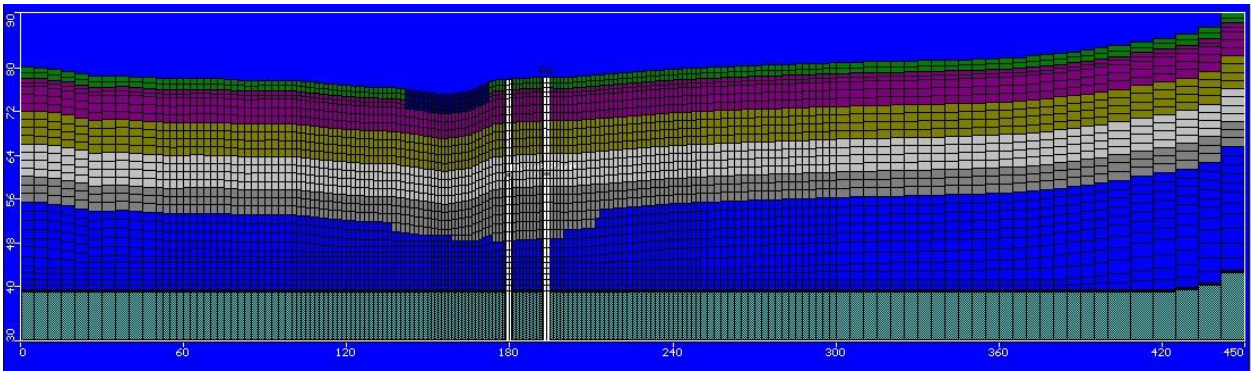

Figure 38: North-South cross-section through the model domain showing HSUs that were assigned unique K values. Also shown are wells PW01 and MW02 that intersect this cross-section.

Hydraulic Properties

Different K zones were defined in the model based on the HSUs shown in Figure 35. Due to the fine vertical discretization, i.e. grid layers are approximately 1.4 m thick, individual HSUs span several grid layers. This is evident on Figure 37 and Figure 38, which show the model grid and different coloured property zones. Each property zone was assigned an initial K value (Table *14*) roughly mid-range of values in Table 13. However, HSU #3 was divided into an upper and a lower zone according to the well logs (Appendix A) and grain size analysis results (Table 3 and Table 4) for PW01 and MW03, which were assigned initial K values one half order of magnitude different. All values were adjusted during calibration (final K values in Table 14). In Table 14, HSUs are shown to have different colours to correspond with the HSUs in Figure 37 and Figure 38.

Table 14*: Initial estimates of K and final values of K in the calibrated model.*

HSU #	$K_{initial}$ (m/s)	K_{final} (m/s)
1	1.0E-03	1.0E-03
2	2.5E-05	6.0E-04
3 upper	1.0E-03	5.0E-04
3 lower	5.0E-04	9.0E-05
4	8.0E-04	5.0E-04
5	1.0E-07	5.0E-05
6	1.0E-10	1.0E-08

Boundary Conditions

Zero recharge was applied to the model because the pumping test simulation period is very short. Moreover, no precipitation fell at the Otter Park site during this time.

The northern and southern boundaries of the model domain were assigned general head boundary conditions. A general head boundary condition is typically used when a source of water with a known hydraulic head exists some known distance away from the boundary (e.g., a distant equipotential contour). Use of this boundary condition allows the domain to be smaller than would be otherwise necessary if the distance source were included. The static water levels from nearby wells WTN92057 and WTN29107 were used to assign the head along the northern and southern general head boundaries. The hydraulic conductivity of the northern general head boundary was assigned a value of 0.001 m/s, while

the southern boundary was assigned a value of 0.0001 m/sec based on the general lithology shown in cross-section #2 (Appendix D). The main function of these general head boundaries was to generate a regional flow field directed toward Bertrand Creek.

Bertrand Creek itself was assigned a stream boundary condition, a type of head-dependent (or Cauchy) boundary condition that allows for leakage to occur across the boundary (i.e. a flux) that depends on the head difference between the aquifer and the stream. Streams are defined by segments. For each segment, the stream stage and volumetric inflow (i.e. streamflow) measured at each end of the segment, along with streambed top elevation, streambed bottom elevation, stream width and streambed K vertical are entered as input. Leakage across the streambed (to and from the underlying aquifer) is calculated using a conductance, C, which is defined as the product of the stream width, cell length and the vertical hydraulic conductivity, divided by the streambed thickness. The model used four stream segments, with ends anchored to the five hydrometric stations (e.g. segment 1 had HS1 at the upstream end and HS2 at the downstream end). Streambed bottom elevation was 2 m below the measured streambed top. The K vertical value was assigned a value 0.001 m/s.

Model Calibration

The model was calibrated by trial and error, primarily against the observed time-varying observations in the hydrometric stations, the groundwater wells and the instream piezometers. Although the overall model calibration was also assessed using standard statistics.

The “calibrated” model is highly non-unique, meaning that other combinations of parameters exist that would lead to an equally “calibrated” model. That said, the model was rather sensitive to relatively minor adjustments in K (but not the storage properties Sy and Ss). If K was lowered too much, particularly for the main aquifer HSUs, then the simulated drawdown was too high, and the model dewatered and crashed.

Use of the stream boundary condition presented challenges for model calibration. First, a stream boundary conditions is placed as a line in the model, but in reality there is some width to a stream. This means that piezometers and hydrometric stations used as observation points for calibration had to be moved into cells through which the stream boundary condition line passed. This was particularly problematic for instream piezometers across the central line of the stream, which are located at different distances from the pumping well. Therefore, only one central piezometer D10 was used to represent the group of piezometers across the center line.

Another issue is that, in reality, pumping wells have some inefficiency. Well inefficiency cannot be modeled in MODFLOW (i.e., well loss effects cannot be simulated). This means that if you attempt to match the drawdown in the pumping well, you would need to use a lower K/Ss than represents the aquifer. This causes the simulated drawdown in observation wells to be too high. Therefore, for this model, more emphasis was placed on calibrating the observation wells, with less drawdown than observed targeted for the pumping well.

Uncertainty in the depths of the piezometers (and thus the logger elevations) led to uncertainties in the calculation of hydraulic head in the piezometers. For the purposes of modeling, piezometers were assigned an initial head with the same value as the nearest hydrometric station. Thus, initial observed heads in the instream piezometers ranged from 74.086 (at D46 referenced to HS2) to 74.083 (at D10 referenced to HS3) to 73.833 (at D34 referenced to HS4), for a total range of 0.253 m.

Ultimately, for the instream piezometer calibration, the uncertainties in having to shift piezometers to bring them closer to the stream boundary condition, the challenges with elevation referencing, and the

similarity of initial heads meant that only relative differences in simulated hydraulic heads could be examined during calibration.

6.4.3 Numerical Modeling Results

Overall Calibration

Figure 39 shows the overall model calibration results for all time steps. Most of the calibration points (instream piezometers and hydrometric stations) are in model layers 3 and 4 (stream sediments) except for HS1 which is located in layer 5, PW01, MW01 and MW02 which are in layer 14, and MW03 which is in layer 21.The coloured symbols are observations at the end of the simulation (11459 minutes), while the black outlined symbols show the head values at different times.

The normalized root mean squared error (RMSE) was 4.8% and the correlation coefficient was 0.974. These excellent calibration results are not unexpected because all calibration points lie within a very small range of the overall range in head across the site.

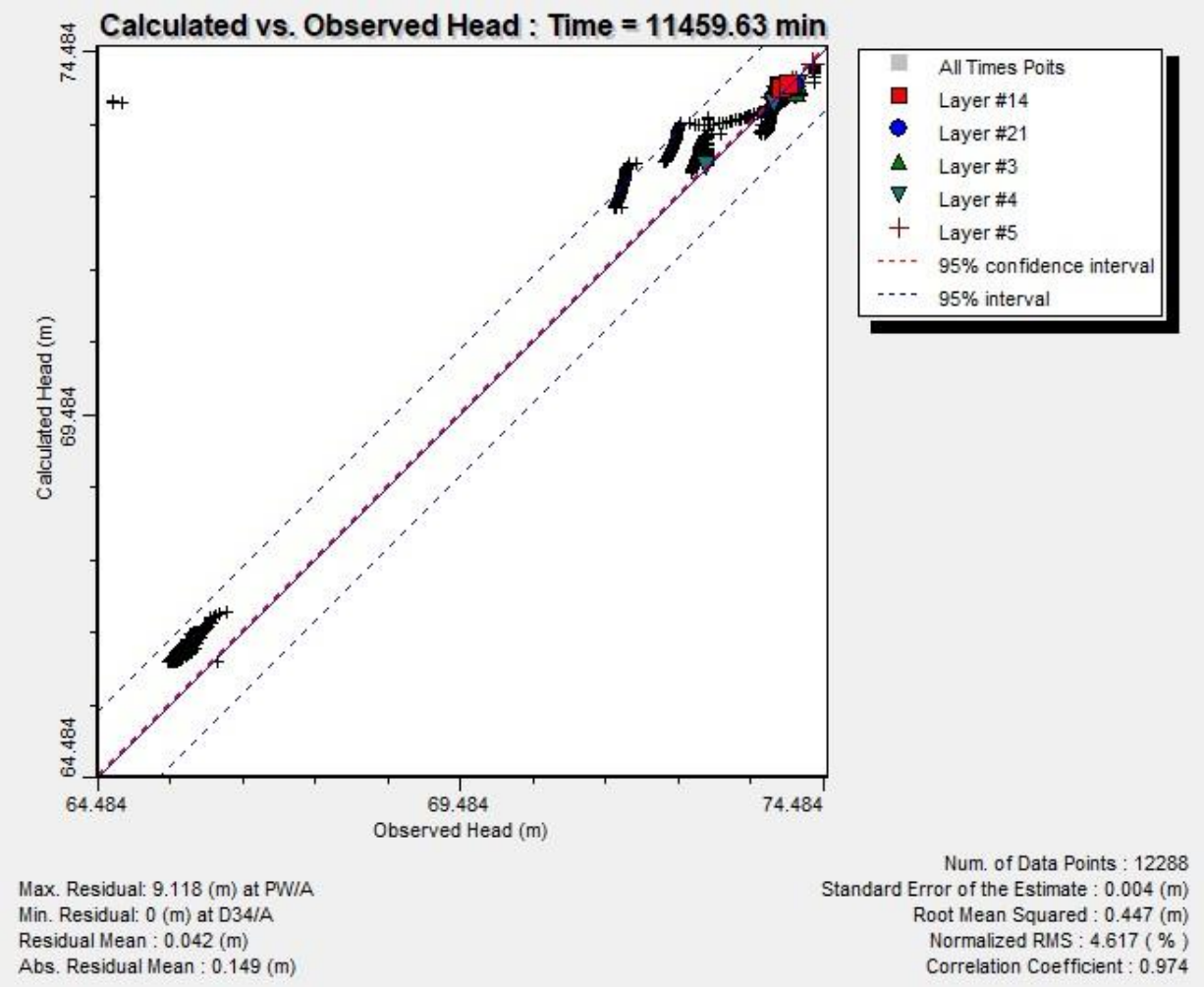

Figure 39: Overall numerical model calibration results. Results are shown for all time steps. The coloured symbols are observations at the end of the simulation (11459 min), while the black outlined symbols represent observations at other times.

Time Series Calibration

Figure 40 shows the time series (head versus time) calibration results for all observation points. The calibration results are shown and discussed separately for the wells, the hydrometric stations, and the instream piezometers.

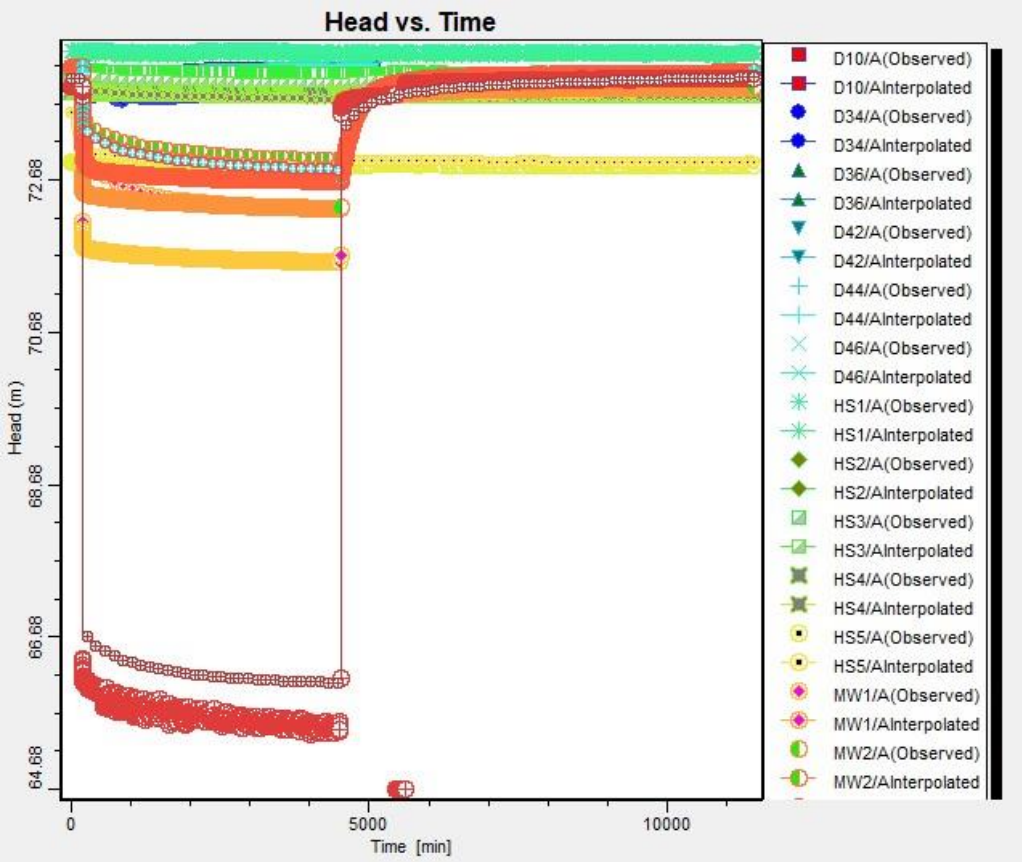

Figure 40: Calibration results for all observation points.

Figure 41 shows the time series calibration results for the wells. As discussed previously, the targeted drawdown in the pumping well was intentionally less than the observed drawdown to account for potential well loss effects. Overall, the simulated drawdown changed more gradually compared to the more abrupt observed drawdown. The responses of MW01 and MW02 (and PW01) were found to be quite sensitive to K. If too low a K was assigned to the lower zone in HSU #3 (where the wells are completed), the model crashed because there was too much drawdown. Ultimately, the K values of upper zone of HSU #3 and HSU #4 were important for buffering the drawdown.

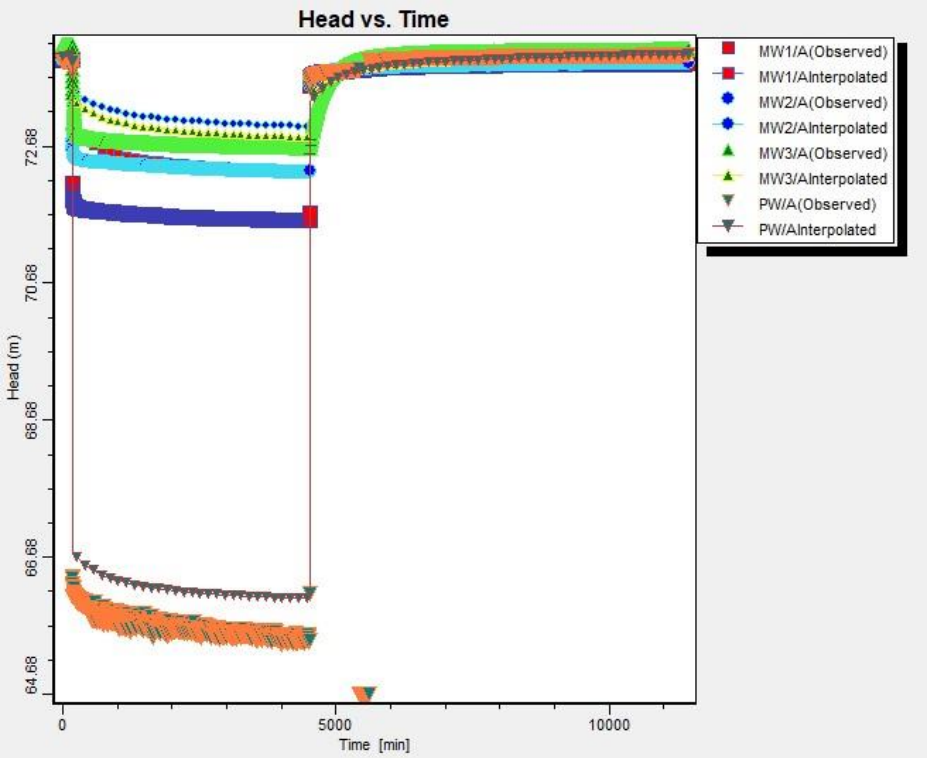

Figure 41: Calibration results for the wells.

Figure 42 shows the time series calibration results for the hydrometric stations. Even though the observed heads (stages) for each hydrometric station were used to define the stream boundary condition, accurate simulation of the heads in the cell where the hydrometric station was located is important. Figure 42 shows some early time head adjustments that are common in many transient models, despite experimenting with different initial head distributions (e.g. previous model runs). Perhaps the most noticeable difference is for HS3, which has a simulated head that is more consistent with what would be expected for its distance downstream of HS2. Notice that the observed head in HS3 overlaps with HS2. It is unclear why the observed heads at HS3 and HS2 overlap to this degree, but the simulation results are reasonable in that they show a progressive reduction in head downstream from HS1 to HS5. The slight reduction in observed stage at around 4000 minutes is accentuated in the simulation results.

Figure 43 shows the time series calibration results for the instream piezometers. The first point to mention is the offset of the observed head in piezometer D34 compared to the other piezometers. D34 is the furthest downstream at the end of a riffle, and the elevation does drop noticeably from D36 to D34. Also, D34 was the only deep piezometer that had more drawdown than its shallower counterpart (see Figure 24). The observed heads for all other piezometers plot as a group with very similar initial heads and responses.

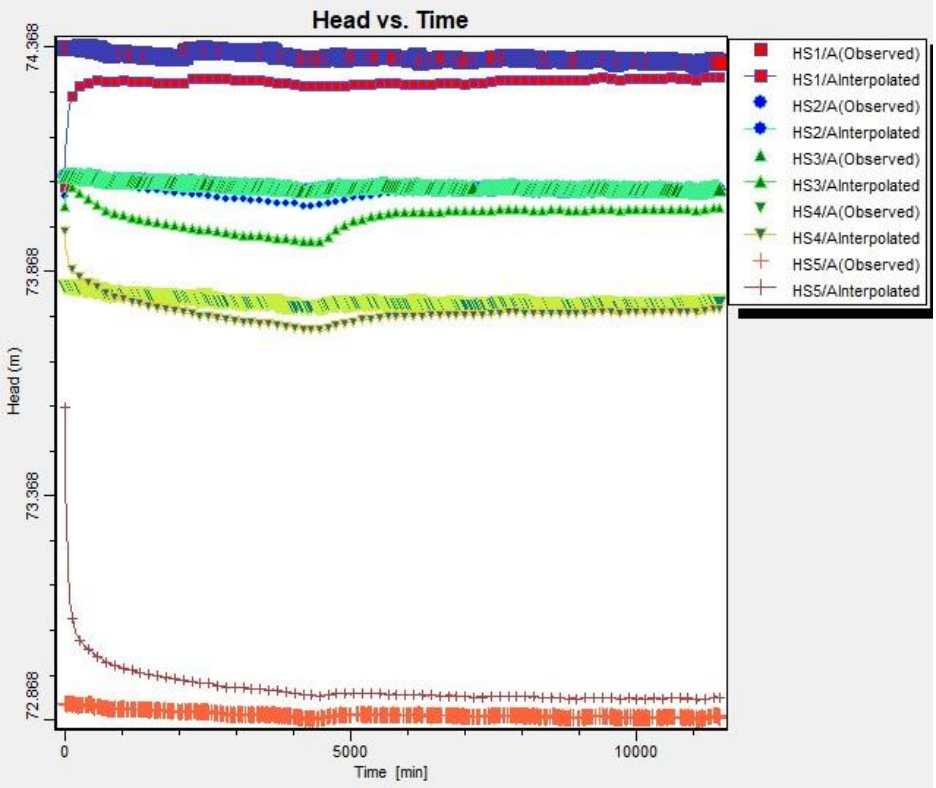

Figure 42: Calibration results for the hydrometric stations.

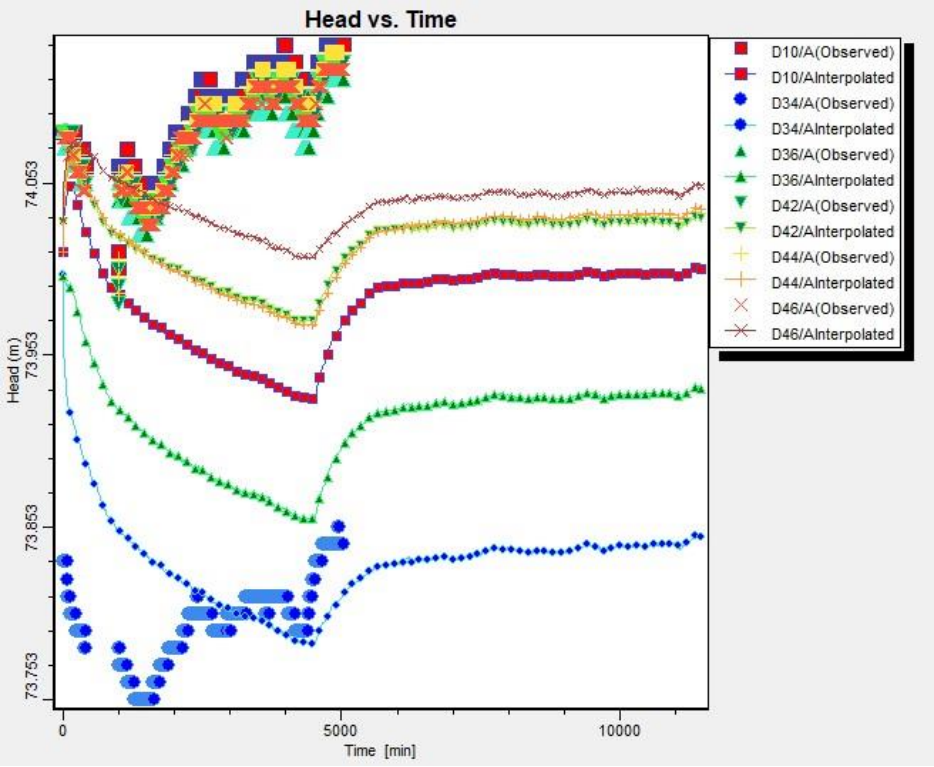

Figure 43: Calibration results for the instream piezometers.

The second point is that the simulation generated more drawdown in all piezometers compared to observed. Moreover, the simulated response of the instream piezometers was overall quite different than the observed response. The simulation produced a typical drawdown response in the piezometers until the end of pumping (at 4520 minutes), followed by recovery. However, the observations show drawdown at early time (until approximately 1500 minutes), followed by a rapid increase in head, and then nearing the end of pumping (at around 4000 minutes), the observed heads in the piezometers drop, similar to what was observed with stream stage. So, something unusual happened in the instream piezometers that could not be reproduced in the model. It is interesting to note that the observed streamflow at HS1 increased on October 12 at 23:45 (this is approximately 28.5 hours into the pumping test or 1710 minutes (see Figure 20), roughly the same time as the heads in the piezometers increased. However, the discharge (and stage) did not similarly increase at the other hydrometric stations. So, the cause of the unusual piezometer heads is not known.

Mass Balance

The overall mass balance ranged from -3.4% to 1.7% (Figure 44). These results are generally satisfactory, as model mass balance discrepancies should be less than 5%. However, the mass balance is not stable throughout the simulation, despite numerous attempts to alter solver settings to improve the mass balance. The maximum total mass balance error is approximately -3.4% at 1500 minutes. This percentage corresponds to a volumetric discrepancy of approximately -224 m^3. This is not an insignificant volume. For comparison, the volume entering the aquifer from the stream is ~820 m^3 and the volume leaving the stream is ~1400 m^3 at 1500 minutes, so a -224 m^3 discrepancy is potentially significant if all of the mass discrepancy is solely associated with the transfer of water between the stream and the aquifer. Unfortunately, the mass balance output does not attribute mass discrepancy to any particular boundary condition, but if this discrepancy is applied entirely to the streambed leakage, then it could account for a significant mass balance error for this component. This suggests the simulated volumetric exchanges associated with streamflow depletion should be viewed with caution.

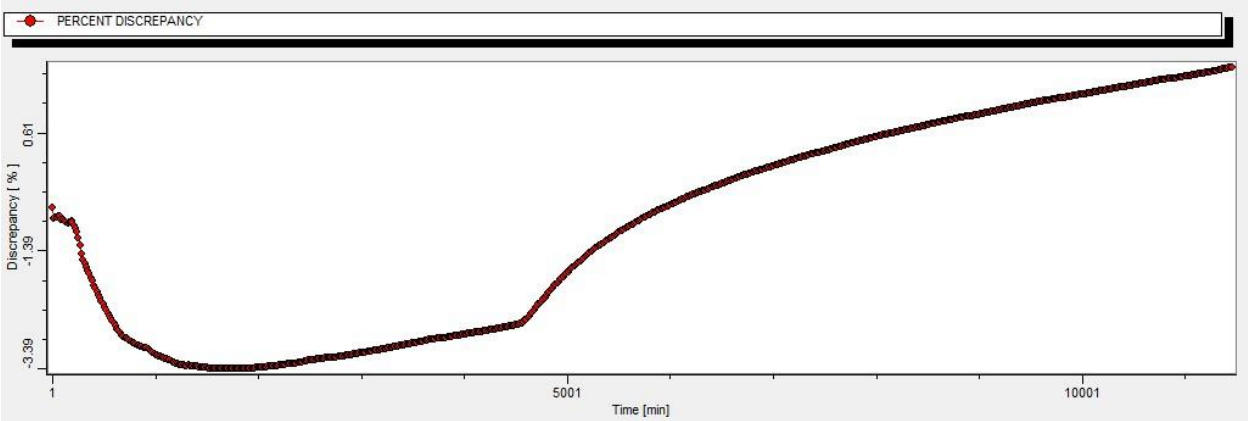

Figure 44: Model mass balance showing percent discrepancy throughout the simulation.

Figure 45 shows the pre-pumping cumulative volumetric water exchange (leakage) between the stream and the aquifer system, where the aquifer system is defined as all HSUs. The lower line on the graph represents leakage from the stream to the aquifer system and the upper line the leakage from the aquifer system to the stream. Thus, throughout this period, the aquifer system was losing water to the stream; although, the rate of loss reduced slightly over time – i.e. the line flattens (simulated volumetric exchanges are annotated).

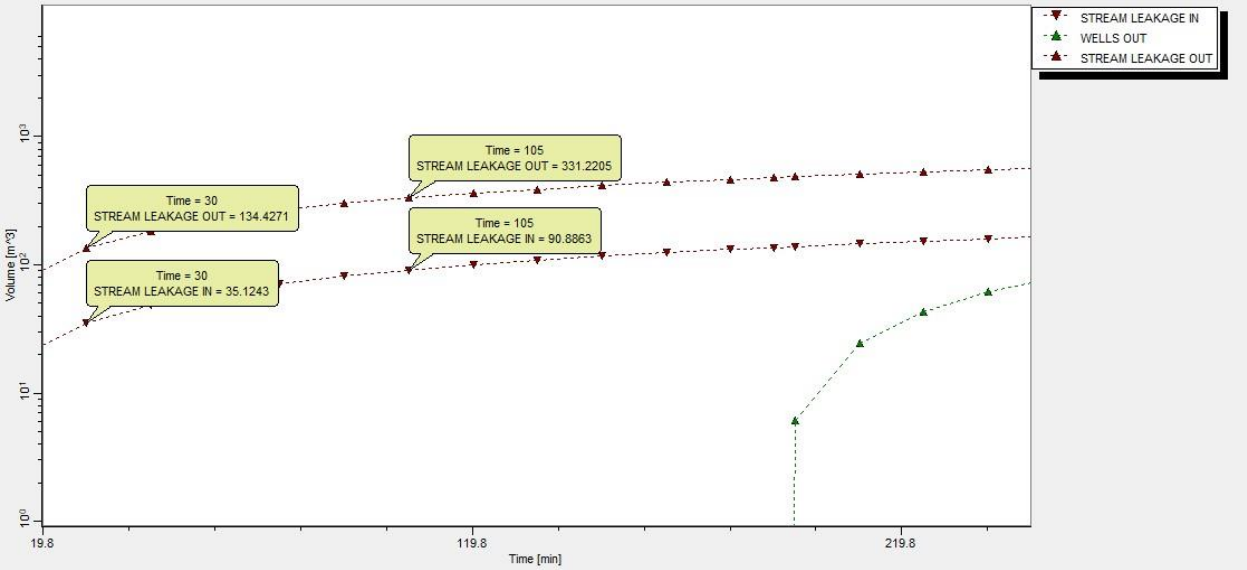

Figure 45: Pre-pumping cumulative volumetric water exchange (leakage) between the stream and the aquifer system. Leakage into the aquifer system is shown as the bottom line and leakage from the aquifer system to the stream is shown as the top line. The pumped volume is shown on the far right when pumping begins.

Figure 46 shows the cumulative volumetric water exchange during pumping. Also shown is the cumulative volumetric outflow from the pumping well. As the volume of water lost through pumping increases, the difference in the leakage in and out reduces. At approximately 2250 minutes (34 hours into the pumping test), the leakage lines cross (arrow). This occurs because the leakage from the aquifer into the stream slows (the line flattens). While, the leakage from the stream into the aquifer system continues to increase.

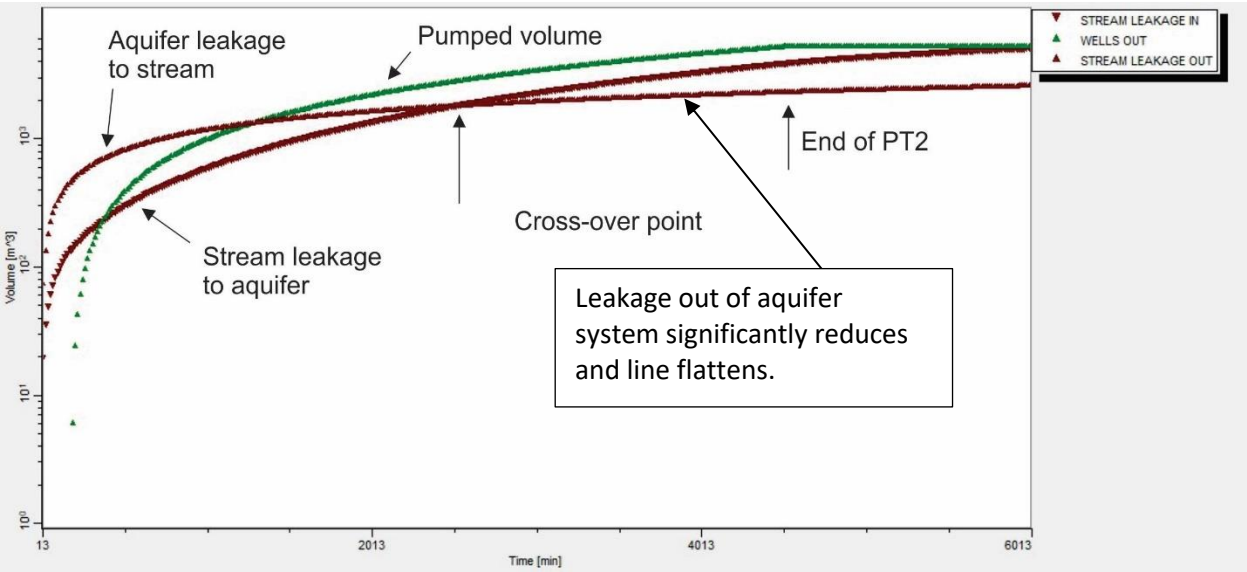

Figure 46: Pumping cumulative volumetric water exchange between the stream and the aquifer system. Leakage from the stream into the aquifer system is initially lower than leakage from the aquifer system to the stream; however, the two lines cross at approximately 2250 minutes (after 34 hours of pumping). The green line shows the cumulative volumetric loss of water from pumping.

At the cross-over point at 2250 minutes in Figure 46 (i.e. when the stream largely switched from being overall gaining to overall losing), the cumulative volumetric exchanges (leakage out of the aquifer to the stream, and leakage from the stream to the aquifer) were both approximately 1856 m^3. At 4520 minutes (end of pumping), the cumulative loss from the aquifer to the stream was 2351 m^3 and the cumulative gain to the aquifer from the stream was 3927 m^3, for difference of **1576 m^3 over a period of 2270 minutes (37 hours) from the cross-over point**. The Hunt model estimated **1460 m^3 over the 72-hour period**, while the piezometry estimate was **1510 m^3 over the 72 hours.**

Based on the simulation results, the stream largely switched from being a gaining stream to a losing stream approximately 36 hours into the pumping test. This is an interesting result, because the despite the model uncertainty, at 4:30 am on October 14th (roughly 33 hours and 15 minutes into the pumping test), the streamflow noticeably dropped at all hydrometric stations (Figure 20).

7. CONCLUSIONS AND RECOMMENDATIONS

The four main objectives of the study were: 1) Estimate the hydraulic conductivity (K) of the aquifer and streambed sediments using grain size analysis and slug testing; 2) Estimate the transmissivity (T), hydraulic conductivity and specific yield (Sy) of the aquifer from pumping test data; 3) Characterize the hydraulic connectivity between the stream and the aquifer; and 4) Quantify streamflow depletion during pumping and evaluate against a streamflow depletion model.

7.1 Hydraulic Properties

Several methods were used to determine the hydraulic properties of the aquifer and the streambed sediments at Otter Park.

Five analytical grain size distribution methods were used to analyze the streambed sediment samples, of which the Chapuis was deemed the most applicable because the majority of the equation's conditions were met. The geomean of the minimum K values was 6.79×10^{-4} m/s and the geomean of the maximum K values was 4.75×10^{-3} m/s (Table 9). The Bouwer-Rice and Hvorslev methods were used to estimate the K of the streambed sediments based on slug testing in the deep and shallow instream piezometers. The deeper piezometers had a geomean K of 1.46×10^{-5} m/s determined by the Hvorslev method and a geomean K of 1.39×10^{-5} m/s using the Bouwer-Rice method (Table 9). The shallower piezometers had a geomean K of 3.41×10^{-5} m/s using the Hvorslev method and a geomean K of 3.77×10^{-5} m/s using the Bouwer-Rice method (Table 9). A student t-test showed the geomean K values for the deep and shallow piezometers are statistically different for the Bouwer-Rice method. However, the deep and shallow K values are still within the same order of magnitude. The slightly lower K of the deeper piezometers may reflect retention of fines of the deeper piezometer in the streambed compared to the shallower piezometers in the streambed.

For aquifer sediments, the Chapuis method was also the most applicable, with geomeans of the minimum and maximum K values ranging from 2.12×10^{-4} to 1.55×10^{-3} m/s for sediments from PW01, and from 1.44×10^{-4} to 1.11×10^{-3} m/s for sediments from MW03 (Table 10). The minimum and maximum K values produced by the Chapuis method bracket the range of K values determined from other methods. For example, for the slug/bail test data, the Hvorslev method gave a K of 7.62×10^{-4} m/s and the Bouwer-Rice method gave a K of 5.49×10^{-4} m/s (Table 10). Using data collected during PT2, a K value of 1.29×10^{-4} m/s was estimated with the Neuman method and a K value of 6.51×10^{-4} m/s from the Theis Recovery method (Table 10).

Overall, the results from all methods suggest that the K value for the aquifer is approximately one half order of magnitude higher than the streambed sediments, which indicates the likelihood of the instream piezometers being screened in a clogging layer (layer of relatively lower K compared to the aquifer). The range of K values for the streambed sediments determined from both grain size analysis and slug testing suggests the streambed sediments are spatially heterogeneous, both laterally and vertically. The implications of heterogeneity in streambed sediments is discussed in Section 7.2.

7.2 Hydraulic Connectivity and Streamflow Depletion

A streamflow rating curve was very difficult to construct for the site. While the rating curve during the early summer likely provides fairly accurate estimates of streamflow at the five hydrometric stations, the accuracy of the rating curve diminished over the late summer (low flow period) due to difficulties in measuring flow, the presence of significant instream vegetation, and beaver activity (Figure 9). Outside the late summer low flow period, HS1 (the most upstream) consistently had the highest discharge, followed by HS2 and HS3. Discharge at HS4 and HS5 were of similar magnitude (curves almost overlapped), despite being closer together than HS3 and HS4. The reduction in streamflow from HS1 to HS5 suggests that Bertrand Creek is losing under natural conditions from upstream to downstream through the site. The lower magnitude decrease in streamflow from HS4 to HS5 suggests that there is little to no groundwater contribution (or indeed loss to groundwater) along this reach.

Prior to PT2, streamflow was declining, which made it difficult to determine whether any streamflow depletion was occurring during pumping. All of the individual instream piezometers had an immediate response to pumping evidenced by a rapid drop in head. Drawdown occurred in all instream piezometers until approximately 24 hours into the pumping test when maximum drawdown was attained. Thereafter, until the end of the pumping test, the drawdown reduced and indeed became negative (water levels in the piezometers were higher than before pumping commenced). Vertical hydraulic gradients at each piezometer pair location were complex both prior to pumping and during pumping. The overall pattern suggests that prior to pumping there was a mix of upward and downward fluxes across the streambed at the site, possibly resulting from variations in streambed morphology in combination with variations in hydraulic conductivity. During the pumping test, most piezometers pairs had downward flows.

Streambed temperatures also differed pre-pumping, during pumping and post-pumping. During PT2, the difference in temperatures at two depths in the streambed gradually increased (i.e. the range increased between Tidbit pairs at some locations). This increase in range was most noticeable in Tidbits located near the stream bank. The cause of the increase in uncertain but is likely related to the streambank locations becoming more exposed as the streamflow declined following a rainy period two days prior to PT2, or possibly due to progressive streamflow depletion during the test. Interestingly, the time lag between Tidbits located upstream to downstream, which had been as high as 2 hours, reduced to near zero during the early recovery period. The streambed temperature data will be examined in more detail as part of ongoing research.

The variability in gaining or losing conditions along the stream made it difficult to characterize streamflow depletion with absolute certainty. However, several lines of evidence suggest that streamflow depletion occurred. 1) During the pumping test, streamflow decreased gradually at all hydrometric stations, but most notably right near the end of the test (Figure 20). The same phenomenon was observed during PT1. The onset of streamflow depletion was delayed as might be expected because pumped water initially derives from storage and it takes time for the pumping effects to propagate to the stream. 2) Once the pump was shut down the streamflow rebounded slightly. 3) Prior to and following pumping, the streamflow at HS4 was consistently higher than at HS5, while during

the pumping test the streamflow was almost the same magnitude as at HS5. 4) During pumping, the streamflow magnitudes at HS1, HS3 and HS4 were more similar than at any other time during non-pumping conditions (Figure 19). The same phenomenon was observed during PT1.

Over the 72 hours of pumping during PT2, streamflow depletion estimated from the vertical hydraulic gradients was 1510 m^3. An estimate of actual streamflow depletion of 500 m^3 was made using the rate of decline of streamflow over the last 14.25 hours of the test. This estimate is highly uncertain because streamflow had been declining prior to pumping. It is not possible to estimate streamflow depletion over the full 72 hours of the test using direct observations, but it was likely higher than 500 m^3.

The Hunt (1999) model estimated streamflow depletion to be approximately 1460 m^3 over the 72 hours, similar to the value estimated from the vertical hydraulic gradients (1510 m^3). The numerical groundwater flow model of the PT2 estimated streamflow depletion at 1576 m^3 over that last 37 hours of the pumping simulation. Prior to 37 hours, the stream continued to be gaining, with a switchover from gaining to losing occurring at 37 hours. Thus, the estimate from the numerical model is based on when the stream switched from being a net gaining stream to a net losing stream. This does not mean that streamflow depletion was not occurring along different sections of the stream earlier in the pumping test. Thus, the estimate of 1576 m^3 should perhaps be considered a lower estimate.

Another important uncertainty related to the estimate of streamflow depletion from the numerical groundwater flow model is the model mass balance error. Mass balance errors arise because the mathematical solution is inaccurate (i.e. the bank account is not balanced). Typically, a mass balance error less than 5% is considered acceptable. Indeed, the total mass balance discrepancy was below 5% over the entire simulation (i.e. it was acceptable); however, the discrepancy was not stable (see Figure 44). During the pumping period, the maximum total mass balance error gradually dropped from -0.88 (right before pumping) to -3.4% (at 1500 minutes). This percentage corresponds to a volumetric discrepancy of approximately -224 m^3. For comparison, at 1500 minutes, the volume entering the aquifer from the stream is ~820 m^3 and the volume leaving the stream is ~1400 m^3, so a -224 m^3 discrepancy is potentially significant if all of the mass discrepancy is solely associated with the transfer of water between the stream and the aquifer. Unfortunately, model mass discrepancy cannot be associated with any particular boundary condition (i.e. mass discrepancy is for the entire model, not its parts). So, the estimate of streamflow depletion from the groundwater flow model is uncertain.

A separate sensitivity analysis was carried out as part of this study (results now shown here). The numerical model was very sensitive to the hydraulic conductivity estimates, particularly those of HSU #4. Lowering K of HSU #4 by any more than 0.0001 m/s caused the model to crash (heads dropped too low in the pumping well). Changes in K values for the other HSUs produced little or no change in calculated hydraulic head values. Similarly, changes in specific storage (Ss) did influence the heads, but much less so than K.

The stream boundary condition presented some challenges with regard to the relative placement of instream piezometers that were used as observation points. Stream boundary conditions are lines having no actual width, so despite having piezometer data across the streambed, only single piezometers were placed at different distances along the stream. Moreover, only one piezometer in the nest was used because the vertical discretization could not be refined sufficiently in the top layer to give a computational layer thickness of 30 cm (the difference in depth between instream piezometers). Nevertheless, stream boundary conditions are really the only suitable option when using a groundwater flow code to simulate streamflow depletion. Other options, such as constant head or river boundary conditions specify the head (stage) along the entire length of the feature, which defeats the purpose of the modeling to explore how exchanges between the aquifer and the stream influence the stage.

In addition, the stream boundary condition was divided into four segments, with the ends of each segment anchored at each of the five hydrometric stations. This means that the stage and streamflow were specified at these five locations, and adjustments to the stream stage due to exchanges between the stream and the aquifer could only occur in between these anchoring points. This is a limitation of the model. Ideally, the stage and streamflow would only be specified at the upstream and downstream ends, allowing stage to vary along the entire stream reach in an unconstrained fashion. An attempt was made to anchor the stream boundary condition at HS1 (furthest upstream) and HS5 (furthest downstream), and thus allow the stage to vary along the entire reach. Unfortunately, the model was too ill-constrained and could not be satisfactorily calibrated. Thus, groundwater models have important limitations for simulating streamflow depletion due to how well model boundary conditions represent the real system. Ideally, an integrated model would be used, which explicitly models the stream and the aquifer, along with the exchanges.

One final consideration related to hydraulic connectivity and streamflow depletion are the implications of streambed sediment heterogeneity. This heterogeneity will impact the response of the instream piezometers to changes in gradient (i.e. relative changes in stream stage and groundwater level), however those may be caused. In fact, the lower K values for the deeper piezometers compared to the shallower piezometers caused the deeper ones to respond more slowly to changes in stream stage, which made the vertical fluxes difficult to interpret.

Perhaps a more important consequence of heterogeneity of the streambed sediments is that analytical models, such as the Hunt (1999) model, do not account for heterogeneity (either in the aquifer or the streambed sediments). Vertical heterogeneity of the streambed sediments can be accommodated in the analytical model by calculating an effective vertical K for layered media (see Freeze and Cherry, 1979); although this was not done in this study. However, lateral heterogeneity cannot be accommodated in the Hunt and similar analytical streamflow depletion models. In contrast, spatial heterogeneity can be accounted for in numerical models by varying the aquifer materials underlying the stream and/or adjusting the conductance values. For this study, the conductance value was uniform along the stream boundary condition. Both the Hunt model and the numerical model were sensitive to changes in vertical K (or conductance), so it is very important to collect sufficient field data to define the spatial variability of K across the site.

7.3 Recommendations

Several recommendations are made for reducing data uncertainty in any follow-up field studies at this site or elsewhere.

A large group of people volunteered to install the instream instrumentation (piezometers, hydrometric stations, etc.) and while this was a great benefit in terms of manpower, this created a somewhat hectic environment, which led to some mistakes and certain details not being recorded accurately. For example, all piezometers were meant to be installed with ~30 cm vertical separation between the nested pair. However, one pair (D37/D38) was installed at approximately the same depth, which increased the difficulty of accurately determining dl, ultimately resulting in anomalous vertical hydraulic gradient data. Increased communication and/or reduced group size for field work could reduce the possibility of details being overlooked.

Removal of dataloggers from instream piezometers and re-deployment following downloading of data and re-programming was a task delegated to different volunteers over the course of the project. While dataloggers did have serial numbers on them, and were associated with specific piezometers, it is possible that one or two got mixed up when being re-deployed in the pair. This could possibly account

for unusual gradient measurements in the full time series. A list of serial numbers / piezometer should be consulted each time a logger is re-deployed.

Data management was a challenge. Fortunately, one individual was responsible for downloading data and re-programming the loggers. That likely helped to reduce error. However, the datafiles accumulated over the course of the project were numerous. Multiple time series data had to be merged together to generate a complete time series. Each time loggers were removed, re-programmed and re-deployed, there were breaks in the data that had to be carefully examined. Ultimately, a huge amount of time was spent collating and filtering data and verifying the continuity and formatting of dates and times so that the data could be plotted in Excel (which does not handle date and time very well).

One possible issue with the dataset relates to time. One site laptop was used as the primary laptop for downloading and reprogramming loggers. However, occasionally a second laptop was used. Part way through the project, the team discovered that the loggers used in the hydrometric stations should standard time, as this is done by convention across Canada. Subsequently, the laptop was changed to standard time (from daylight savings time), but this could have resulted in a shift of an hour in the datasets that was not properly accounted for in the collated data. It is recommended that standard time be used in future, regardless of provincial time.

Another was barometric compensation. The research team had used several barologgers (for redundancy), but the sampling intervals were often inconsistent - some logged every second or at other intervals (for background and pumping test measurements in wells and instream piezometers), while some logged every 15 minutes (for the hydrometric stations). Solinst Leveloggers were used in the wells/instream piezometers, while Hobo loggers were used in the hydrometric stations. Having at least one (and ideally two) barologgers specifically associated with each logger type and purpose is recommended.

Streamflow rating curves proved challenging to construct. Two flow meters were used for development of the rating curve at Bertrand Creek, and they were estimated at to have a 10% difference in streamflow readings. Additionally, increasing the precision of the stream stage readings on the hydrometric station would also result in an increase in precision and reduce the uncertainty associated with stream discharge. In this study, most streamflow measurements were made in May, prior to the low flow period when the rating curve became inaccurate. Streamflow should be measured at regular intervals.

During PT1, an adjustment to the flow was made by the pumping contractor to keep the discharge at the agreed upon level prior to pumping. This adjustment significantly compromised the pumping test data. For the second pumping test, the pumping contractor was given clear direction not to make any adjustments to the pumping rate, and the data curve was much improved. Pumping rates should not be adjusted during the test, particularly at the beginning of the test.

7.4 Continuing Research

Continuing research at the site in Phase 3 involves a hydroecological component to develop a more comprehensive understanding of the linkages between instream flow conditions (streamflow, groundwater exchanges, streambed temperature, streambed morphology, water chemistry) and aquatic communities. The study is currently focusing on benthic invertebrates but may be expanded to include fish, notably the endangered Nooksack Dace. Phase 3 will include an in-depth analysis of the datasets acquired during Phase 2 under summer background (non-pumping conditions) alongside new datasets collected in summer 2020.

During Phase 2, the research team noted significant declines in streamflow during the late summer at Otter Park. To explore and quantify exchanges between the aquifer and Bertrand Creek at a regional scale, a numerical groundwater flow model of Bertrand Creek Watershed has been developed. Details on the model design and findings will be described in a forthcoming Water Science Series report.

REFERENCES

American Society of Testing and Materials. 2014. ASTM D422-63: Standard test method for particle-size analysis of soils.

Armstrong, J.E. 1981. Post-Vashon Wisconsin Glaciation, Fraser Lowland, British Columbia. Bulletin 332, Geological Survey of Canada.

Bertrand Creek Enhancement Society (BCEC). 2008. Where is the Bertrand Creek watershed? Available from: http://www.bertrandcreek.ca/ (accessed July, 2018).

Beyer, W. 1964. Zur Bestimmung der Wasserdurchlassigkeit von Kieson und Sanduen aus der Kornverteilung, Wasserwirt. Wassertech, 14: 165–169.

Bouwer, H., and R. Rice. 1976. A slug test for determining hydraulic conductivity of unconfined aquifers with completely or partially penetrating wells. Water Resources Research, 12(3): 423-428.

Butler, J.J., Jr. 1998. The Design, Performance, and Analysis of Slug Tests (1st ed.). New York: Lewis Publishers, 252 pp.

Chapuis, R.P. 2004. Predicting the saturated hydraulic conductivity of sand and gravel using effective diameter and void ratio. Canadian Geotechnical Journal, 41(5): 787-795.

Cooper, H.H. and C.E. Jacob, 1946. A generalized graphical method for evaluating formation constants and summarizing well field history, Am. Geophys. Union Trans., 27: 526-534.

Fetter, C.W. 2001. Applied Hydrogeology (4th ed.). Upper Saddle River, New Jersey: Prentice Hall.

Freeze, A.R. and Cherry. J.A. 1979. Groundwater. Prentice-Hall, Inc. Englewood Cliffs, New Jersey, 29 pp.

Hall, G. 2017. Investigation of Aquifer-Stream Connectivity at Steele Park, Langley BC. BSc Honours Thesis, Department of Earth Sciences, Simon Fraser University.

Hall, G. D.M. Allen, M. Simpson, H. Tolera, B. Jackson, M.A. Middleton, and M.A. Lepitre, M. 2017. Assessment of Hydraulic Connectivity Related to Groundwater Extraction on Selected Sensitive Steams: Phase 1 Field Investigation. Water Science Series, WSS2017-02. Prov. B.C., Victoria B.C., 79 pp.

Hunt, B. 1999. Unsteady stream depletion from ground water pumping. Ground Water, 39(1): 98-102.

Hvorslev, M. 1951. Time Lag and Soil Permeability in Ground-water Observations. Waterways Experiment Station. Vicksburg, Mississippi: Corps of Engineers, U.S. Army.

Johnson, B. 2018. Aquifer-Stream Connectivity at Otter Park, Langley, BC. BSc Honours thesis, Department of Earth Sciences, Simon Fraser University, 141 pp.

Middleton, M.A. and D.M. Allen. 2017. Assessment of Hydraulic Connectivity Related to Groundwater Extraction on Selected Sensitive Streams: Stream Vulnerability Mapping. Water Science Series, WSS2017-04. Prov. B.C., Victoria, B.C., 28 pp.

NAVFAC. 1974. Soil mechanics, foundations, and earth structures. Naval Facilities Engineering Command (NAVFAC) design manual DM7. U.S Government Printing Office Washington, D.C.

Neuman, S.P. 1975. Analysis of pumping test data from anisotropic unconfined aquifers considering delayed gravity response. Water Resources Research, 11(2): 329-342.

Pearson, M.P. 2004. The Ecology, Status and Recovery Prospects of Nooksack Dace (rhinichthys cataractae spp.) and Salish Sucker (catostomus sp.) in Canada. Ph.D. Thesis, University of British Columbia, Vancouver.

Starzyk, C.A. 2012. Simulating Surface Water-Groundwater Interaction in the Bertrand Creek Watershed, BC. Ph.D. Thesis, Department of Geologic Engineering, University of British Columbia, Vancouver, BC.

Theis, C.V. 1935. The relation between the lowering of the piezometric surface and the rate and duration of discharge of a well using groundwater storage, American Geophysical Union Transactions, 16, 519-524.

Vukovic, M., and A. Soro. 1992. Determination of Hydraulic Conductivity of Porous Media from Grain-size Composition. Water Resources Publications, Littleton, Colorado, USA.

Waterloo Hydrogeologic Inc. 2019. AquiferTestPro, version 9.0. Waterloo Hydrogeologic Inc.

Whistler, A. 2018. Investigating the Thermo-Hydraulic Regime of Union Creek, Langley B.C. B.Sc. Honours Thesis, Department of Earth Sciences, Simon Fraser University, 96 pp.

APPENDIX A. BOREHOLE LOGS.

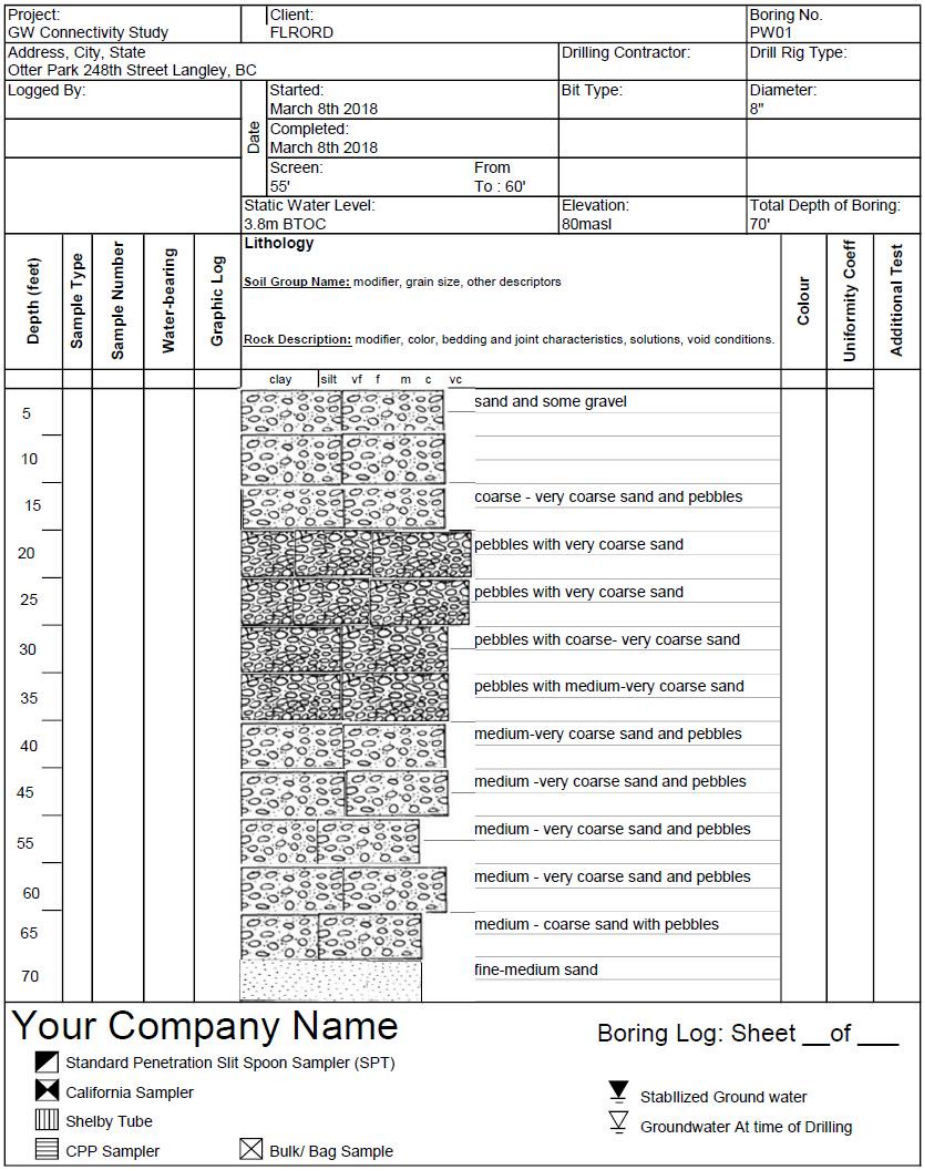

Figure A1: Well log for Pumping Well PW01 at Otter Park, Langley.

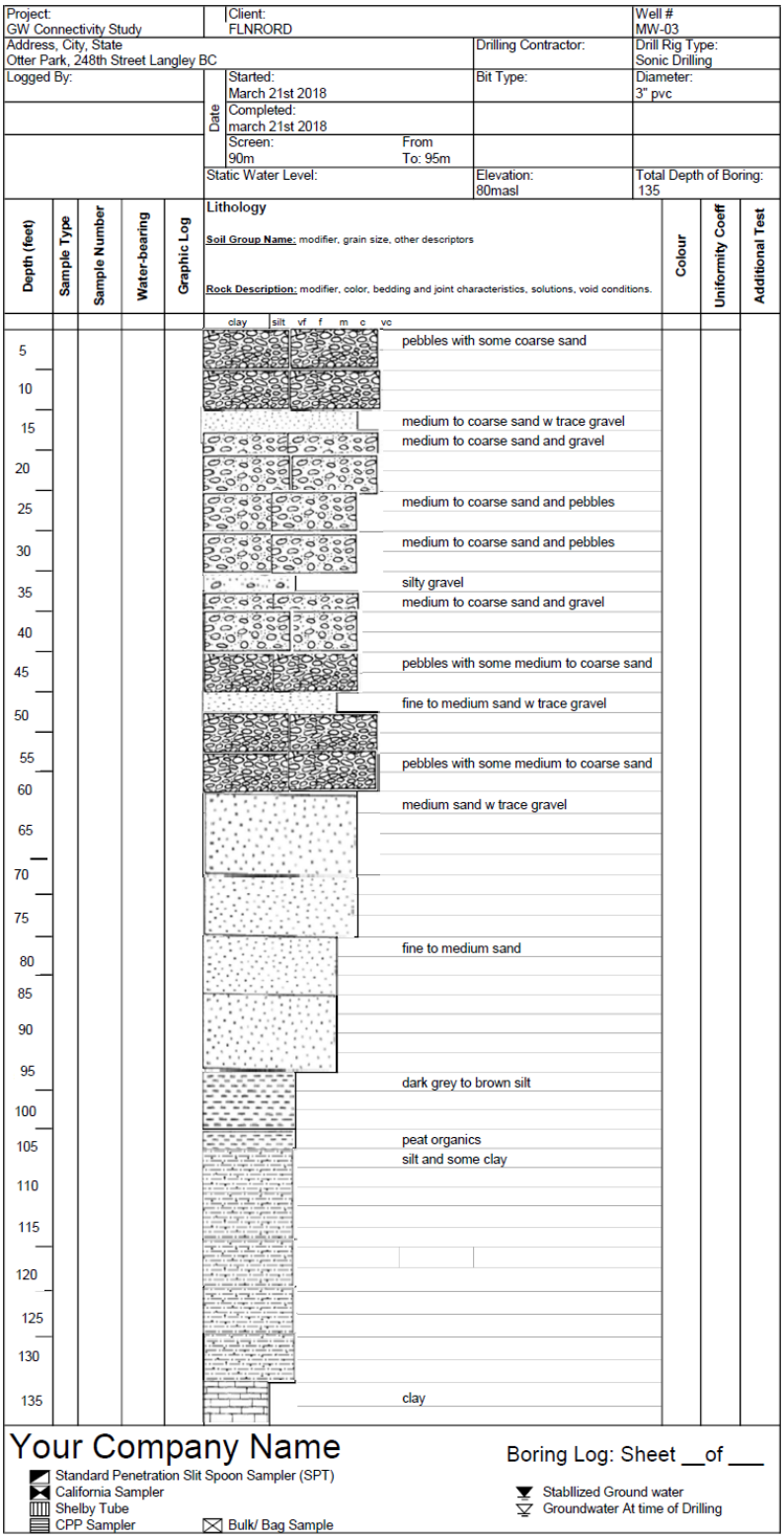

Figure A2: Well log for Monitoring Well MW03 at Otter Park, Langley.

Figure A3: Location of nearby water wells relative to PW01 (source: iMapBC)

APPENDIX B. CORRECTIONS FOR CALCULATING VERTICAL HYDRAULIC GRADIENT IN INSTREAM PIEZOMETERS.

Calculating the hydraulic gradient between the nested piezometers was a multi-step process. Two approaches were used depending on whether the piezometer was installed vertically or at an angle. All variables used in Equations B1 to B4 are displayed in Figure B1.

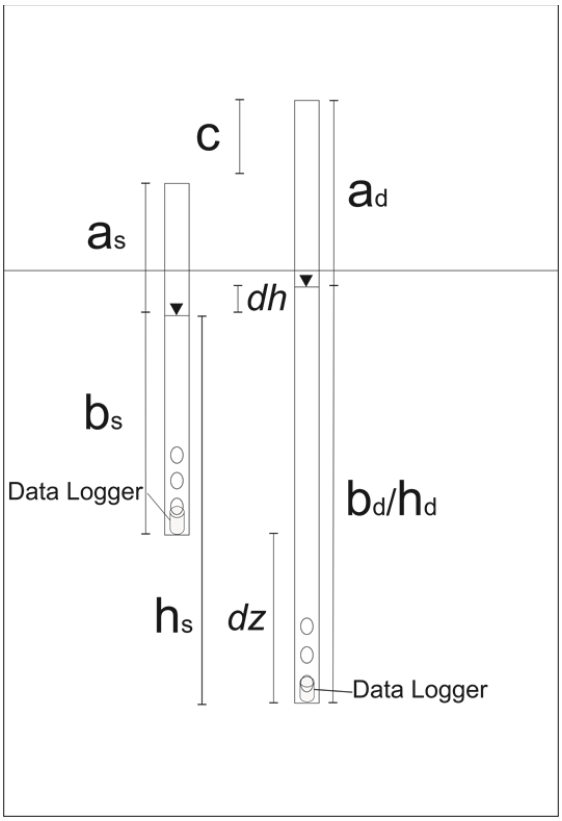

Figure B1: Piezometer geometry for conceptually calculating the hydraulic gradient between nested pairs. The subscripts s and d represent the shallow and deep piezometers, respectively.

The difference in hydraulic head, dh, between each piezometer pair was calculated by first referencing a single point in time water level measurement made by the logger against the depth to water level measured from the top of casing using a water level tape. The relative elevations of top of casing of each piezometer had been surveyed on May 11th 2018. The difference in the hydraulic head was calculated using $dh = a_d \pm (a_s + c)$ Equation B1, where the piezometer with the higher top of casing elevation was the reference point. As illustrated in Figure B1, the equation is:

$$dh = a_d \pm (a_s + c) \quad \text{Equation B1}$$

where:

a_d = depth to water in the deeper piezometer; measured with a Solinst water level tape

a_s = depth to water in the shallower piezometer; measured with a Solinst water level tape

c = the difference in elevation of the top of casing of the piezometers.

This single point in time dh value was then used to calculate the exact difference in logger depth between each pair, dz, using Equation B2:

$$dz = (b_d \pm dh) - b_s \quad \text{Equation B2}$$

where:

± is determined by whether the shallow or deep piezometer has a higher hydraulic head

b_d = the height of the water column in the deep piezometer

b_s = the height of the water column in the shallow piezometer

dh as calculated using Equation 1.

The separation dz should be the same as dl if the loggers indeed rested on the bottom of the piezometers. The dz value was used calculate h_s (Equation B3) for use in Equation B4 to calculate the hydraulic gradient.

$$h_s = b_s + dz \quad \text{Equation B3}$$

$$hydraulic\ gradient = \frac{dh}{dl} = \frac{|hd - hs|}{dl} \quad \text{Equation B4}$$

where:

dh = the difference in head between the data loggers in nested pairs

dl = the separation between the bottom depths of the nested pairs (assumed to be equal to the separation between logger depths (dz))

h_s = hydraulic head in the shallow piezometer

h_d= hydraulic head in the deep piezometer

Because it was not possible to install all piezometers vertically (as in Figure B1) due to cobbles in the streambed, corrections had to be made for piezometers that were installed at angles (Figure B2). The corrected length(s) were then applied to the vertical hydraulic gradient calculations when necessary for dl in Equation B5. As for the vertical piezometers, dz was assumed equal to dl.

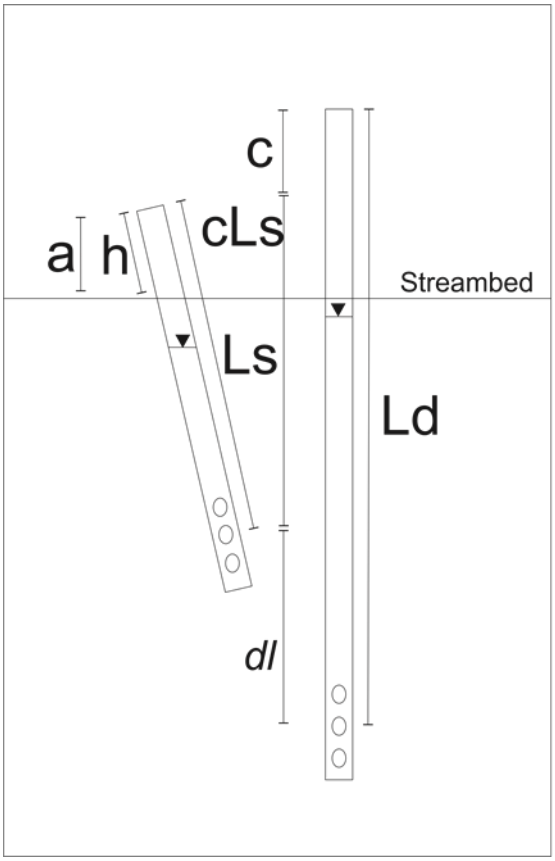

Figure B2: Piezometer geometry for calculating the hydraulic gradient between nested pairs when one (or both) is not installed vertically.

$$\theta = cos^{-1}\frac{a}{h}$$ Equation B5

$$\mathrm{c}Ls = \cos(\theta) * Ls$$ Equation B6

where:

a = is the adjacent length in the angle between the piezometer and the vertical; it was measured from the top of the piezometer straight down to the streambed

h = the hypotenuse value in the angle between the piezometer and the vertical; it was measured from the top of the piezometer to the streambed along the length of the piezometer

θ = the angle of tilt

cLs = corrected length of the shallow piezometer

For tilted piezometers, no correction for dh is needed because only the vertical component of pressure is measured by the transducer. Thus, the values for b_d or b_s remain unchanged.

APPENDIX C. DRAWDOWN AND HYDRAULIC GRADIENT MEASURED IN INSTREAM PIEZOMETER PAIRS DURING PUMPING TEST 2 (PT2)

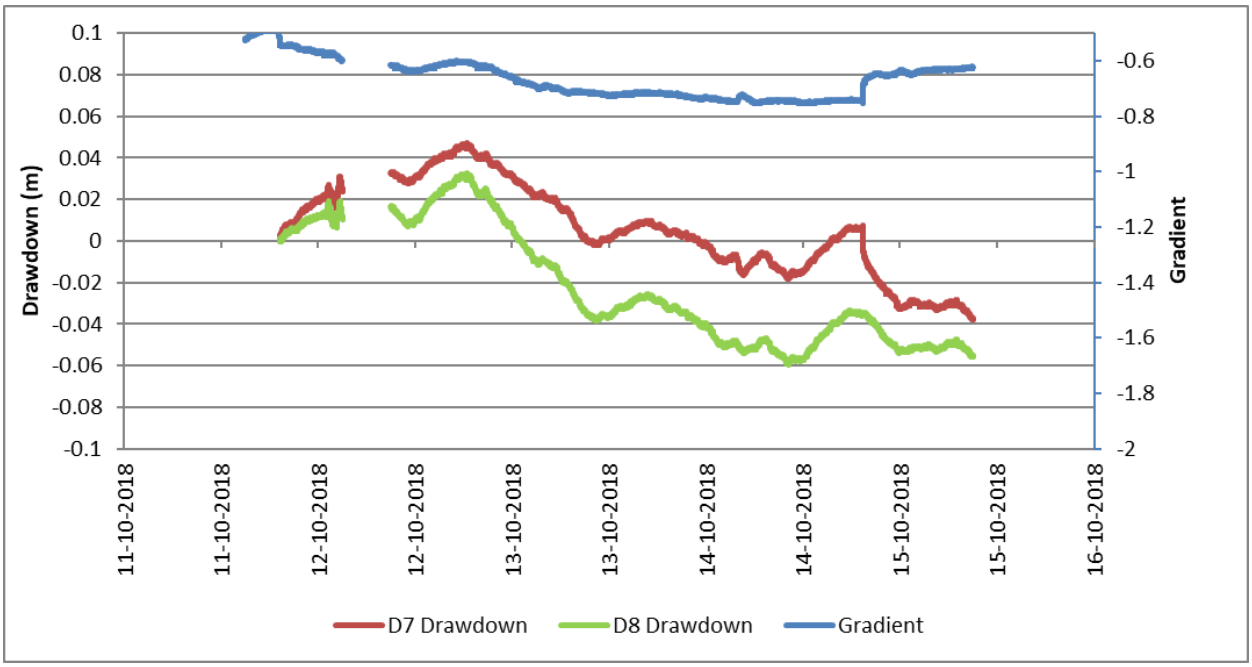

Figure C1: Drawdown and vertical hydraulic gradient in D7/D8 during PT2.

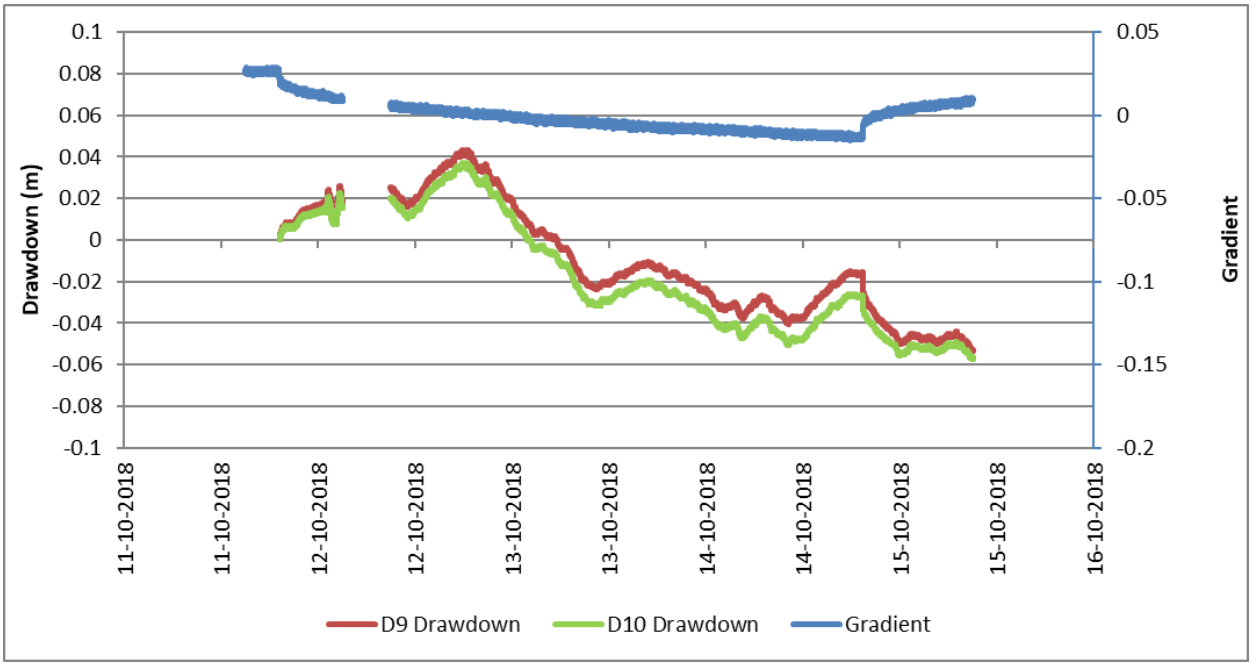

Figure C2: Drawdown and vertical hydraulic gradient in D9/D10 during PT2.

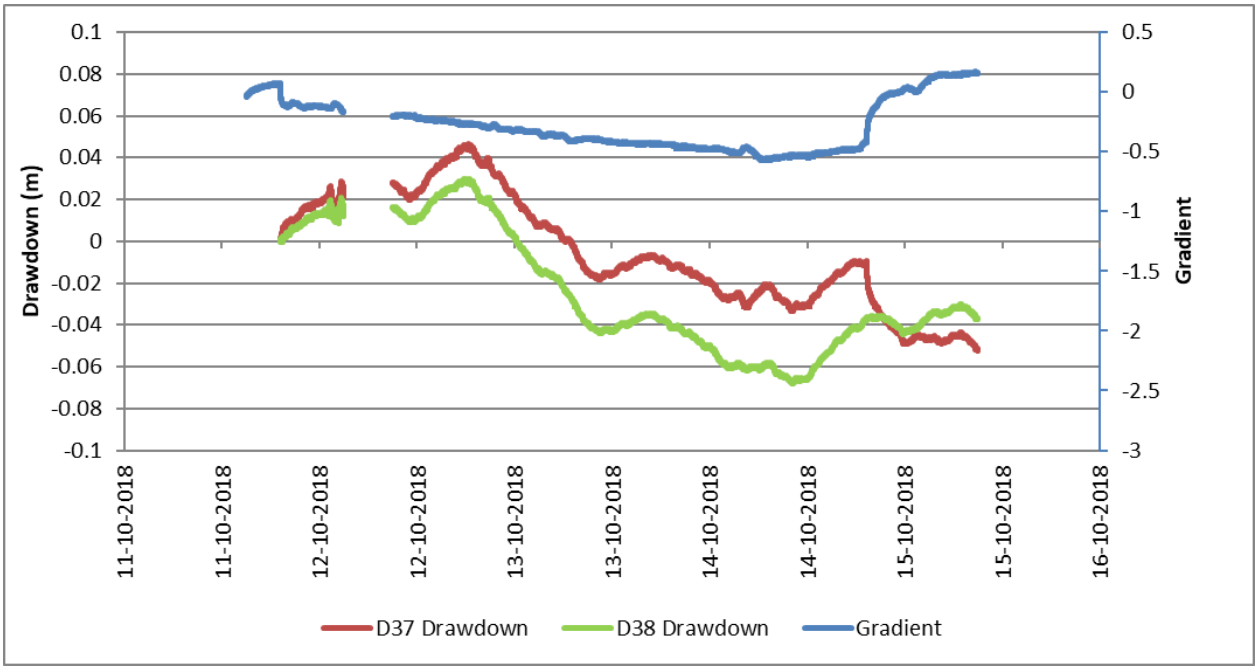

Figure C3: Drawdown and vertical hydraulic gradient in D37/D38 during PT2.

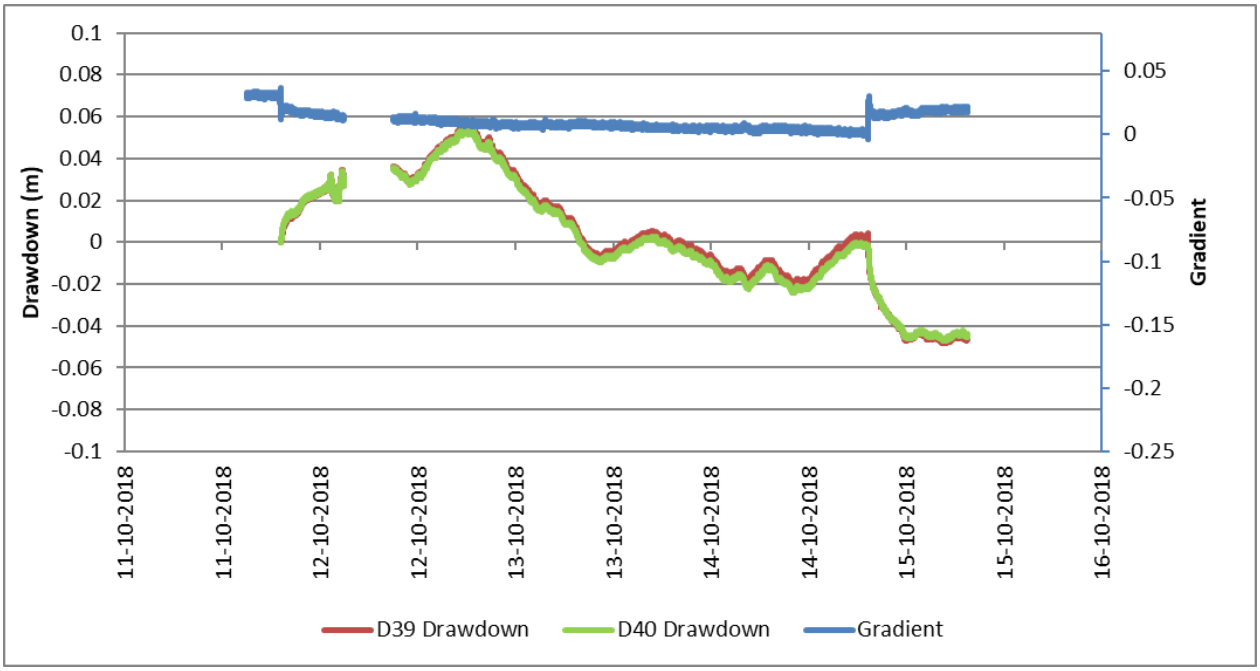

Figure C4: Drawdown and vertical hydraulic gradient in D39/D40 during PT2.

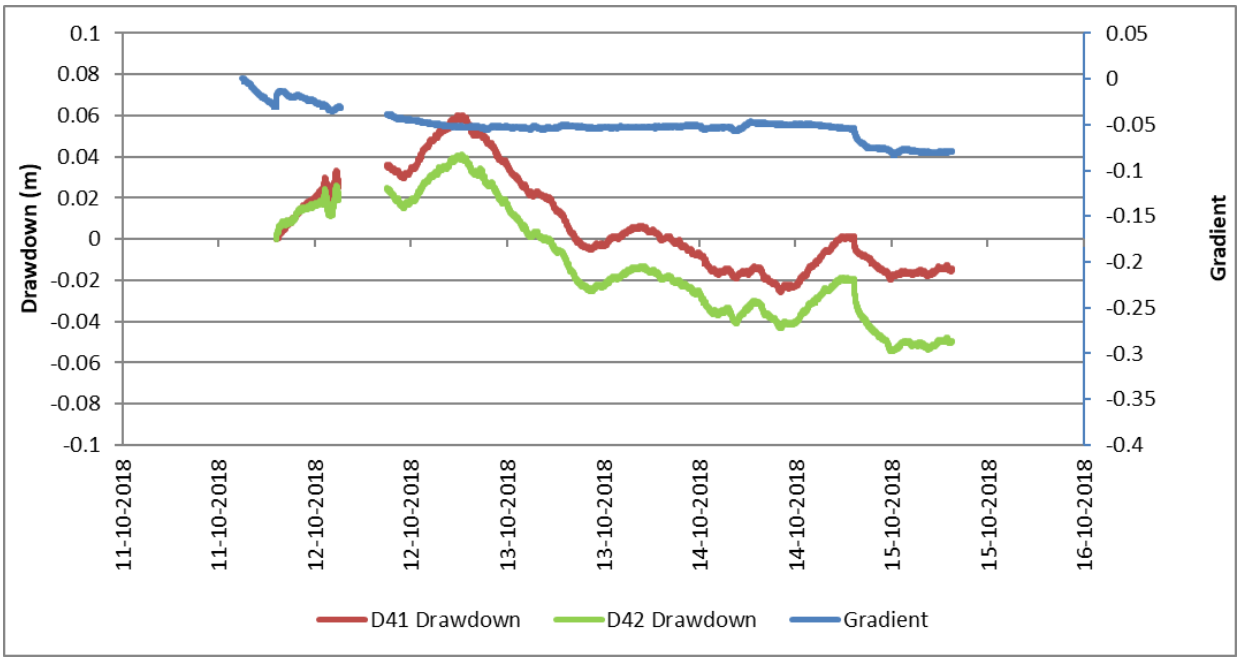

Figure C5: Drawdown and vertical hydraulic gradient in D41/D42 during PT2.

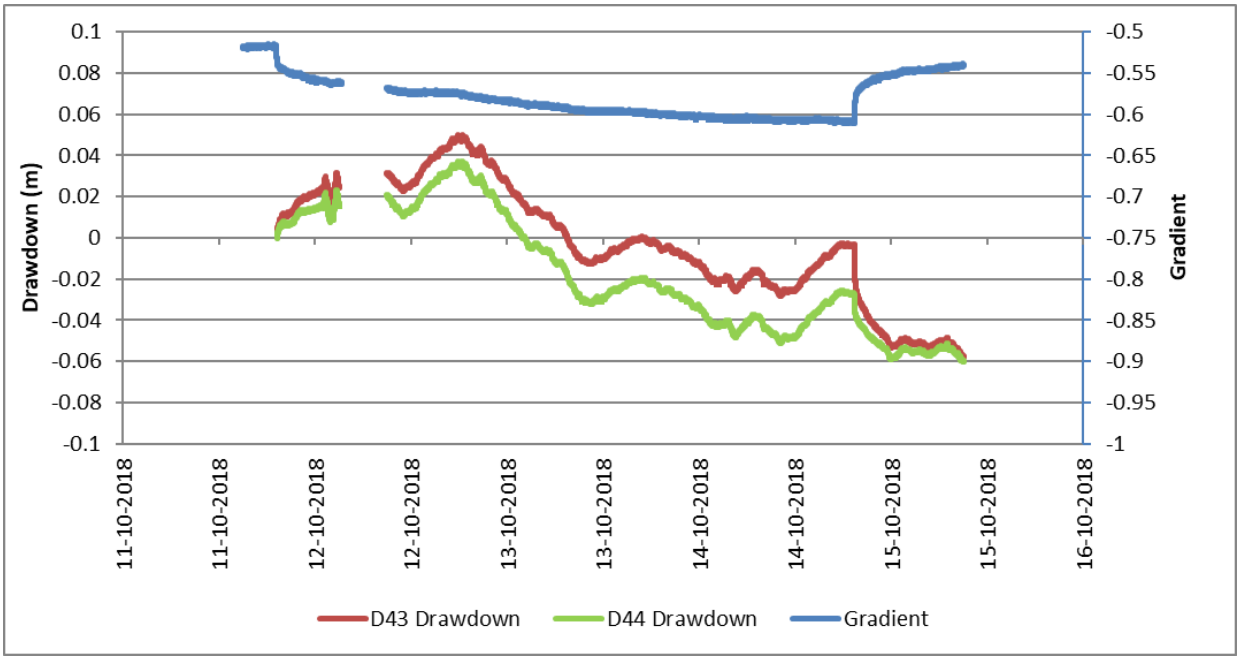

Figure C6: Drawdown and vertical hydraulic gradient in D43/D44 during PT2.

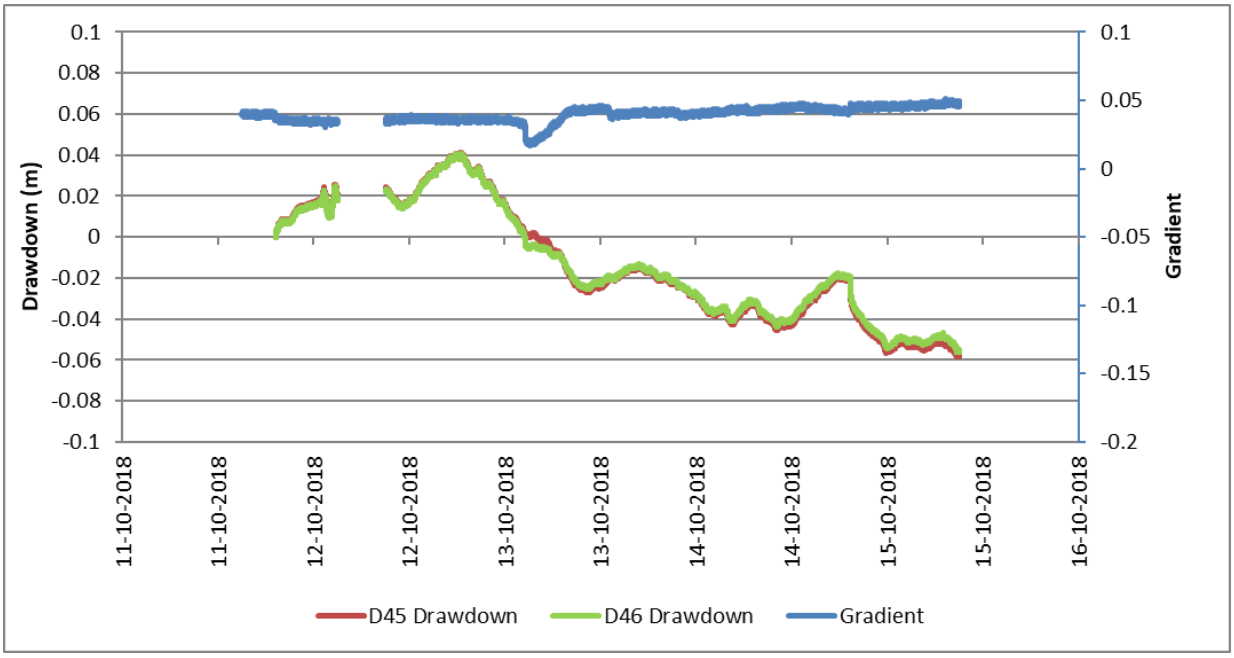

Figure C7: Drawdown and vertical hydraulic gradient in D45/D46 during PT2.

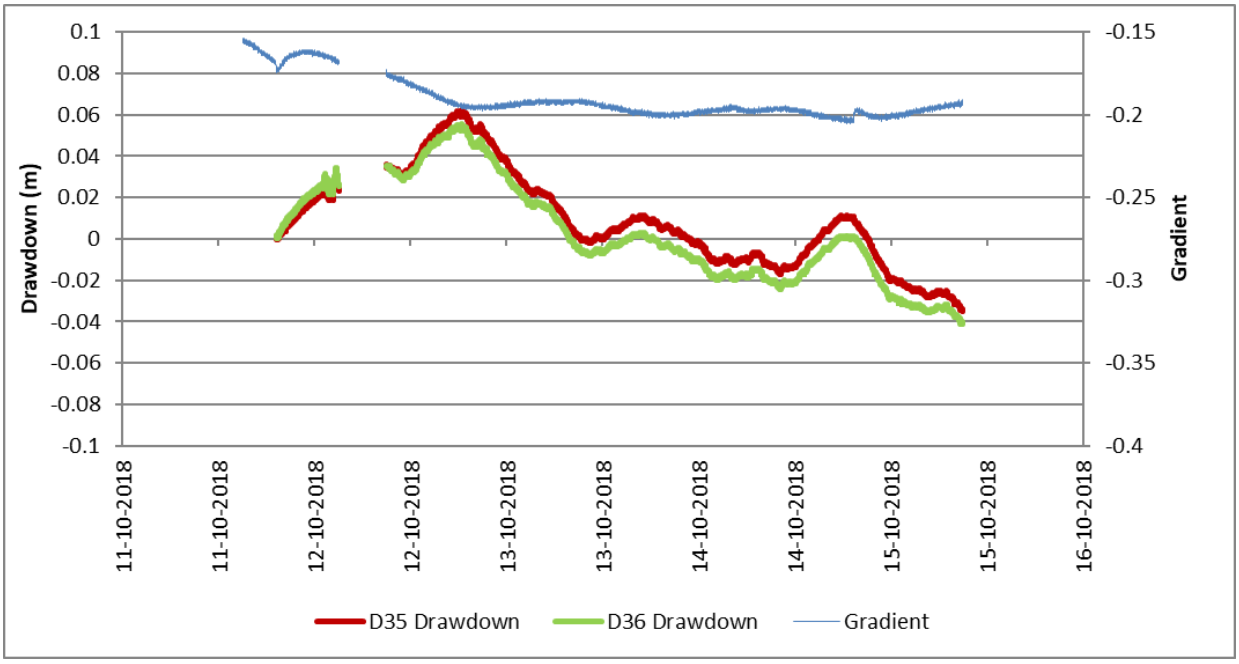

Figure C8: Drawdown and vertical hydraulic gradient in D35/D36 during PT2.

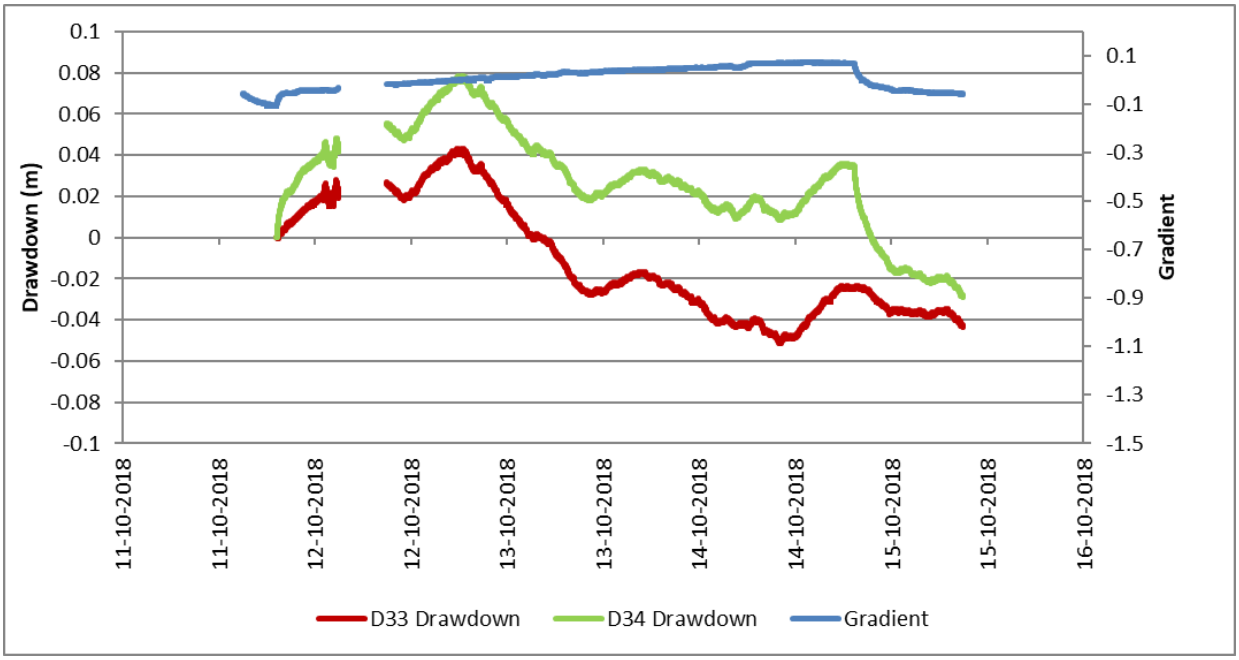

Figure C9: Drawdown and vertical hydraulic gradient in D33/D34 during PT2.

APPENDIX D. GEOLOGICAL CROSSS-SECTIONS THROUGH OTTER PARK

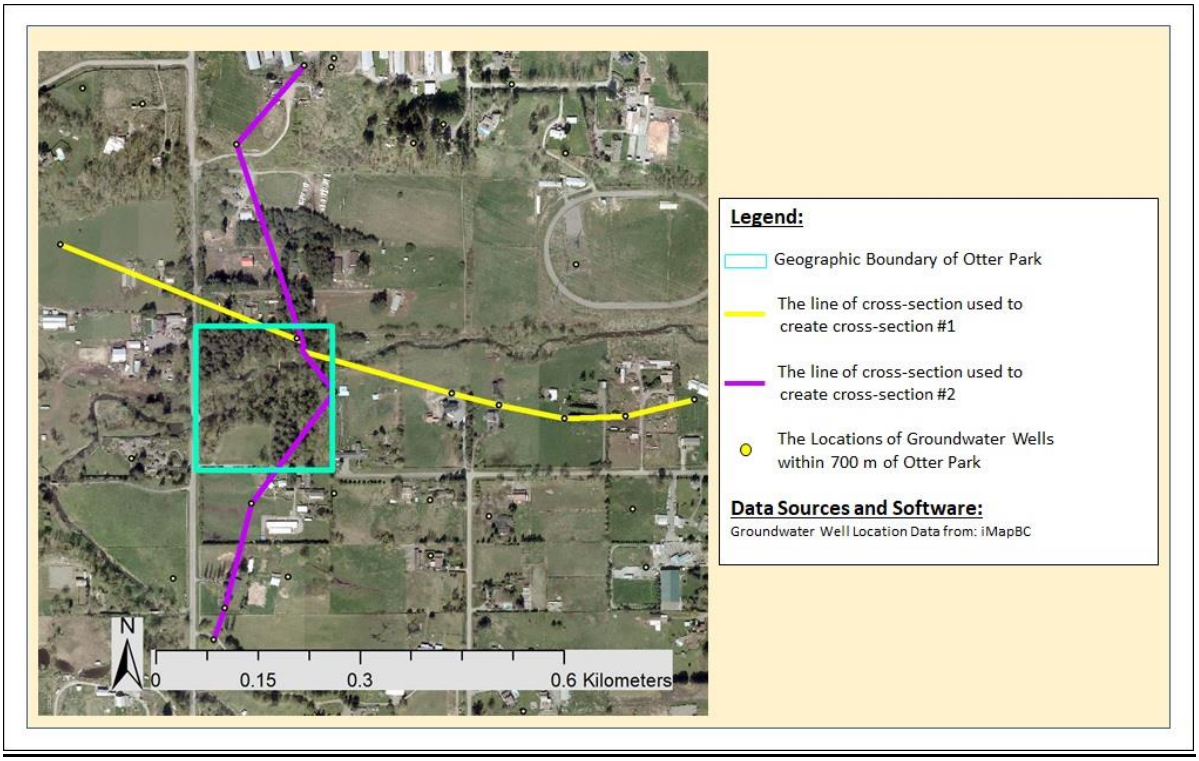

Figure D1: Location of cross-section lines passing through Otter Park.

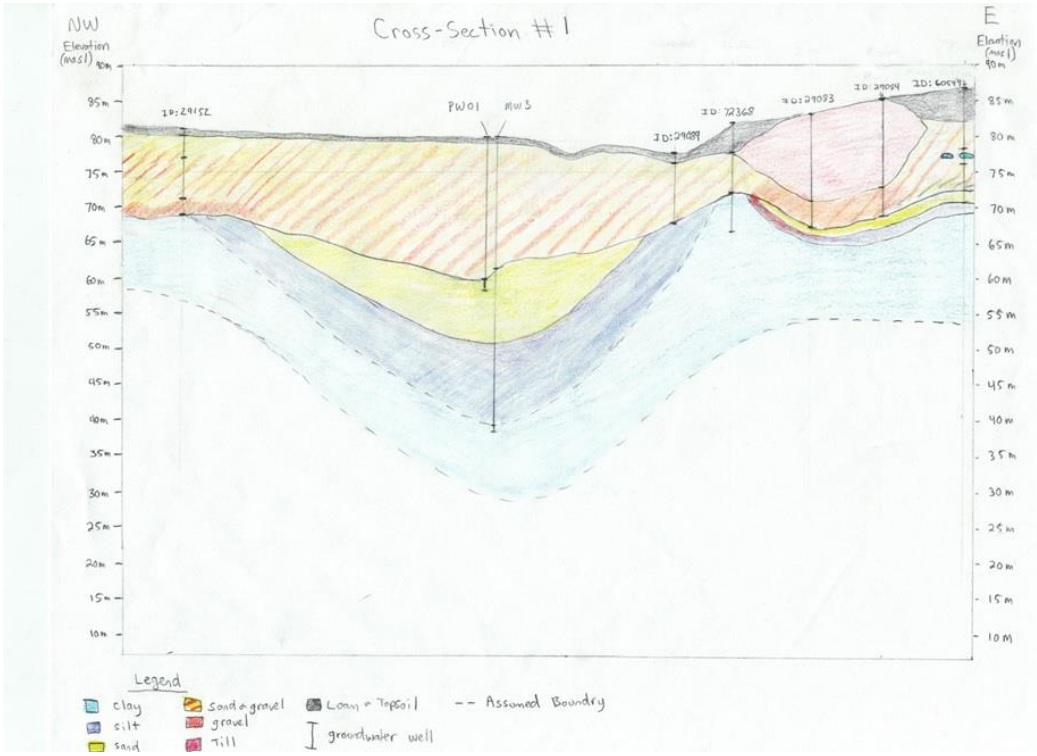

Figure D2: Geological cross-section #1 (see Figure D1 for location).

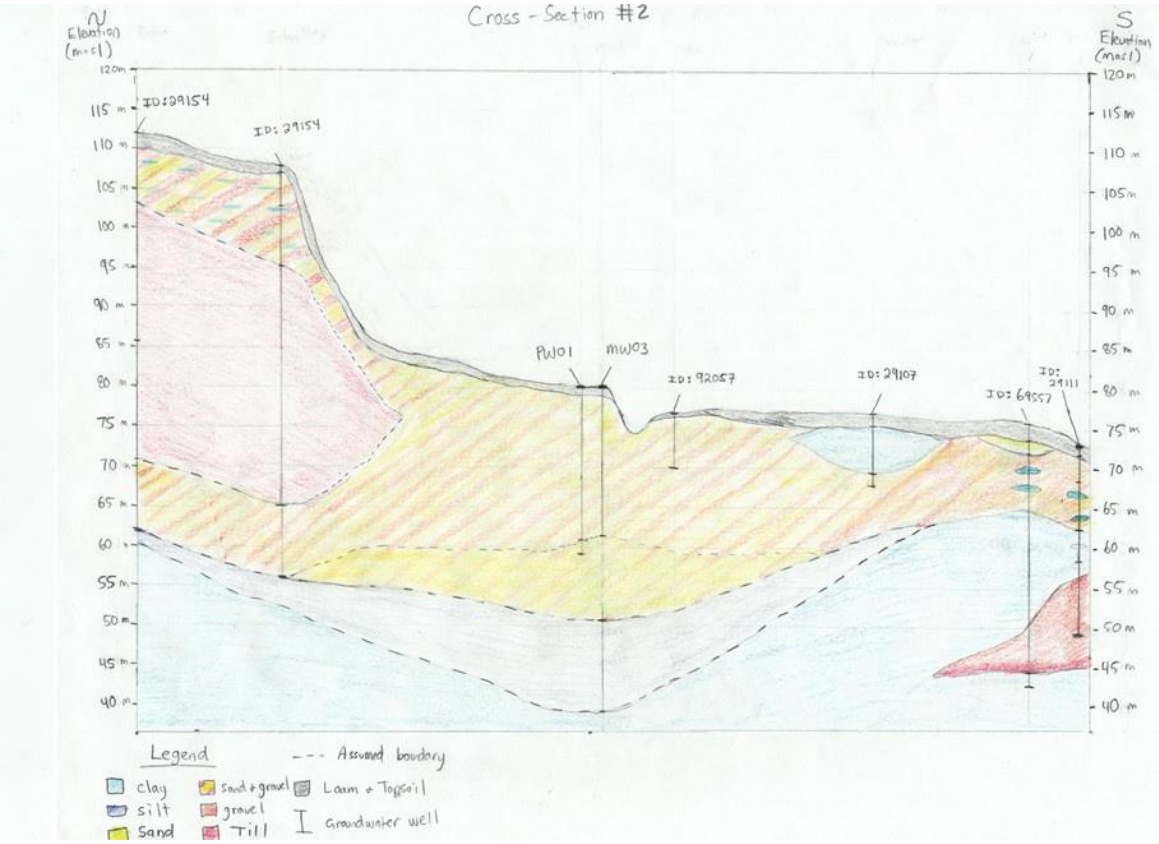

Figure D3: Geological cross-section #2 (see Figure D1 for location).